Characterisation of the Photosystem 2 reaction centre complex

Thesis presented for the Degree of

Doctor of Philosophy in

the University of London

by

Christalla Demetriou

Department of Biology

University College London

London

February 1990

ABSTRACT

The reaction centre components of Photosystem II are bound to a heterodimer of the D1 and D2 polypeptides, in analogy with the L and M subunits of the bacterial reaction centre. This was confirmed with the isolation of a photochemically active complex consisting of the D1/D2/cytochrome b_{559} polypeptides. The complex however does not contain bound quinone and is light and temperature labile.

In this thesis, esr and laser flash spectroscopy were used to characterise the components of the reaction centre complex of higher plants. The isolation of the complex from a variety of organisms is also reported.

Both silicomolybdate (SiMo) and ferricyanide (FeCN) were shown to act as electron acceptors at cryogenic temperatures in the D1/D2/cyt b_{559} complex. In the presence of either SiMo or FeCN, two radicals at g=2 were observed from $P680^{+}$ (0.8mT) and the accessory monomeric chlorophyll (1.0mT). A radical attributed to tyrosine radical (D^{+}/Z^{+}) was also observed in a small number of centres.

The complex was found to be more stable under anaerobic conditions. This suggests that photodamage of the complex may arise as a result of the reaction of

the triplet form of chlorophyll with oxygen to form oxygen radicals. A possible role of cyt b_{559} in the prevention of photodamage is presented.

The addition of exogenous quinone, in the form of decylplastoquinone, to the complex facilitated the reduction of cyt b_{559}, although no evidence of specific binding was observed. However, experimental evidence of specific binding was obtained in the presence of the exogenous quinone, dibromothymoquinone.

Acknowledgments

I would like to thank my supervisor, Dr. Jonathan Nugent for his help and encouragement throughout my PhD and for the loan of his office while writing up my thesis. I would also like to thank the following members, past and present, of the UCL Photosynthesis Group ; Prof. Mike Evans, Andrew Corrie, and Stuart Ruffle, Dr. Julia Hubbard for her assistance with the laser flash spectroscopy experiments and for her friendship and to Dr. G. Bredenkamp for his advice and encouragement while writing my thesis. I would finally like to thank Prof. Jim Barber and Dr. Alison Telfer for the collaborative work on the PSII reaction centre complex.

TABLE OF CONTENTS

Chapter 2 MATERIALS AND METHODS

Chapter 3 ISOLATION OF THE REACTION CENTRE COMPLEX

FIGURES

ABBREVIATIONS

ATP	adenosine triphosphate
BChl	bacteriochlorophyll
BPhe	bacteriopheophytin
Chl	chlorophyll
cyt	cytochrome
D	tyrosine residue 160 of the D2 polypeptide
D1/D2	reaction centre polypeptides of PSII
DBMIB	dibromothymoquinone
DCMU	3-(3,4-dichlorophenyl)-1,1-dimethylurea
DPC	1,5- diphenylcarbazide
DPQ	decylplastoquinone
Esr	Electron spin resonance
G	Gauss (10^{-4} tesla)
FeCN	potassium ferricyanide
LHC	Light harvesting chlorophyll
MES	2- (N-morpholino) ethanesulfonic acid
$NADP^+$	nicotinamide adenine dinucleotide phosphate
OEC	oxygen evolving complex
Phe	pheophytin
PSI	Photosystem I
PSII	Photosystem II
PQ	plastoquinone
Q_A	primary quinone acceptor
Q_B	secondary quinone acceptor
SiMo	silicomolybdate
SPT	spin polarised triplet

Tris	tris (hydromethyl) aminomethane
UQ	ubiquinone
Z	tyrosine residue 161 of the D1 polypeptide

CHAPTER 1

INTRODUCTION

1.1 Summary of photosynthesis

The light reactions of photosynthesis begin with the absorption of incident radiation by the antenna chlorophyll molecules. This results in the redistribution of the electrons of the antennae, forming an excited singlet state (Figure 1.1). The antennae are organised into arrays to maximise light absorption. The excitation energy is then transferred from one antenna pigment to the next, towards longer wavelength species until it reaches a photosynthetic reaction centre. Reaction centre molecules absorb less energetic photons (i.e. of longer wavelength) than the antennae, and as a consequence there can be no back transfer into the antennae and only photochemistry can follow.

The arrival of the excitation energy at the reaction centre promotes a charge separation, where an electron is lost from an occupied orbital of the donor molecule and transferred to an unoccupied orbital of an acceptor molecule. The charge separation is then stabilised by a series of electron transfer steps. As a consequence of this electron transfer, a transmembrane proton gradient is formed which is used to drive ATP

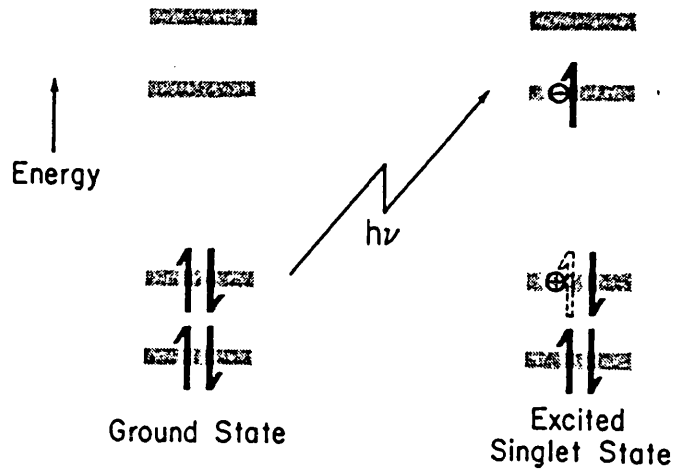

Figure 1.1. Energy level diagram associated with the formation of an excited singlet state.

In the ground state, all electrons are paired. The two highest-energy occupied molecular orbitals and the two lowest unfilled orbitals are represented. Following the absorption of a photon, one of the ground state electrons is transferred to a previously unoccupied orbital, leaving a positive hole. If electrons remain paired i.e. with spins opposed, then the excited state is called a singlet. If the spins are parallel, a triplet state is formed. (Diagram from Sauer, K. 1986).

synthesis. Reduced coenzyme NADH (in bacteria) or NADPH (in plants) is also formed as a result of linear electron flow, and both the NAD(P)H and ATP are used to fix CO_2.

1.2 General aspects of photosynthetic systems

The conversion of light energy to chemical energy is carried out by a number of organisms including higher plants, algae, cyanobacteria and bacteria. The sunlight incident on the earth's surface is in the range of 300 to 1150nm, with an intensity maximum at approximately 600nm.

Higher plant photosynthesis involves the absorption of light between 700 and 350nm. Wavelengths shorter than 350nm can cause ionisation and are therefore potentially harmful to plants and other organisms. The wavelength of light absorption absorbed by algae and cyanobacteria is influenced by the light transmitting properties of the water. At the far end of this spectrum are bacteria which can utilise photons with wavelengths as long as 1050nm.

Higher plants, algae and cyanobacteria have two reaction centres (PSI and PSII) and undergo oxygenic photosynthesis. The photosynthetic bacteria have just one reaction centre and utilise low redox potential compounds as the source of reductant.

1.3 Photosynthetic pigments

There are two main groups of pigments important in photosynthesis, the tetrapyrroles and the carotenoids. Chlorophyll (Chl) and bacteriochlorophyll (BChl) belong to the tetrapyrrole group, these being macro-cyclic, as opposed to the carotenoids and bilins which are linear.

1.3.1 Cyclic Tetrapyrroles

The basic structure of chlorophyll is a chlorin system, made up of four pyrrole rings linked together by methylene groups to form a ring system. In the centre of the chlorin ring is a magnesium atom, complexed with the nitrogen atoms of the four pyrrole rings. Chlorophyll *b* differs from chlorophyll *a* in that it has a formyl group in place of a methyl group on one of the pyrrole rings (Figure 1.2a).

Bacteriochlorophylls are saturated in rings II and IV, the chlorophylls only in ring IV. In the green and purple bacteria, the primary pigment is bacteriochlorophyll *a* except in a few species, such as *Rhodopseudomonas viridis* where the main pigment is bacteriochlorophyll *b*.

Higher plants contain both chlorophyll *a* and *b* , while cyanobacteria have chlorophyll *a* together with phycobilins as accessory pigments . Pheophytin has the

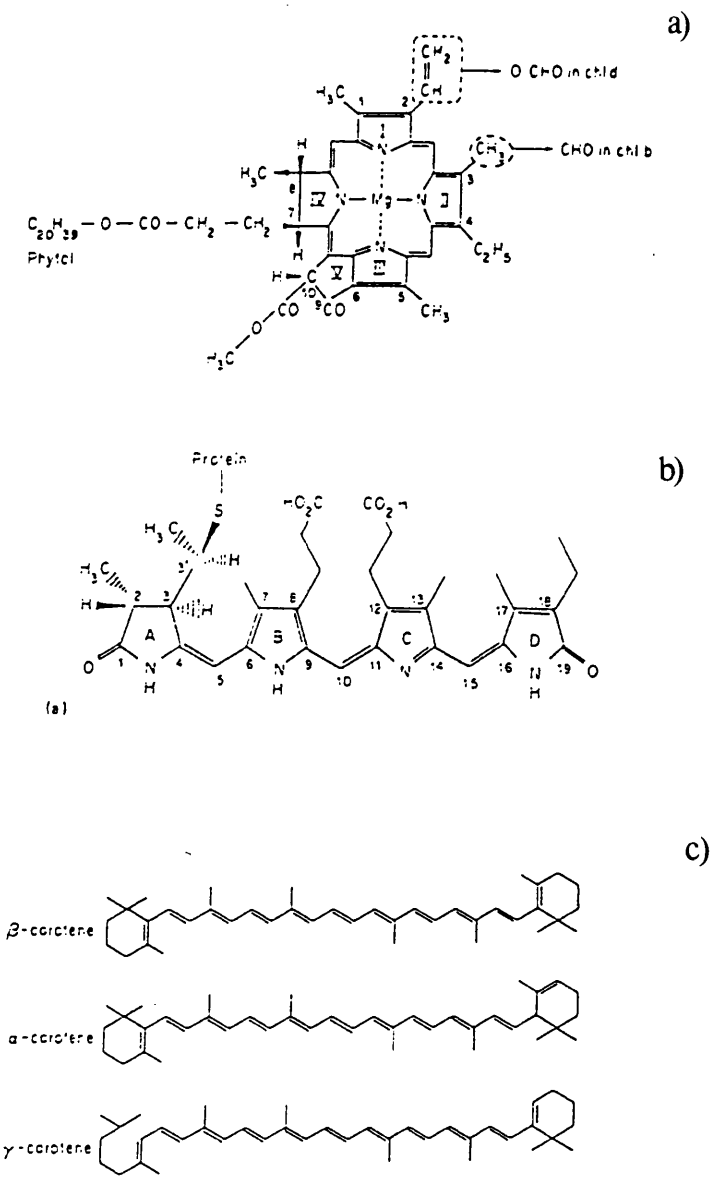

Figure 1.2. Chemical structure of photosynthetic pigments

a) Chlorophylls and bacteriochlorophylls are the primary photosynthetic pigments. Chlorophyll a and b differ in that chlorophyll b has a methyl group in place of the methyl. Bacteriochlorophylls are saturated in both rings II and IV. b) A phycocyanobilin chromophore i.e. a bilin (linear tetrapyrrole) complexed with protein. Phycobilins form part of the antenna system of cyanobacteria and red algae.(Diagram from Glazer, A.N. (1984) Biochim. Biophys. Acta 768, 29-51). c) Carotenes relevant to chlorophyll-dependent photosynthesis are based on a C-40 structure. They are present in most photosynthetic organisms and play a photoprotective role.

same basic structure as chlorophyll a except that it has two protons in place of the magnesium atom.

The pigment molecules are conjugated with polypeptides to form protein pigment complexes. This arrangement holds the pigment in a specific orientation to allow efficient energy transfer by minimising energy loss by fluorescence or radiationless de-excitation.

1.3.2 Linear tetrapyrroles (bilins)

Chlorins can be degraded by the oxidation and removal of the methene bridge, to form linear tetrapyrroles known as bilins (Figure 1.2b). These are complexed with proteins (phycobiliproteins) to form phycobilisomes, which form part of the antenna system in cyanobacteria and red algae.

1.3.3 Carotenoids

These long chain unsaturated hydrocarbons absorb light of wavelengths below about 550nm and hence extend the spectral region of the light harvesting pigments. Mutants of algae and photosynthetic bacteria lacking carotenoids are killed by a combination of the presence of light, O_2 and chlorophyll/bacteriochlorophyll and therefore carotenoids are also thought to play a photoprotective role.

Singlet excitation of chlorophyll has a short lifetime and is relatively immune to reaction with agents such as oxygen which is in a triplet form. However, the singlet state formed on chlorophyll excitation can convert to a triplet state (Figure 1.1) which has a longer lifetime. The carotenoids deactivate the triplet state of chlorophyll, preventing damaging reactions with oxygen.

1.4 The photosynthetic apparatus

1.4.1 Algae

In the case of algae such as Chlorophyceae (e.g. Chlamydomonas, Scenedesmus) the photosynthetic apparatus is located on membranes within a chloroplast structure. In some species, an additional membrane of the chloroplast envelope exists as with the Cryptophyceae, Haptophyceae, Chrysophyceae (golden-brown algae) and Xanthophyceae (yellow-green algae). These extra membranes have ribosomes attached to the outer membrane and this is continuous with the outer membrane of the nuclear envelope.

The light harvesting complexes of algae resemble those of higher plants. However, red algae and the Cryptophyceae have phycobilins and are thought to have evolved from cyanobacteria.

1.4.2 Cyanobacteria

The prokaryotic cyanobacteria have a light harvesting complex in the thylakoid membrane comparable to that of higher plants , but in addition have an extrinsic antenna system on the stromal surface of the thylakoid membrane , the phycobilisome (Figure 1.3). The phycobilisomes are large assemblies of many phycobiliprotein subunits, each containing many covalently attached accessory phycobilin pigments. The proteins are globular, water soluble heterodimers of alpha and beta chains, which form aggregates of trimers and hexamers.

The phycobilins have a layered arrangement within the phycobilisome with phycoerythrin (absorption maximum at 570nm) outermost, phycocyanin (630nm) next , then allophycocyanin (650nm) followed by allophycocyanin B (670nm) closest to chlorophyll a (670-680nm) in the membrane (Figure 1.3). This chlorophyll a acts as an antenna for the reaction centres of PSI and PSII. The density of the phycobilisomes is regulated by light intensity so that under conditions of low light intensity, more phycobilisomes are produced which then aggregate into rows (Zuber et al, 1986).

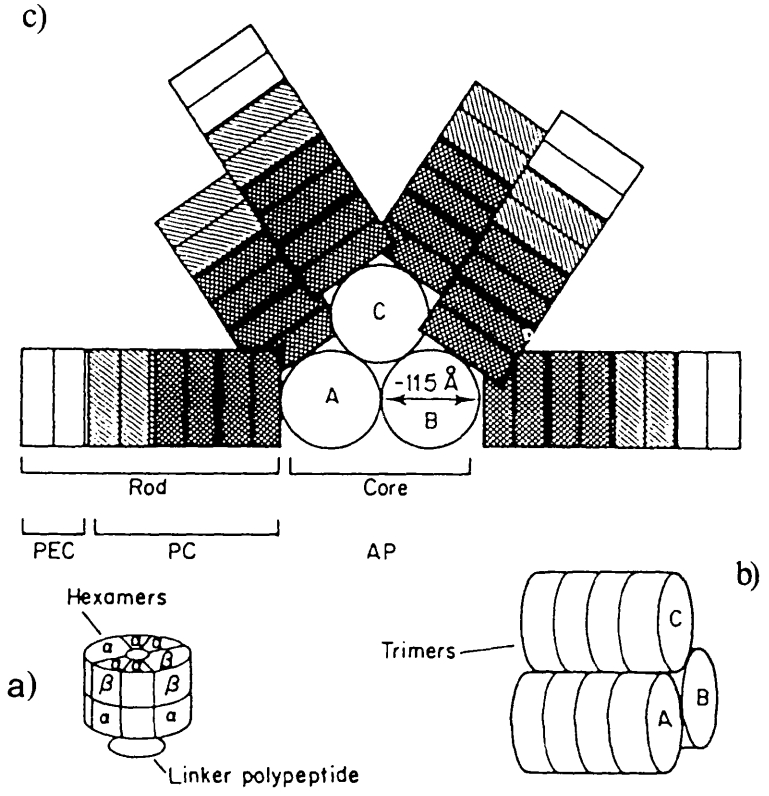

Figure 1.3. Structure of the phycobilisome

The phycobilisome is formed by a) formation of sets of hexamers ($\alpha_3 \beta_3$) around a linker peptide. b) the phycocyanin (PC) and phycoerythrin (PEC) hexamers are stacked to form rods and c) the rods are then arranged around a core of allophycocyanin (APC) dimers. (Diagram from Zuber, 1986).

1.4.3 Higher plants

In higher plants the photosynthetic apparatus is located in the chloroplast (Figure 1.4). The chloroplast is bound by an outer envelope of two continuous membranes, with the inner membrane regulating the transport of metabolites into and out of the chloroplast. The outer envelope is highly permeable to low molecular weight substances. The interior contains the stroma, which consists of an aqueous solution containing various low molecular weight compounds plus a high concentration of protein, mainly the enzyme ribulose biphosphate carboxylase and other enzymes of the Calvin cycle. The stroma houses an intricate lamellar system composed of flattened sacs, or thylakoids which are arranged in stacked, appressed regions (grana) and interconnecting, non-appressed stromal lamellae (Kahn and Wettstein, 1961).

It is these membranes which contain the photosynthetic pigments and electron transport systems which generate the NADPH, and by a process of photophosphorylation, the ATP required to drive CO_2 fixation by the Calvin cycle in the stroma.

Both PSI and PSII have a specific antenna system (LHCI and LHCII respectively). LHCII is the major antenna system of chloroplasts, consisting of

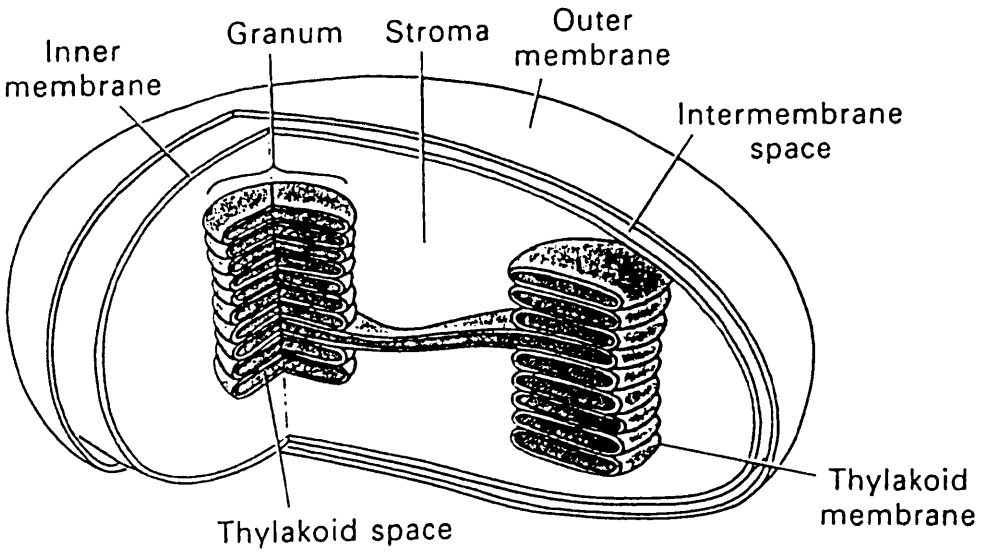

Figure 1.4. Chloroplast structure

The photosynthetic apparatus of higher plants is the chloroplast.The thylakoids associate by appression, forming grana structures within the stroma. (Diagram from Wolf,S.L (1972) Biology of the Cell).

half the total chlorophyll a and almost all the chlorophyll b. LHCII is composed of several polypeptides, some of which were sufficiently similar to co-crystallise (Kuhlbrandt, 1984).

LHCII is involved in a regulatory mechanism of energy distribution between PSI and PSII. The complex is reversibly phosphorylated by a 64 kDa kinase, located in the thylakoid. The activity of the kinase is controlled by the degree of reduction of the PQ pool, i.e. the more reduced it is, the greater the rate of phosphorylation. LHCII is dephosphorylated at a constant rate by a phosphatase.

The phosphorylation of the LHCII is thought to increase the negative charge of the antenna complexes, which then detach due to electrostatic repulsion, thereby causing them to move from the appressed regions containing PSII, to the stroma exposed ones of the thylakoid membrane.

The PSI antenna (LHCI) differ from LHCII in that they are not readily detached and do not show the association - dissociation behavour of LHCII. The antenna complex LHCI was first isolated by Haworth et al (1983), and found to consist of chlorophyll a and b in a ratio of 3:7. Since then two antenna complexes have been resolved LHCIa and LHCIb from their

fluorescence properties.

1.5 Electron transfer in higher plants

The photosynthetic components are located in pigment protein complexes embedded in the lipid bilayer of the thylakoid membrane. Five membrane spanning complexes have been recognised, these being the light harvesting complex (LHC), Photosystem I (PSI) and Photosystem II (PSII) reaction centre complexes , the cytochrome b_6f complex and the CF_1-CF_0 ATPase complex (Figure 1.5a).

The complexes have a heterogenous distribution throughout the thylakoid membrane (Figure 1.5b). Fractionation studies revealed that the PSI and ATPase complexes are located in the stroma lamellae and in regions of the grana that are exposed to the stroma. In contrast, PSII complexes are primarily located in the appressed regions of the grana (Anderson and Andersson, 1982).

Due to this lateral heterogeneity, it has been proposed that plastoquinone and plastocyanin act as mobile electron carriers between PSI and PSII. It has also been proposed that light energy is distributed between the asymmetrically positioned photosystems via the phosphorylation of the light harvesting

a)

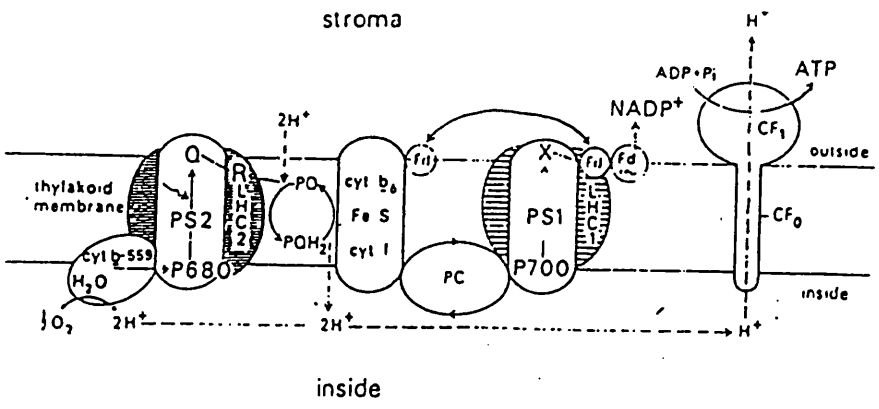

b)

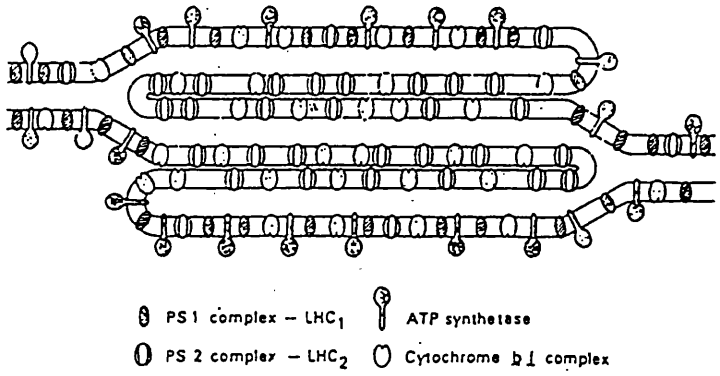

Figure 1.5a. Arrangement of the membrane spanning regions of the pigment-protein complexes in the thylakoid membrane.

Photosynthetic electron transfer (–) and proton transport (--) are shown in the figure. The proton gradient is used to drive ATP synthesis. The NAD(P)H and the ATP formed as a result of electron transfer are used to fix CO_2 in the Calvin cycle.

Figure 1.5b Distribution of the pigment-protein complexes in the thylakoid membrane.

The majority of the PSII complexes are situated within the grana stacks, while PSI occupies the stroma exposed regions. Detergent treatment of the thylakoids results in the digestion of the ends of the grana stacks, allowing separation of the photosystems. (Diagram from Anderson and Andersson, 1982).

polypeptides as explained above (Barber, 1982).

For a general review of the structure and function of the membrane proteins, see Marder and Barber, (1989).

1.6 Electron transfer through the complexes

Absorption of a photon by the P680 reaction centre chlorophyll leads to charge separation. The displaced electron is passed through the PSII complex, via a series of electron carriers, to the plastoquinone (PQ) pool. From PQ, electrons flow on through the cytochrome b_6f complex. This complex contains one c-type cytochrome (f) and two b-cytochromes and a Rieske - type iron - sulphur centre. Electrons are accepted from PSII via plastoquinol, and are delivered to plastocyanin (PC), a protein containing two atoms of copper per molecule.

The photooxidation of the P700 reaction centre chlorophyll leads to a second charge separation. Electrons are passed onto a chain of iron-sulphur electron acceptors and are replaced by electrons from PC (Figure 1.5b). Electron acceptors from PSI donate electrons to NADP via ferredoxin (Fd), the reaction being catalysed by a flavoprotein enzyme, ferredoxin NADP oxidoreductase. The NADPH so produced is then used to operate the Calvin cycle of CO_2 fixation in the

stroma.

In higher plants and cyanobacteria, the electrons from the PSII reaction centre are replaced by electrons from water. Four successive charge separations in the PSII reaction centre create the oxidising equivalents which are necessary to oxidise $2H_2O$ to O_2, releasing four protons.

Electron transport through PSI and PSII results in the transport of protons from the stroma into the intrathylakoid lumen. The proton gradient is used by the ATP synthetase complex to make ATP. The ATP synthetase consists of a hydrophobic membrane sector (CF_o) and a peripheral coupling factor (CF_1)

Two types of photophosphorylation can occur, non-cyclic where ATP synthesis is associated with the flow of electrons from water to NADP, and cyclic where the electron in bound Fd is transferred to the cytochrome b_6f complex to form a cycle around PSI.

The subject area of this thesis is the characterisation of the electron transfer components of the reaction centre of PSII . The following sections outline the electron transfer components of PSII (Figure 1.6).

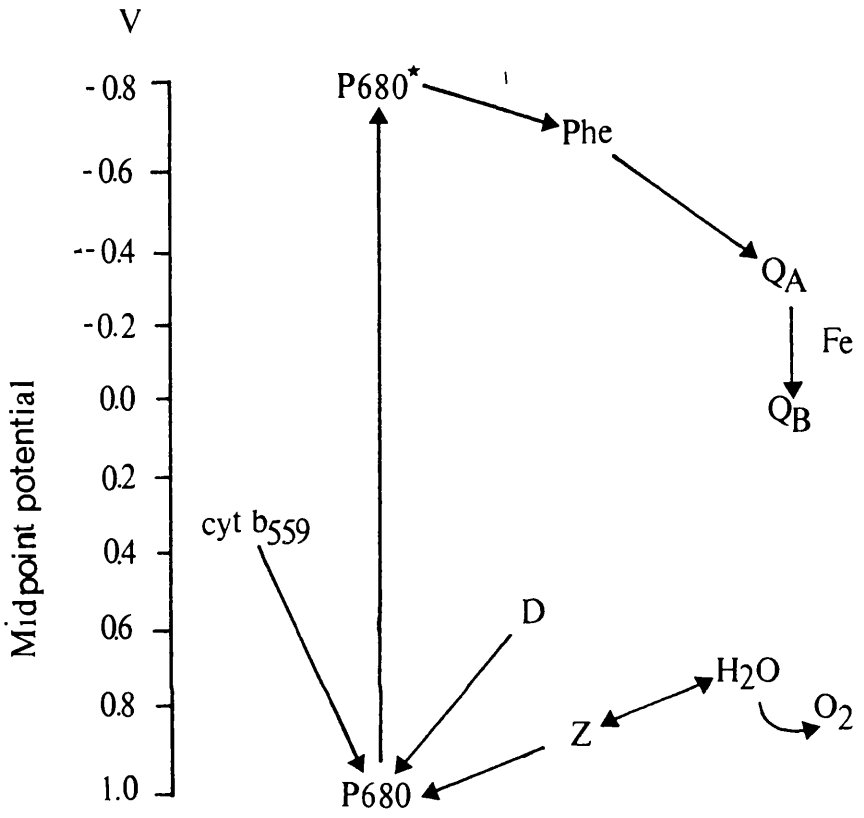

Figure 1.6 Schematic diagram of the reaction centre components of PSII.

The photooxidation of the reaction centre chlorophyll, P680, results in charge separation. Charge stabilisation occurs as a result of electron transfer to the intermediate electon acceptor, pheophytin, and then onto the secondary acceptors, Q_A and Q_B. Z is thought to be a transient electron carrier between the oxygen-evolving complex and P680. D may play a role in the deactivation of the 'S' states of the water oxidation complex. The role of cytochrome b_{559} is as yet undetermined, although it may be involved in a cyclic system which operates under high light intensity to prevent photodamage of the reaction centre.

Structural and functional concepts of the PSII reaction centre have mainly been based on the well characterised purple bacterial reaction centre and from amino acid sequence data of the PSII polypeptides.

1.7 The electron acceptor components of PSII

1.7.1 The reaction centre chlorophyll, P680

The absorption spectrum of P680 was first obtained by Doring et al (1969) by flash spectroscopy. The spectrum showed major bleachings at 682 and 435nm and it was subsequently proposed that P680 was a specialised chlorophyll a .

P680 has a high redox potential of + 1.0 V and as a consequence it can oxidise a neighbouring pigment molecule in the absence of a normal electron donor. It is therefore difficult to accumulate $P680^{+}$ for longer than a few ms. The oxidised form of P680 however, displays an esr signal at low temperature at g=2.002. The esr signal is characteristic of a free radical with a linewidth of approximately 8G. This narrow linewidth could indicate a chlorophyll a dimer as in the case of the purple bacterial bacteriochlorophyll dimer (Norris et al, 1971). However, the reduction in linewidth may also be a result of a highly specific environment rather than of the delocalisation of the electron over two chlorophyll molecules. This is an area of great

uncertainty and will be discussed in Chapter 4 .

1.7.2 The first electron acceptor, pheophytin

The intermediate electron acceptor of PSII is pheophytin. It's role was demonstrated by Klimov et al (1977) by the reversible photoinduced absorbance changes in PSII enriched particles, upon illumination when Q_A was reduced (i.e. at redox potentials below -300mV). The midpoint redox potential of the intermediate was found to be -610mV (Klimov et al, 1977).

The difference spectrum showed a decrease at 680nm, 545nm, 515nm and 422nm and an increase at 448nm and 605nm , these changes being characteristic of the formation of a pheophytin anion radical (Fuijita et al, 1978). Further to this, a light induced esr signal of approximately 13 gauss wide near g=2 was observed (Klimov et al, 1980).

1.7.3 The secondary electron acceptors, Q_A and Q_B

Q_A was first detected from the dependence of fluorescence yield on its redox state (Duysens and Sweers, 1963) , and was later assigned to a plastoquinone by Stiehl and Witt (1969). Investigations into the mechanism of charge accumulation using a series of single turnover flashes, resulted in the

discovery that electron release from PSII showed damped oscillations with a periodicity of two (Bouges-Bouquet, 1973).

These results were interpreted in terms of another electron acceptor, Q_B acting in series with Q_A. Q_B acts as a two electron gate as follows: with the first turnover of the reaction centre, the electron is stabilised on Q_A and then within a few tens of ms is transferred onto a secondary quinone acceptor Q_B. Following a second turnover of the reaction centre, the events are repeated, forming a doubly reduced Q_B. At some stage during this process, two protons are taken up from the stroma side to form a fully reduced and protonated plastoquinol. This quinol is loosely associated with the quinone binding site and its dissociation from the PSII reaction centre is probably the mode of reduction of the plastoquinone pool. The vacated quinone site can then bind a PQ.

Both Q_A and Q_B are magnetically coupled to a high spin ferrous iron, Fe^{2+}. The discovery of an esr signal in PSII particles provided evidence of the involvement of a semiquinone-iron complex. This esr signal, was analogous to the signal observed in bacterial reaction centres which was attributed to the interaction between $BPhe^-$ and $Q_A^-Fe^{2+}$ (Klimov et al, 1980).

The observation of the light induced $Q_A^-Fe^{2+}$ signals at g= 1.82 and 1.90 provided further information of the involvement of a semiquinone-iron complex on the acceptor side of PSII (Nugent et al, 1981; Rutherford and Mathis, 1983). Two forms of the signal can be seen under different conditions. A g=1.8 signal (Nugent et al, 1981) is observed at low pH and in the presence of formate (Vermass and Rutherford, 1984) and a g=1.9 which is observed at high pH (Rutherford and Zimmerman, 1984). Nugent et al (1988) have proposed that bicarbonate binds at or near the non-haem iron and influences the $Q_A^-Fe^{2+}$ esr signal. Formate treatment of PSII removes the bicarbonate, resulting in a change from the g=1.9 to the g=1.8 form of the semiquinone-iron signal.

1.8 The electron transfer components on the donor side of PSII

1.8.1 The oxygen evolving complex

The oxidised P680 is reduced by electrons obtained from the oxidation of H_2O to O_2. The latter process is performed by the oxygen evolving complex (OEC) of PSII. In order to oxidise $2H_2O$ into O_2 and $4H^+$, a stepwise accumulation of four oxidising equivalents in the OEC by four consecutive oxidations of P680 is required. Thereby it has been proposed that the OEC passes

through five different states, called the S-states (S_0 to S_4) (Figure 1.7). O_2 is released during the conversion of S_4 to S_0. This model was based on the oxygen yield of isolated chloroplasts following a sequence of single saturating laser flashes. The oxygen yield had a four flash periodicity after a four hour dark adaptation period (Kok et al, 1970).

The S_0 and S_1 states are relatively stable in the dark, with the S_0 states present in 25% of the PSII centres. However, during periods of long dark adaptation, S_0 is slowly oxidised to S_1 to give 100% S_1 in long dark adapted samples (Joliot et al, 1971; Vermaas et al, 1984; Beck et al ,1985). It is now accepted that the 'S' states represent the oxidation states of the Manganese (Mn) of the water splitting enzyme (Dismukes, 1986). The Mn may also act as a binding site for the water molecules which are undergoing oxidation (Rutherford, 1989). Electrons are removed from the oxygen evolving complex by Z, which is an intermediate between P680 and the OEC.

Data on the organisation of the Mn cluster is obtained mainly from esr and X-ray absorption studies. Two esr signals arise from the Mn cluster. Firstly, the multiline signal around g=2, which arises from the S_2 state (Dismukes and Siderer, 1980).

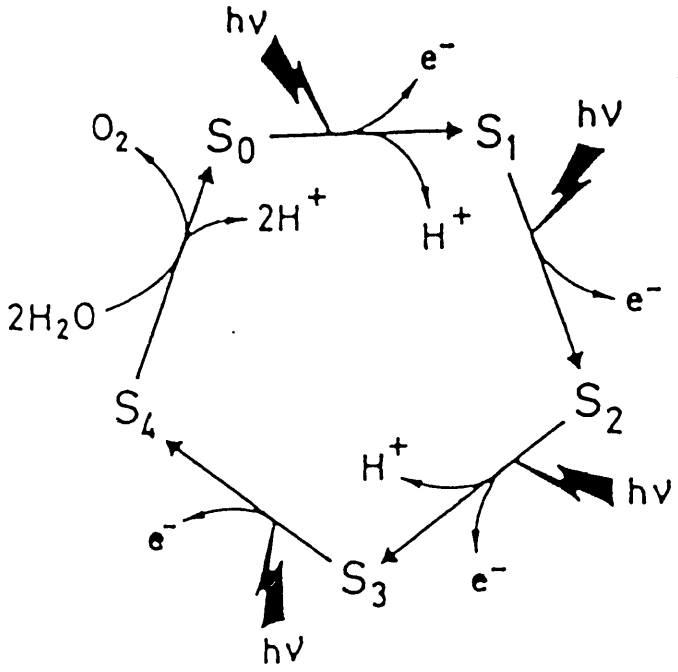

Figure 1.7. A kinetic model for the accumulation of four positive charges, based on Kok's model (1970)

The 'S' states are defined by the number of the positive charge equivalents accumulated (S_0 to S_4). S_0 and S_1 are relatively dark stable, although S_0 is slowly oxidised by D^+ to form S_1. S_2 and S_3 can back react to form S_1 in a few secs. S_4 is a transient state, rapidly forming the S_0 state. Protons are possibly released at the points shown on the diagram. (Diagram from Rutherford, 1989).

Most of the features of this signal implicate a mixed valence dimer, most likely to be Mn^{3+} Mn^{4+} (for a review see Rutherford, 1989). A second esr signal close to g=4 is also attributed to the S_2 state. This g=4 state is thought to be a precursor which gives rise to the multiline signal.

The structure of the Mn complex is still uncertain, although there are probably four Mn ions involved (Babcock, 1987). Various proposals have been put forward for the organisation of the Mn cluster (Brudvig and Crabtree , 1986; Dismukes, 1988; Rutherford, 1989).

1.8.2 The electron donors D and Z

The two components on the electron donor side of PSII, D and Z, both give rise to free radical esr signals at g=2.0046, called signal II. This signal was one of the first to be observed in photosynthetic material (Commoner et al, 1956; Kohl and Wood, 1969). A number of forms of signal II were found at room temperature and were subsequently named according to their decay kinetics, signal II_{vf}, II_f, II_m and II_d.

The similarity in the esr signals indicated that the origin and the environmental surroundings of the radicals were similar. It was initially thought that D

and Z were plastoquinones, based on reconstitution experiments with deuterated quinone (Kohl and Wood, 1969).

A narrowing of the D^+ signal resulted. Several other authors agreed with this proposal, based on the interpretation of spectroscopic properties of D^+ and Z^+ (O'Malley and Babcock, 1984). However, the assignment of Z/D to a quinone was unreliable due to a number of considerations;

1) Quantification experiments of the amount of quinone in the reaction centre indicated that quinone was not present in adequate amounts to account for Z,D and the acceptor quinones (de Vitry et al, 1986; Tabata et al, 1985).

2) The g values of the model quinone cation radicals are in the range of 2.0034-2.0038, significantly lower than the 2.0046 value measured for Z^+ and D^+ (Sullivan and Bolton, 1968).

The spectral and physical properties of the Z^+/D^+ species are consistent with it being a tyrosine radical. In vivo deuteration of the tyrosine in cyanobacteria resulted in the narrowing of signal II. No change in width of the signal was observed in cyanobacteria grown to form deuterated quinones. This in addition to the inconsistences of the previous

experiments have led to the proposal that D and Z are tyrosine radicals (Barry and Babcock, 1987; Debus et al, 1988a; Debus et al, 1988b, Vermaas et al, 1988).

Site directed mutagenesis experiments have shown that Z and D are located symmetrically on D1 and D2 respectively. Changing the tyrosine residue 160 of the D2 polypeptide of the cyanobacterium Synechocystis 6803 to a phenylalanine results in the organism being able to grow photosynthetically but it lacks the D^+ esr signal.

Z is a transient electron carrier between $P680^+$ and the OEC. D plays a role in the oxidation of S_0 to S_1 state (Vermaas et al, 1984), and the deactivation of S_2 to S_3 (Babcock and Sauer, 1973; Velthys and Visser, 1975). This role in deactivation was confirmed by Nugent et al, (1987), by monitoring the rise of D^+ (signal II) and the loss of the S_2 multiline signal.

1.8.3 Cytochrome b_{559}

Cytochrome b_{559} occurs in two forms with different midpoint oxidation - reduction potentials. A high potential form exists with an E_m of 380mV and a low potential form with E_m 80mV. Esr spectra of both forms can also be observed following illumination at cryogenic temperatures. A definite role for cytochrome

b_{559} has not yet been assigned, although it may play a protective role in high light conditions which may lead to photoinhibition.

1.9 The polypeptide composition of PSII

The structure of the thylakoid membrane follows the fluid mosaic model, i.e. a lipid bilayer in this case consisting of glycolipids, sulpholipids and phospholipids into which various proteins are embedded. Both extrinsic and intrinsic polypeptides are associated with the thylakoid membrane. The extrinsic proteins are loosely attached to the membranes via ionic forces to polar groupings of membrane lipids and proteins can be removed with high salt treatments. The intrinsics are located in the hydrophobic membrane interior and therefore require detergents to remove them. A large fraction of PSII is made up of the light harvesting chlorophyll (LHCII) proteins (Delepaire and Chua, 1981). Figure 1.8 summarises these polypeptides and the genes which code for them.

The chlorophyll a , chlorophyll b and xanthophylls of LHCII are non-covalently associated with two major apoproteins of 28 and 26 kDa . The remainder consists of at least seven polypeptides which are involved in binding the reaction centre. A number of small molecular weight polypeptides are also present although their functions are not as yet clear (for a

review, see Marder and Barber, 1989).

The OEC had long been thought to be a protein complex separate from the photochemical reaction centre complex . However, it is now known that the site of O_2 evolution is tightly bound to the photochemical reaction centre.

1.9.1 The proteins of the oxygen evolving complex

Investigations into the function of the extrinsic polypeptides of the OEC have been performed on PSII particles (Berthold et al, 1981) and inside out thylakoid preparations. The latter are prepared by a two-phase partition method following high pressure treatment of intact thylakoids (Andersson and Akerlund, 1978). These preparations expose the site and proteins involved in oxygen evolution to the bulk aqueous phase, which can then be dissociated by mild treatments. This makes for easy manipulation and allows reconstitution experiments to be performed in order to give an indication of the role of various polypeptides in water oxidation.

Treating PSII particles or inside-out particles with Tris-HCl buffer of high pH and concentration, results in three proteins of molecular weight, 33, 24 and 18 kDa being lost, with concomittant loss of O_2

evolution (Kuwabara and Murata, 1982; Akerlund and Jansson, 1981; Yamamoto et al, 1981). Treatment of PSII particles with 2M NaCl removes the 24 and 18 kDa polypeptides only (Akerlund et al, 1982; Miyao and Murata, 1983; Kuwabara and Murata, 1983).

The function of the extrinsic 18 and 24 kDa polypeptides can be replaced with low concentrations of chloride and/or calcium ions. The 18 kDa polypeptide can be replaced by 5mM Cl^- and the 24 kDa with with 5mM Ca^{2+} and 30mM Cl^-. Oxygen evolution can occur even in the absence of the 33 kDa polypeptide although at a slower rate, in the presence of 200mM Cl^- (Miyao et al, 1987).

The removal of the 33 kDa also results in the loss of some manganese (Mn) and is therefore thought to play a role in Mn binding, perhaps maintaining the conformation of the Mn cluster required for oxygen evolution. The 33 kDa protein may provide ligands directly to the Mn cluster, which can be replaced by Cl^- in the protein's absence (Dismukes, 1988).

A fourth nuclear encoded polypeptide is thought to be associated with the three extrinsic polypeptides. This 10 kDa protein can be released by washing with 1M NaCl and 0.06% Triton X-100.The predicted folding pattern of this 10 kDa indicates a hydrophobic segment

long enough to span the the lipid bilayer in an alpha helix. This in turn is flanked by a large N-terminal region located towards the thylakoid lumen and a short C-terminal hydrophilic domain. The role of this polypeptide is uncertain at present, but it may act as a docking protein for the 24 kDa polypeptide.

1.9.2 The intrinsic polypeptides of PSII

At least six chloroplast encoded intrinsic polypeptides are thought to be involved in the reaction centres of oxygenic photosynthetic organisms (Marder and Barber, 1989). The core complex consists of two chlorophyll proteins, CP47 and CP43 (approximately 47,000 and 43,000 M_r respectively), two proteins D1 and D2 (32,000 and 34,000 M_r) and the two apoproteins of cytochrome b_{559}, psbE and psbF (10,000 and 4,000 M_r). A 9 kDa phosphoprotein (psbH) of unknown function is also is also present in the core complex. Figure 1.8 summarises these polypeptides and the genes which code for them.

There was controversy over which of these polypeptides were involved in binding the reaction centre components. Initial attempts to identify the reaction centre polypeptides concentrated on the two chlorophyll binding proteins, CP47 and CP43. The isolation of both the CP47 and the CP43 polypeptides

Figure 1.8. The intrinsic and extrinsic polypeptides of PSII

Chloroplast encoded proteins of PSII

Complex	Gene designation	Gene product
Intrinsic core of PSII	psbA	32 kDa Q_B protein, D1
	psbB	47 kDa Chl *a* protein
	psbC	44 kDa Chl *a* protein
	psbD	34 kDa Q_A protein, D2
	psbE	9 kDa cytochrome b_{559}
	psbF	4 kDa cytochrome b_{559}
	psbG	24 kDa polypeptide
	psbH	10 kDa phosphoprotein
	psbI	4.8 kDa protein
	psbJ	-
	psbK	2.0 kDa protein
	psbL	3.2 kDa protein

Nuclear encoded proteins of PSII

Light harvesting proteins	cab type 1	26-28 kDa LHCII
	cab type II	24 kDa LHCII
Extrinsic polypeptides	oee	33 kDa polypeptide
	oee2	23 kDa polypeptide
	oee3	16 kDa polypeptide
	-	10 kDa polypeptide

using non-denaturing SDS-PAGE, indicated that they were both chlorophyll a binding proteins, as judged from the absorption maximum at 670nm (Nakatani et al, 1984). When investigated using low temperature fluorescence spectroscopy, the CP47 exhibited a fluorescence emission band at 695nm attributed to the presence of reduced pheophytin. CP47 was therefore thought to bind the reaction centre components and the CP43 was assigned the role of light harvesting polypeptide. The proposed model for the assembly of the polypeptides of PSII is shown in Figure 1.9.

Substantial progress has been made following the crystallisation and subsequent X-ray crystallography of the related reaction centre of the purple bacterium, Rhodopseudomonas viridis (Deisenhofer et al, 1984, 1985a and 1985b) and of Rhodobacter sphaeroides (Feher ,1983 ; Allen and Feher, 1984). This together with the determination of the amino acid sequences of the polypeptides has provided detailed information on both the structural and functional properties of the reaction centre.

1.10 The crystallisation of the reaction centre of purple bacteria

Before the crystallisation of the bacterial reaction centre the cofactors had been identified using

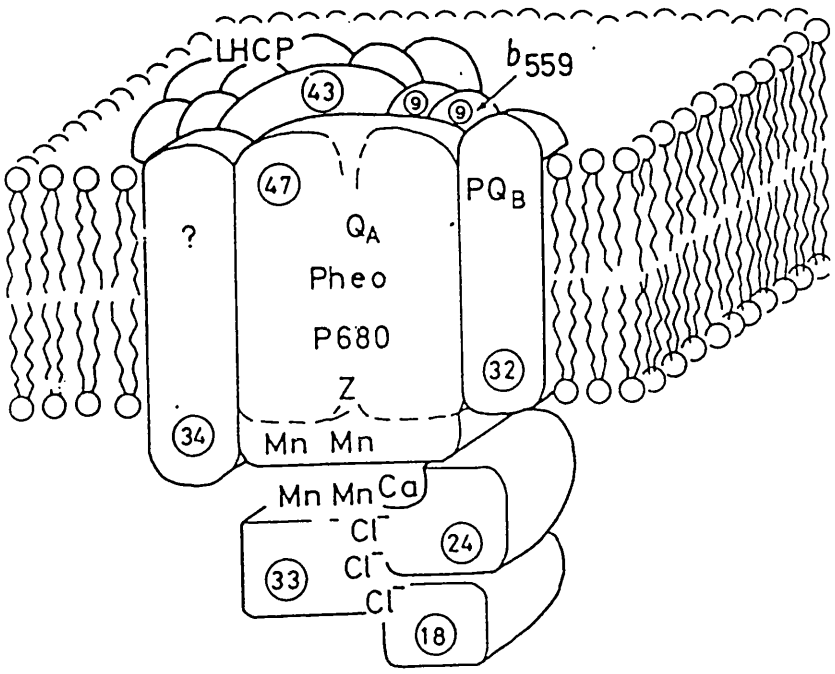

Figure 1.9. Initial model for the organisation of the PSII polypeptides

The model shows the arrangement of the intrinsic and the three extrinsic polypeptides embedded in the lipid bilayer. Following the work of Nakatani et al, (1984) and Satoh, (1979) it was proposed that the reaction centre components were bound to the 47 kDa polypeptide. (Diagram from Murata and Miyao, 1985).

a number of techniques including esr, endor and optical spectroscopy. The reaction centres from two non-sulphur purple bacteria have been particularly well studied, these being the bacteriochlorophyll a containing Rhb. sphaeroides and the bacteriochlorophyll b containing Rps. viridis. Both reaction centres consist of three protein subunits, L, M and H (for light, medium and heavy protein bands on SDS-PAGE) but reaction centres from Rps. viridis have an additional cytochrome subunit.

Reaction centres of purple bacteria contain four bacteriochlorophyll molecules, two bacteriopheophytin molecules (BPhe) (BPhe a in Rhb. sphaeroides and BPhe b in Rps. viridis), a non-haem iron, a primary quinone, Q_A (menaquinone in Rps. viridis and ubiquinone in Rhb. sphaeroides) and a secondary quinone, Q_B (ubiquinone in both species). The crystallisation of the reaction centre of Rps. viridis and the determination of its structure to 0.3nm resolution allowed the spatial arrangement of the cofactors to be determined (Deisenhofer et al, 1985a).

A three dimensional structure has been elucidated from the X-ray crystallographic data in conjunction with the determination of the amino acid sequences of the reaction centre polypeptides.

1.10.1 Structure of the bacterial reaction centre as revealed by X-ray crystallography

The X-ray data of Rps. viridis revealed that the reaction centre had an elongated shape, with the L and M subunits forming a central structure. Although L is shorter than M (L, 273 residues: M, 323 residues), the folding pattern is generally similar. It was confirmed that both L and M consisted of five membrane spanning helices (A - E). Each transmembrane segment consists of about 25 amino acids of which at least 19 are hydrophobic. Cysteine, methionine, alanine, serine and histidine residues are well represented in the helices with prolines and glycines at the ends of the transmembrane segments.

The H subunit can be divided into three structural regions a) a small transmembrane helix (24 residues) at the N terminal segment b) a region consisting of a short helix and two, double stranded antiparallel beta sheets which runs along the surface of the L-M complex. This region appears to derive stability from the contact with the L and M subunits, c) there is a globular domain consisting of an alpha helix and an extended system of antiparallel and parallel beta sheets, the latter forming a pocket with a hydrophobic interior.

1.10.2 Arrangement of the cofactors of the bacterial reaction centre

The cofactors were found to have a symmetrical arrangement, forming two branches, termed the L and M branches. The primary donor (P960), was confirmed to be a bacteriochlorophyll b dimer as was implicated from esr and endor data. The rings of the dimer are stabilised by the acetyl groups being H-bonded to amino acid side chains and other H-bond interactions. The monomeric bacteriochlorophyll b are each placed approximately 1.3 nm from closest ring of the dimer. Each bacteriochlorophyll b is in contact with bacteriopheophytin b, with a distance between the rings of 1.1 nm.

A two-fold rotation axis runs from the non-haem iron to the dimer. A bound menaquinone corresponding to Q_A is found close-by the bacteriopheophytin. Q_B is more loosely bound and is lost during the purification process (Shopes and Wraight, 1985; Gast et al, 1985). The Q_B site in Rps. viridis is found by soaking competitive inhibitors e.g. terbutryn into the crystals in order to find the binding pocket. The non-haem iron is located midway between the two quinones which implicates a role in electron transfer. However, its role in electron transfer between the quinones seems to

be a minor one (Kirmaier et al, 1986).

The reaction centre of Rhb. sphaeroides was also crystallised (Allen and Feher, 1984, Chang et al, 1985) and its structure has been shown to be very similar to that of Rps. viridis (Allen and Feher, 1984; Allen et al, 1986; Chang et al, 1986; Chang et al, 1985; Feher et al, 1989).

The secondary donor in Rhb. sphaeroides is an exogenous water soluble cytochrome c_2, where in the case of Rps. viridis the donor is a multihaem cytochrome which forms an integral part of the reaction centre.

The cofactors of Rhb. sphaeroides were again found to have a symmetrical arrangement, forming two branches, the L and M branches. The primary donor is a dimeric form of bacteriochlorophyll a . Each branch has an accessory bacteriochlorophyll, a bacteriopheophytin and a quinone. The non-haem iron is located midway between the two quinones.

Despite the symmetry displayed by the two branches there are certain asymmetrical features, including the side chains of the accessory bacteriochlorophyll b's , the transmembrane helix of the H subunit and the carotenoid molecule in contact with the accessory

bacteriochlorophyll b's (Deisenhofer and Michel, 1989).

There is a preferential direction of electron transfer down branch L, the reasons for this unidirectional charge separation remain uncertain although there may be a number of contributory factors. Firstly, the non-planarity of the two bacteriochlorophyll b ring systems of the special pair may result in unequal charge distribution between two components of the special pair. Secondly, there are subtle deviations in the symmetry of the L and M branches. The two branches can be rotated on top of each other and it was consequently found that the angle between the special pair and the accessory bacteriochlorophyll on the L branch differs by 6 degrees relative to that of the M branch. There are also differences in the structural order of L and M i.e. phytyl chains of the bacteriochlorophyll and bacteriopheophytin of the M subunit are partially disordered at their ends compared to those of the L subunit which are more ordered. Finally there is only 25% homology of the amino acid residues binding the cofactors in each branch.

The reason for this asymmetrical arrangement may be to increase the efficiency of energy transfer. In the situation where both electron transport chains were functional, the first excitation will result in the

transfer of one electron to the end of one pigment branch. The resulting semiquinone is unstable and its electron lost in the time range of seconds. Energy will only be stored in the form of quinol if the semiquinone receives a second electron. The probability of the second electron being funnelled into the same chain and to the same quinone is only 50%. The solution to this problem is to have two quinones in series with only the second quinone protonated and subsquently released as is the case in reaction centres of bacteria and PSII.

1.11 Amino acid sequence homology of L and M with D1 and D2

Comparison of the amino acid sequences for the L and M subunits of the bacterial reaction centre with those of D1 and D2 from PSII, revealed areas of homology between the two sets of polypeptides (Deisenhofer et al, 1985; Deisenhofer and Michel, 1989; Barber, 1987; Feher et al, 1989).

The homology was particularly strong in the region corresponding to the fourth transmembrane segment of the bacterial reaction centre. The two histidines involved in binding the Mg atoms of the special pair of the bacterial reaction centre are conserved on the D1 and D2 polypeptides . The ligands involved in

binding the non-haem iron also show a high degree of homology, since histidines D1-198, D2-298, D1-272, D2-269 are conserved. The tryptophan on D2 at 254 may equate with the tryptophan 250 on the M subunit, similarly for the alanine residues D2-261 and M-258 which suggest a likely binding site for Q_A. A Phe-255 and Ser-264 on D1 may correspond to Phe-216 and Ser-223 on the L subunit, thus forming the binding site for Q_B.

This led to the proposal that the D1 and D2 were in fact the reaction centre binding proteins of PSII in analogy with the L/M of the bacterial reaction centre.

1.12 Current model of the organisation of the PSII reaction centre complex

Experimental support for this proposal was provided by Nanba and Satoh, (1987). A pigment - protein complex consisting of the D1/D2/cyt b_{559} polypeptides was prepared by treating spinach PSII particles with the detergent Triton X-100, followed by ion-exchange chromatography. An additional band of approximately 60 kDa was also observed on polacrylamide gels. This was thought to represent an aggregate of the D1/D2 polypeptides since it co-reacted with antibodies prepared against D1/D2. The complex does not appear to have an H subunit equivalent as in the case of the bacterial reaction centre.

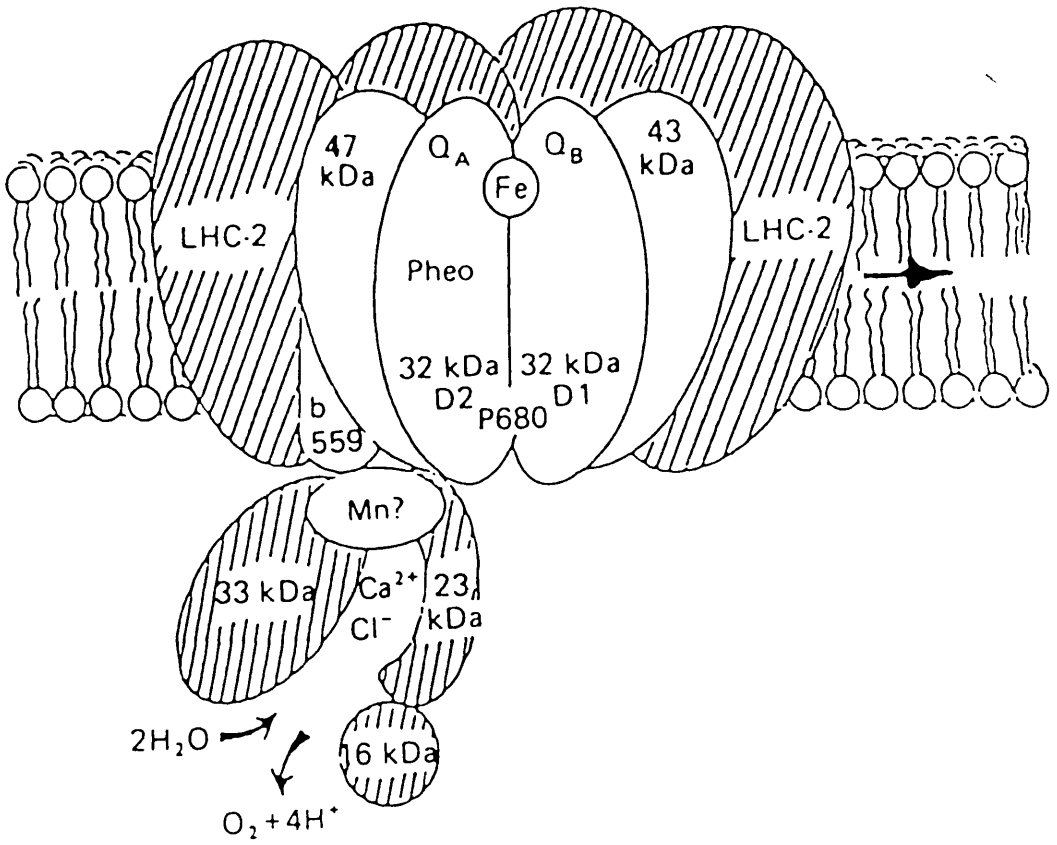

Figure 1.10 The current model of the organisation of the polypeptides of PSII.

The shaded polypeptides are nuclear encoded while the unshaded ones are products of the chloroplast genome. P680, pheophytin, Q_A, Q_B, the non-haem iron, D and Z are thought to be bound to the D1 and D2 heterodimer, as shown in the diagram. The 47 and 43 kDa polypeptides are assigned the role of binding antennae chlorophyll. The site of interaction of the 33 kDa extrinsic polypeptide is still uncertain. (Diagram from Gounaris et al, 1986).

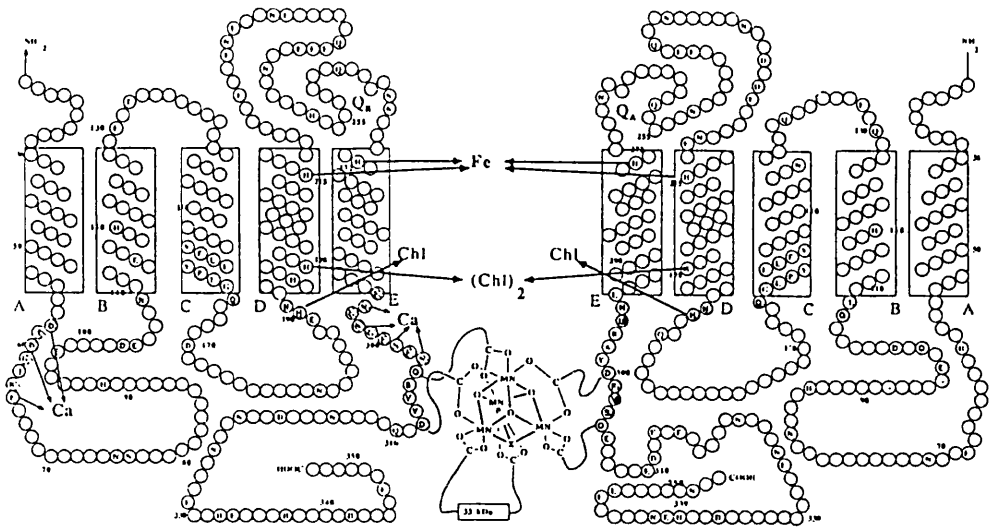

Figure 1.11 Model of the proposed binding sites of the reaction centre components of PSII

The five membrane spanning regions of D1 and D2 are shown (based on the folding model of Trebst, 1986). The locations of the histidine (H), aspartate (D), glutamate (E), glutamine (Q) and asparagine (N) residues are shown. The proposed binding site of the Mn cluster is also shown. Possible ligands involved in binding the chlorophyll special pair, the non-haem iron and those residues thought to form the Q_A and Q_B binding pockets are indicated (based on amino acid homology with the bacterial reaction centre L and M subunits). Diagram from Dismukes,1988).

The complex was demonstrated to be photochemically active by the photoaccumulation of reduced Phe in the presence of methyl viologen and dithionite. The characteristic absorption spectrum consists of negative peaks at 422, 515, 545, 682nm and positive peak at 450nm (Klimov et al, 1977). The complex also displayed the triplet esr spectrum, which results from charge recombination of Phe^- and $P680^+$, as observed in the bacterial reaction centre (Okamura et al, 1987).

It now generally accepted that D1/D2 are the reaction centre polypeptides and these polypeptides have since been extensively studied. The current model for the organisation of the PSII polypeptides is shown in Figure 1.10. Dismukes, using the D1/D2 folding model of Trebst has proposed binding sites for the reaction components in PSII (see Figure 1.11).

The subject of this thesis is the study of the electron transfer reactions of the D1/D2/cyt b_{559} complex.

CHAPTER 2

MATERIALS AND METHODS

2.1 Preparation of PSII particles from spinach and peas

Thylakoid membranes were prepared by the method of Ford and Evans (1983) from greenhouse grown pea Pisum sativum var, Feltham First and market grown spinach Spinacea oleracea . 100g of cut leaves were ground using a Braun blender for 10 s bursts, in 300mM sorbitol, 0.2mM $MgCl_2$, 20mM MES, pH 6.5 (grinding medium) and 1mM ascorbate. The homogenate was poured through nine layers of muslin and then centrifuged at 3,000 g for 5 mins. The pelleted chloroplasts were resuspended in 5mM $MgCl_2$ for approximately 30 secs to osmotically lyse them and then an equal volume of grinding medium was added. The mixture was centrifuged at 3000 g for 20 mins to pellet the thylakoid membranes.

PSII particles were then prepared by the method of Berthold et al (1981) with modifications as in Ford and Evans (1983). The thylakoid membranes were resuspended at a final concentration of 4 mg $Chl.ml^{-1}$ in 5mM $MgCl_2$, 15mM NaCl and 20mM MES pH 6.3 (resuspending medium). The chlorophyll concentration was calculated according to the method of Arnon (1949). After a dark adaptation period of 90 mins at 4°C, Triton X-100 was added to 5%

at a final thylakoid membrane concentration of 2 mg Chl.ml^{-1} . After a 25 min detergent treatment in the dark on ice, the PSII particles were pelleted by centrifugation at 40,000 g for 30 mins. The pellet was resuspended in resuspending medium plus 20% glycerol (v/v) and stored at 77K.

2.2 Preparation of PSII particles from Scenedesmus obliquus

The LF1 mutant strain of Scenedesmus obliquus was grown heterotrophically in the light in 10uM KNO_3, 5uM $ZnSO_4$, 10uM $CaCl_2$, 100 uM Na_2HPO_4, 5uM $MnCl_2$, 10uM $FeSO_4$, 300mM glucose and 2.0g yeast extract/litre. The cell suspension was incubated in an orbital shaker maintained at 30°C. The cells were harvested after approximately seven days and membranes prepared using a method based on that of Bishop (1971) and Metz and Seibert (1984).

Cells were collected by centrifugation at 3000 g for 3 mins and washed three times with resuspending medium. The washed cells were resuspended in a solution of 20% glycerol, 10mM HEPES/NaOH, 5mM PO_4^{3-}, 5mM $MgCl_2$, pH 7.5 and disrupted in a bead beater (Biospec Products, Bartlesville OK, USA), half-filled with 0.5mm diameter glass beads . The ratio of beads to

cell suspension was approximately 1.5 : 1.0.

5-10, 1 min blending periods were used with a 1 min cooling period between. The beads and homogenate were separated by passing the mixture through a piece of gauze. The thylakoid membranes were pelleted by centrifugation at 40,000 g for 30 min, and PSII prepared as for peas and spinach.

2.3 Growth conditions and preparation of PSII from Phormidium laminosum

P. laminosum was grown at 45°C, in medium D of Castenholz (Castenholz, 1970) under continuous illumination with a 150 W tungsten filament spot lamp and gassed with 5% CO_2/95% air. The cells were harvested in late growth phase. Thylakoid membranes were prepared using a method based on Stewart and Bendall, (1979).

The thylakoid membranes were incubated in 0.5% (w/v) N-dodecyl-N, N-methylammonio-3-propanesulphonate (SB12) (Serva, Heidelberg) at a chlorophyll concentration of 1 $mg.ml^{-1}$, for 40 min at 4°C (Schatz and Witt,1984). The sample was centrifuged at 100,000 g for 60 min at 4°C. The PSII enriched supernatant was concentrated by precipitation with 10% (w/v) poly(ethylene) glycol 6000, and centrifuged at 100,000 g for 20 min at 4°C. The pellet was resuspended and

washed twice in 10mM HEPES, 10mM $MgCl_2$, 5mM Na_2HPO_4 and 25% (v/v) glycerol (pH 7.5) (Buffer C) and frozen at 77K until required. The PSII particles prepared with this method evolved oxygen at a rate between 1500 to 2000 uMoles O_2 mg $Chl^{-1}.hr^{-1}$.

2.4 Isolation of the D1/D2/cyt b_{559} complex from higher plants

PSII reaction centre complexes were prepared by the method of Nanba and Satoh (1987) and modified as in Barber et al (1987). The extrinsic polypeptides were removed by incubating PSII particles with 1M Tris/HCl, pH 8.8 for 60 min at 0°C in room light, followed by centrifugation at 40,000 g for 30 min. This procedure was carried out in room light as the slow turnover of the 'S' states of the OEC increases the chances of release of the extrinsic polypeptides. The membrane pellet was resuspended in 50mM Tris/HCl buffer, pH 7.2 and then incubated in 4% Triton X-100 and 1mM orthophenanthroline, at 1 mg Chl. ml^{-1} for 90 min with stirring at 4°C. This suspension was centrifuged at 40,000 g for 30 min and the resulting supernatant loaded onto a 30cm^3 column pre-equilibrated with 50mM Tris/HCl , 0.2% Triton X-100, 30mM NaCl and 1mM orthophenanthroline, pH 7.2.

DEAE 650S fractogel
The column was washed with approximately 400ml of

the same buffer solution, until the eluate was colourless. This eluted the majority of the chlorophyll content including the 47 kDa, 43 kDa and light harvesting complex binding polypeptides. The column was then subjected to a NaCl gradient in steps from 30-120mM NaCl in the same running buffer.

The reaction centre containing fraction was usually eluted at 120mM NaCl although there were some variations. The fractions were concentrated mainly by placing each sample into dialysis tubing which was then sealed and surrounded with the hygroscopic compound, polyethylene glycol (PEG) , molecular weight 15-20,000. The fractions were assayed for purified reaction centre by using esr measurement of the spin polarised triplet spectrum and measurement of the absorption spectrum.

Dodecylmaltoside reaction centres were prepared by the same method but substituting the Triton X-100 for 4mM dodecylmaltoside in the final elution stages.

Some of the experiments described in this thesis were carried out in collaboration with Dr. Alison Telfer from Imperial College, using reaction centre preparations exchanged into maltoside buffer. In most cases, the reactions were duplicated in reaction centres prepared at both IC and UCL. Confirmation of the identification of the D1/D2 and cytochrome b_{559}

polypeptides was performed by blotting with specific antibodies (at Imperial College).

2.5 Preparation of PSII particles and reaction centre complexes from deuterated Scenedesmus obliquus

Deuterated preparations were made from Scenedesmus obliquus grown on deuterated media (a gift from Henry L. Crespi and Marion Thurnauer, Argonne National Lab. U.S.A.). PSII particles and reaction centre complexes were prepared as for Scenedesmus mentioned previously.

2.6 Spectroscopic techniques

2.6.1 Esr measurements

Esr measurements were performed with a JEOL X-band spectrometer with a 100 kHz field modulation and an Oxford Instruments cryostat. 0.3ml samples of the reaction centre preparation were placed in 3mm diameter calibrated quartz tubes, and either dark adapted for 15 min and frozen to 77K in the dark or illuminated at 4°C for the time stated in the text and subsequently frozen in the light. Illumination at 4°C and in the cryostat at cryogenic temperatures was provided by a 150W white light source (400u einsteins.$m^{-2}.s^{-1}$) directed by a light guide.

Quantification of esr radicals was done by double integration of the first derivative signal taken at

non-saturating microwave powers. Approximately four spectra were recorded of each esr signal, and averaged to reduce the noise to signal ratio. The spectra were then transferred to a Tektronix 4051 computer for plotting.

To prepare the anaerobic samples, esr tubes containing reaction centre samples were flushed out with oxygen-free nitrogen gas and then the following additions made in the indicated order: glucose (5mM), catalase (200ug. ml^{-1}) and glucose oxidase (100ug. ml^{-1}),(McTavish et al,1988).

Silicomolybdate (SiMo ; $H_4SiMo_{12}O_{40}$) was purchased from Pfaltz and Bauer Inc. The electrochemistry of SiMo was investigated on a freshly made anaerobic solution of SiMo in 50mM Tris/HCl pH 8.0. using a mercury dropping electrode. Ten scans of -2.0V to +2.0V at 500mV/s were performed. Several weak and strong troughs were seen during reduction, the significant steps for our experiments occurring at approx. +300mV attributed to the reduction of Mo (VI) to Mo (V). The SiMo as delivered contains a mixture of Mo (V) and Mo(VI) forms, as determined by esr.

2.6.2 Laser flash spectroscopy

Absorption changes at 820nm were measured at room temperature in a 1cm path-length cuvette. A purpose

built single-beam spectrophotometer was used (Ford and Evans, 1985). A type PIN 10-D photodiode (United Detector Technology, A, U.S.A.) was used as the detector, coupled to a low-noise diferential amplifier (EG/G Princeton Applied Research, Model 113). The resolution time limit was approximately 5 us. The measuring beam was provided by a 250 W tungsten filament lamp powered by a Coutant direct current supply (Model ASC3000 PC).

Signals were recorded with a Datalab 920 transient recorder and averaged with a Datalab 4000B signal averager. Samples were excited at 0.5 Hz at 337nm with an 800ps flash supplied by a N_2 laser (LN 1000, Photochemical Research Associates, Inc.). The samples were suspended in either 0.2% Triton X-100, 120mM NaCl and 50mM Tris-HCl , pH 8.0 or 4mM maltoside, 120mM NaCl and 50mM Tris-HCl, pH 8.0.

2.6.3 Absorption spectroscopy

Absorption spectra of column fractions were performed at room temperature using a Phillips PU 8740 UV/VIS scanning spectrometer. Scans were run between 350nm and 720nm using a 1cm path length 1ml quartz cuvette.

2.7 Polyacrylamide gel electrophoresis

The polypeptide composition was determined using vertical SDS-PAGE by the method of Laemmli (1970) and Chua and Benoun (1975). 12.5% slab gels and 10-22% gradient gels were run.

2.7.1 12.5% slab gels

The separating gel was a 12.5% (w/v) acrylamide, 0.32% (w/v) bis acrylamide, slab gel containing 0.4 % (w/v) SDS and 0.375M Tris-HCl, pH8.8, polymerised with 0.06% (w/v) freshly made ammonium persulphate and 100ul N,N,N'N'-tetramethylethylenediamine (TEMED). A 1-2 cm 6% (w/v) acrylamide stacking gel, containing 0.16% (w/v) bis acrylamide, 0.4% (w/v) SDS and 0.125M Tris-HCl, pH 6.8 was polymerised in the same manner onto the separating gel.

Samples were solubilised in 4% (w/v) SDS, 5% mercaptoethanol, 5% glycerol, 0.2 % bromophenol blue and 90mM Tris-HCl, pH 6.8 for 30 mins at room temperature. The running buffer used consisted of 0.375 M Tris-HCl, 0.4 M glycine and 0.1% (w/v) SDS pH 8.3. The gel was run at 30 mA for approximately 3 hrs. The gels were stained with Coomassie Brilliant Blue R250 in 50 % methanol, 10 % acetic acid for 2 hrs and then destained with 10 % methanol, 10 % acetic acid.

2.7.2 10 -22 % gradient gel

Gradient gels were run using the method based on Chua and Benoun (1975). The separating gel was a 10 -22 % acrylamide, 0.25 -0.58 % bis acrylamide gradient slab gel containing 0.1 % (w/v) SDS, 80 mM Tris-HCL, pH 9.18 and polymerised with 0.02 % ammonium persulphate, 10 ul TEMED. The stacking gel consisted of 4 % (w/v) acrylamide, 0.1 % (w/v) bis acrylamide, 0.1 % (w/v) SDS and 80 mM Tris -sulphate , pH 6.1 and was polymerised with 0.06 % ammonium persulphate, 10 ul TEMED.

The samples were solubilised in the same buffer as for the 12.5 % (w/v) acrylamide slab gels. The upper reservoir buffer was 2mM Tris-borate, pH 8.64, containing 0.1% (w/v) SDS. The lower reservoir buffer was 100mM Tris-HCl, pH 9.18. All other procedures were as for the non- gradient gels.

2.8 ELECTRON SPIN RESONANCE (ESR)

The main technique used in this thesis was low temperature electron spin resonance (esr) or electron paramagnetic (epr) spectroscopy. Esr is a technique which permits the detection of paramagnetic species i.e. molecules with unpaired electrons.

Figure 2.1a shows a block diagram of an esr spectrometer. Electromagnetic waves (microwaves) are generated and are then led through a microwave guide to the sample compartment (cavity), and pass through the sample to the detector. The sample cavity holds the sample in the proper orientation for exposure to the microwaves entering from the waveguide and also holds the sample between the magnetic poles of the magnet. The sample is thus exposed to both fields. The detectors and recorders measure the net absorption of energy at resonance and record the signal. In the case of our esr spectrometer, the recorder was connected up to a PDP-11 mini computer. Actinic light, either continuous or flash illumination can be provided through the front of the cavity.

As with other forms of spectroscopy, electromagnetic radiation is used to induce a change in the energy state of the sample. In the case of optical spectroscopy, the radiation promotes electrons from their ground state to electronic excited states. However, in esr spectroscopy, the electromagnetic radiation is not used to change the electronic state of the system but its spin state.

An unpaired electron has a magnetic moment associated with its electron spin. The spin of the unpaired electron is assigned the formal value 1/2.

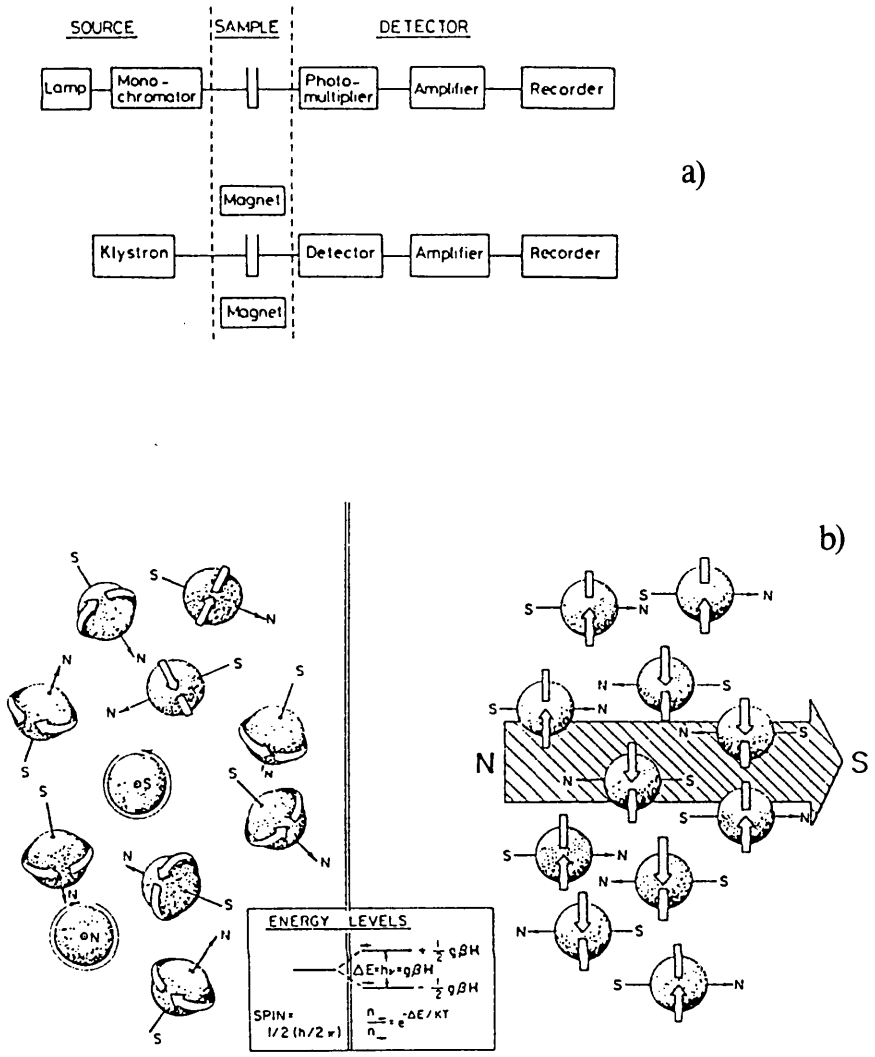

Figure 2.1a. Block diagram of an esr spectrometer (below) compared with an absorption spectrophotometer (above). In the case of the spectrophotometer, a beam of light passes through the sample. The changes in transmitted light are detected and recorded. In the esr spectrometer, a beam of microwaves passes through the sample in a magnetic field and changes of intensity are measured. In the Jeol FE1X esr spectrometer, the microwave source was a Gunn-diode as opposed to a Klystron. (Diagram from Evans, M.C.W. 1977).

Figure 2.1b. Molecules with an unpaired electron can interact with a suitable magnetic field. They can be oriented either parallel or antiparallel to the field, which segregates them into two subsets with a small energy difference. If electromagnetic waves of appropriate frequency (resonance frequency) are now supplied, energy transitions can occur. At resonance, there are more parallel than antiparallel electrons and hence a net absorption of energy is observed. This is detected and amplified to give the esr signal observed. (Diagram from Swartz et al, 1972).

Under normal conditions, the free radicals and their spin magnetic moments are randomly oriented and are in the same average energy state. However, if an external magnetic field is applied to a paramagnetic sample, the spins become oriented either parallel or antiparallel to the direction of the field (Figure 2.1b) . The energy of the spin state is lower for the parallel than the antiparallel direction and unaltered when it is perpendicular to the magnetic field.

The magnetic field can therefore split a single energy state into two or more, each subset having a very small energy difference ΔE. Energy transitions can now take place, whereby the orientation of the electron spins will change. This process can occur if the spins, which are lined up by the applied magnetic field, are also coupled with electromagnetic waves of appropriate frequency (high frequency microwaves). If the quantum energy of the high frequency field corresponds to the energy difference ΔE between the parallel and antiparallel electron magnetic moments, transitions will occur. The electrons can resonate with the radiation field, i.e. they can take energy from it where the electron jumps from a lower to a higher energy level or give energy to it,resulting from the electron dropping to a lower energy level.

As already mentioned, a state can be split into two or more by a magnetic field. In the case of organic radicals where the spin=1/2, two interactions with the magnetic field are allowed, parallel and antiparallel and therefore the state is split into two in the presence of a magnetic field to form a doublet (Figure 2.2a).

When the spin =1 or unity as in the case of an excited molecule with two parallel spins, three kinds of interaction are allowed, parallel, antiparallel and perpendicular. The state is split into three by the magnetic field and this kind of state is called a triplet state (Figure 2.2b).

When the spin is zero, for example as with organic molecules in their ground state, the magnetic field has no effect and the state is referred to as a singlet state.

If we take the example of the spin = 1/2 system, the difference in the energy levels of the two populations formed in an external magnetic field is:

$$\Delta E = h\gamma = g\beta H$$

where h is Plank's constant and g is the frequency of radiation used to induce transitions between the two levels, g is the electronic g value, B is the Bohr

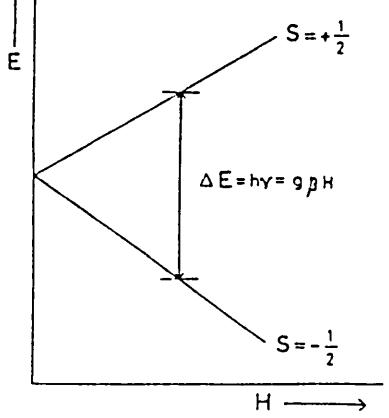

a)

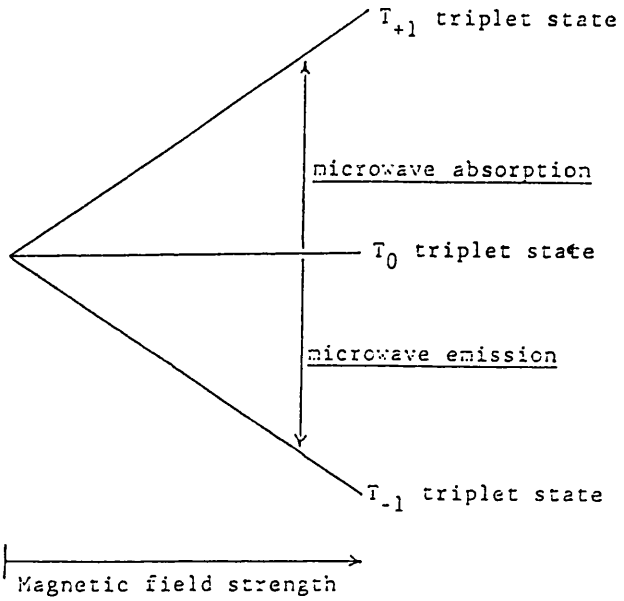

b)

Figure 2.2a. In the case of a spin = 1/2 state, (i.e. a molecule with one unpaired electron), the state is split into two in the presence of a magnetic field. The energy difference between the two states is linearly related to the magnetic field strength. Resonance occurs when at a given field, microwave radiation is supplied.

Figure 2.2b. When the spin=1, as in the case of an excited molecule with two parallel spins (e.g. radical pair recombination), three energy states are formed. The T_0 state has no net magnetic moment in the direction of the field. The part- absorption and part-emission peaks of the triplet signal are due to the transitions T_0 to T_{+1} and T_0 to T_{-1} respectively. (Diagrams from Swartz et al, 1972).

magneton and H is the applied magnetic field. As the energy difference between the two states is very small, there is only a slight preference for the lower spin state. In practice relatively low microwave powers are necessary (uW or mW) in order to allow the spin lattice relaxation to counteract the tendency of the radiation to equalise the two populations.

2.8.1 Presentation of spectra

Esr spectra can be obtained by either changing the microwave frequency at a constant magnetic field or by scanning the magnetic field at a fixed wavelength (Figure 2.3a). In practice, the latter procedure is more convenient. Resonance occurs at a specific magnetic field strength, called the 'g' value. Esr spectra are normally presented as the first derivative of the absorption spectrum. This is as a result of the application of a technique known as phase sensitive detection, whereby a small a.c. magnetic field (100 kHz) is superimposed on the d.c. field . The signal to noise ratio is greatly improved. Absorption spectra can be obtained by integrating the first derivative spectrum, but as esr absorption spectra are often too broad and indistinguishable, they are rarely presented in this form.

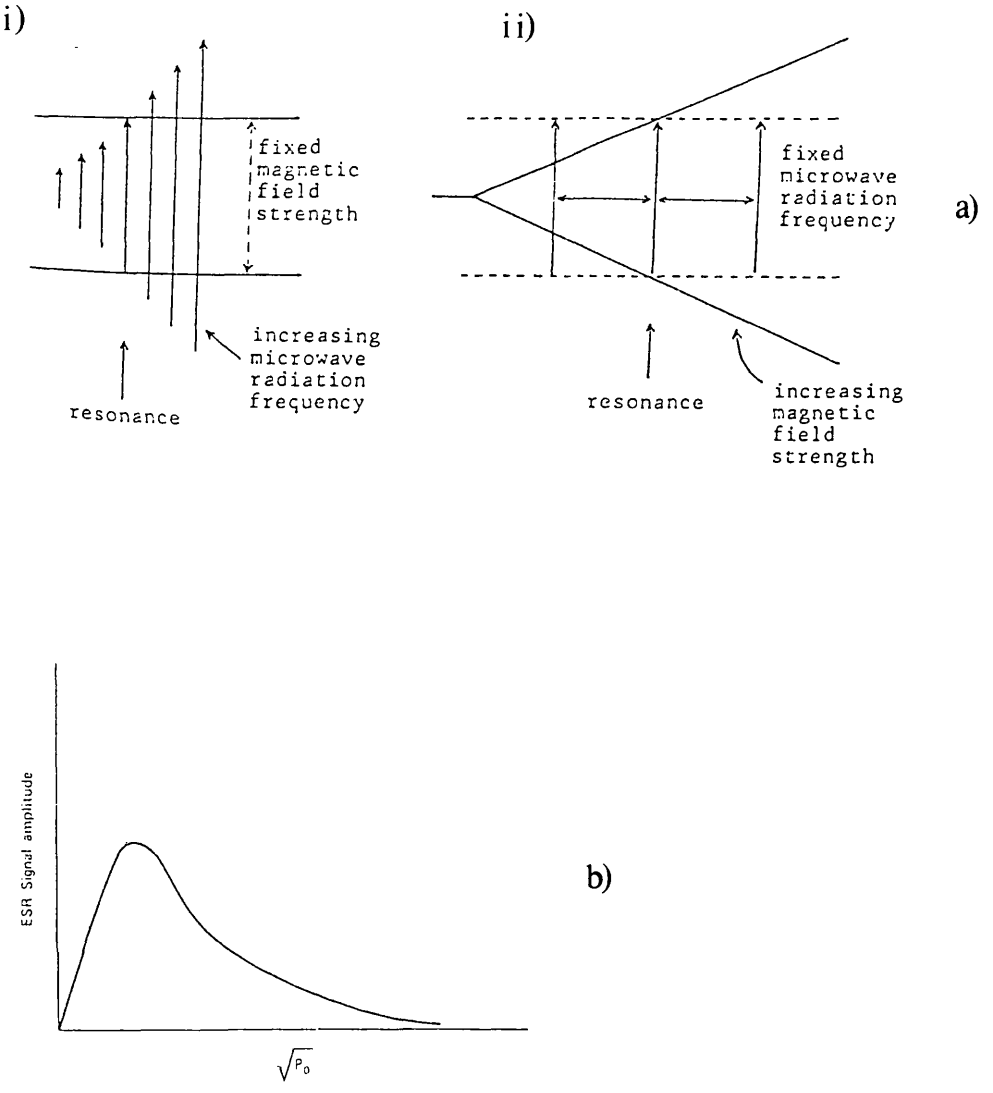

Figure 2.3a An esr spectrum can, in theory, be obtained by one of two methods i) changing the microwave frequency at a constant magnetic field and resonance frequency, and the resonance frequency where microwave absorption occurs monitored or ii) the microwave frequency can be kept constant and the magnetic field scanned until resonance occurs. In practice, method ii) is used.

Figure 2.3b Variation of esr signal amplitude with microwave power (P_o). (Diagrams from Swartz et al, 1972).

2.8.2 Low temperature esr

The spin lattice relaxation effect refers to the interaction of the paramagnetic ion with its surrounding environment, and the spin-spin relaxation describes the interaction of the ion with other paramagnetic species to a distance of about 1nm . Both these effects can alter the width of the absorption peak. At higher temperatures, these relaxation rates are fast and as a result the absorption lines can be very wide and difficult to resolve. Sharper lines are obtained at lower temperatures as the relaxation rates are slower. This is one of the main reasons for using low temperature esr.

2.8.3 Microwave power saturation

The size of an esr signal is proportional to the square root of the microwave power ($\sqrt{P}$) up to the saturation point (Figure 2.3b). This is because the rate of microwave transitions between the two energy levels is proportional to $\sqrt{P}$. Beyond the saturation point, further increases in power actually decrease the signal size as the radiation induced transfer results in the a net increase in the population of the upper energy level until the difference between the two populations is very small. As a result, the difference between the microwave absorption and the stimulated emission is too

small to detect. The power saturation effect increases with decreasing temperature. It is therefore important to find the optimum combination of power and temperature for each signal. The power saturation can be used to distinguish between signals with similar spectra.

2.9 Triplet formation by radical pair recombination

The spin polarised triplet is indicative of a radical pair charge recombination. Triplet states have two unpaired electrons which couple together to form an S=1 state. In a magnetic field this state can be split into three energy levels T_0, T_{-1} and T_{+1} (Figure 2.2b). The T_0 state has no net magnetic moment in the direction of the applied magnetic field and therefore the energy of this state is independent of the magnetic field strength.

Charge separation makes the two unpaired electrons on P^+ and A^- essentially independent of each other and their spins begin to dephase, i.e. they no longer precess around the direction of the applied magnetic field with the same frequency. The recombination of the two radicals can result in the formation of one of two states. If the electrons are antiparallel (i.e. one aligned with the direction of the magnetic field and

one against it), then recombination results in a singlet state. If however, the charges recombine when the spins are parallel, the T_0 state is formed. At very low temperatures where spin relaxation is quite slow, differential entry / exit rates into / from the three magnetic levels of the triplet state, results in spin polarisation. This spin polarisation results in the esr absorption and emmission signals, with six lines observed symmetrically arranged around g=2 . The triplet signal consists of both absorption and emmision peaks and these represent the T_0 to T_{+1} and T_0 to T_{-1} transitions respectively. The observation of a spin polarised triplet is characteristic of the radical pair mechanism and requires charge separation to take place.

CHAPTER 3

Isolation of the PSII reaction centre complex

3.1 Introduction

It is now accepted that the D1 and D2 polypeptides bind the reaction centre components in analogy with the L and M subunits of the bacterial reaction centre . Experimental support for this proposal came from the isolation of the complex consisting of the D1, D2 polypeptides, the two apoproteins of cytochrome b_{559} and a 60 kDa aggregate (Nanba and Satoh, 1987). The copurificaton of a small molecular weight polypeptide has also been reported in the D1/D2/cyt b_{559} complex (Webber and Gray, 1989; Ikeuchi and Inoue, 1988).

The pigment composition of the reaction centre complex was determined by Nanba and Satoh (1987) using HPLC analysis. The complex consisted of five chlorophyll a, two pheophytin a , one beta carotene and one to two cytochrome b_{559} haem(s) (based on an extinction coefficient of 15 $mM^{-1}.cm^{-1}$).

The complex has been shown to be photochemically active in a number of ways . The spin polarised triplet has been observed (Okamura et al ,1987; Demetriou et al, 1988) as has the photoreduction of pheophytin (Nanba and Satoh, 1987; Barber et al, 1987). Electron

transport from the artificial electron donor, diphenylcarbazide (DPC) to the artificial electron acceptor silicomolybdate (SiMo) has also been used as an assay of activity (Barber et al, 1987; Chapman et al, 1988).

The complex prepared using the Nanba and Satoh procedure is highly labile. Akabori et al (1988) reported an 85% loss in triplet yield following the incubation of the complex at 25°C for 5 hrs. Similarly, Chapman et al (1988) observed a reduction in rate of light induced electron transfer activity in the complex at temperatures above 4°C.

The loss of activity has been associated with a shift to shorter wavelengths of the major peak in the 676nm region of the characteristic room temperature absorption spectrum (Telfer and Barber, 1989; Chapman et al, 1988; Seibert et al, 1988). The detergent, Triton X-100 has been proposed to be responsible for this instability and attempts to increase the stability of the complex have been based on the incorporation of milder detergents in the isolation procedure. Akabori et al (1988) have recently shown that if the Triton X-100 is exchanged for a milder detergent such as n-octyl glucopyranoside, the complex is photochemically more stable. Similarly, increased stability of the

complex occurs when the TX-100 is exchanged for dodecylmaltoside, either immediately after isolation of the complex (Seibert et al, 1988) or as part of the chromatographic method (Ghanotakis et al, 1989).

Following the isolation of the reaction centre complex from spinach PSII (Nanba and Satoh 1987), the complex has since been prepared from peas (Barber et al, 1987) , the alga Scenedesmus (Demetriou et al, 1988) and the cyanobacterium Synechocystis (Gounaris et al, 1988).

Cyanobacterial electron transport is comparable to that of higher plants, in terms of electron transfer components, on both the electron acceptor and donor side. The cyanobacterium Phormidium laminosum has been shown to be a good source for the isolation of PSII with high rates of oxygen evolution (Stewart and Bendall, 1979) .

The LF1 mutant of the alga Scenedesmus obliquus has provided much information on the role of D1 in binding the Mn complex of the OEC (Metz and Bishop, 1980; Metz et al, 1988). Thylakoid membranes isolated from the LF1 mutant bind approximately 40% of the Mn bound by wild-type membranes (Metz, 1980) and the mutant does not evolve oxygen (Metz, 1980). This was attributed to the loss of a processing step with D1

resulting in a large polypeptide unable to bind Mn or the polypeptides involved in water oxidation (Metz and Seibert, 1984; Rutherford et al, 1988).

The D2 proteins are the same in both the mutant and the wild type but the unprocessed D1 protein of the LF1 mutant has an apparent moleculer weight about 2 kDa larger than that of the normal protein. In the presence of added electron donors, PSII activity can be restored in the mutant (Metz et al, 1985).

In this Chapter, the isolation of reaction centre complexes from higher plants (spinach and peas), the alga Sc. obliquus and the cyanobacterium P. laminosum is reported. The polypeptide composition and spectroscopic characteristics of these complexes were investigated.

Results

3.2 Preparation of reaction centre complexes from spinach and pea PSII particles.

Detergent treated PSII particles were loaded onto an ion-exchange column. Fractions were collected at increasing NaCl concentrations as described in the Materials and Methods. The addition of 1mM ortho-phenanthroline (OP) throughout the purification procedure increased the yield of reaction centre

SENATE HOUSE, MALET STREET WC1E 7HU
Tel 01-636 8000 · Fax 01-636 0373

With the compliments of
Examinations Division

complexes. This was thought to be due to the OP facilitating the release of quinones and/or the non-haem iron. As the 47 kDa polypeptide has been linked with the binding of Q_A/Q_B (Yagamuchi et al, 1988) , this treatment may also increase the release of the 47 kDa polypeptide.

Figure 3.1 shows the room temperature absorption spectra of the four major fractions eluted at 40, 60, 90 and 120mM NaCl concentrations. An enrichment in the D1/D2/cyt b_{559} complex in the fractions was determined by the ratio of the two peaks in the blue region of the absorption spectrum. The fraction containing the reaction centre complex was indicated by a predominant peak at 417nm relative to the 432nm peak (Figure 3.1d). The 417nm peak is due to pheophytin a (Fuijita et al, 1978) and the Soret band of oxidised cytochrome b_{559}, (Babcock et al, 1985) while the 432nm peak is the Soret band of chlorophyll a. The major peak at 417nm is therefore indicative of a higher concentration of pheophytin and/or cytochrome b_{559} relative to chlorophyll a concentration.

The 40, 60 and 90mM fractions were contaminated with the 47 and 43 kDa polypeptides. They subsequently showed a major peak at 432nm due to chlorophyll a (Figure 3.1 a-c).

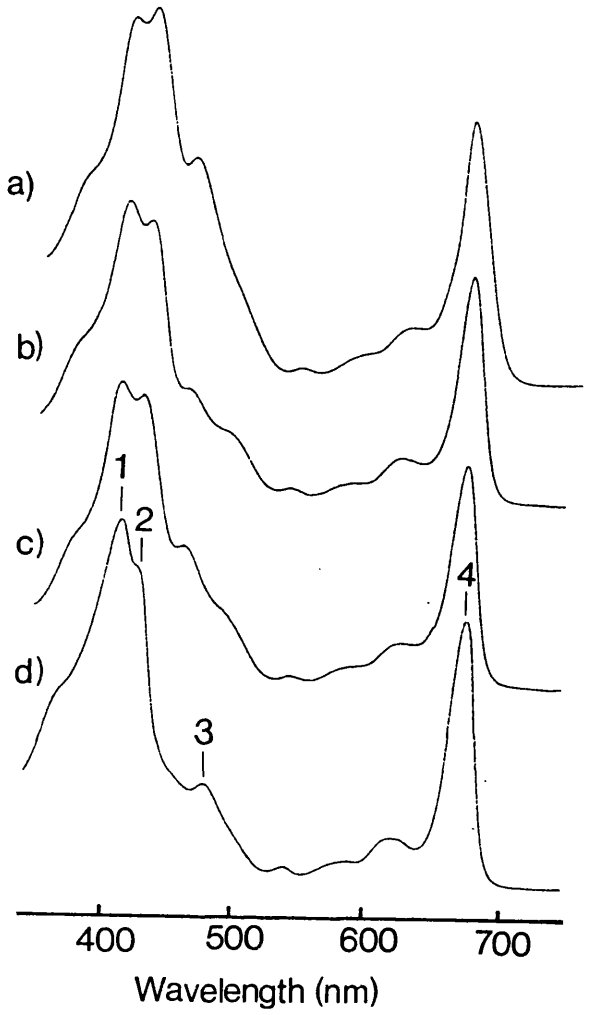

Figure 3.1. Absorption spectra of the fractions eluted off the DEAE ion-exchange column at increasing NaCl concentrations.

Spectra a-d represent the fractions eluted at 40,60,90 and 120mM NaCl. An enrichment in the reaction centre complex (in this case pea) was indicated by a predominant peak at 417nm (peak 1) relative to the peak at 432nm (peak 2). The presence of carotenoid is indicated by an absorption shoulder at approx. 480nm (peak 3). The chlorophyll a absorption peak in the red region was observed at 673 -676nm (peak 4).

3.2.1 Polypeptide composition of the PSII reaction centre complex

The polypeptide composition of spinach PSII is as shown in lane 3, Figure 3.2. Of the intrinsic polypeptides, the 47 and 43 kDa and the two apoproteins of cytochrome b_{559} are visible but the D1 and D2 proteins are obscured. The three polypeptides of the oxygen evolving complex removed as a result of the tris-wash are shown in Figure 3.2, lane 1.

The polypeptide composition of the reaction centre complex is shown in Figure 3.2, lane 2. The two bands in the 30-32 kDa region are attributed to D1 and D2. The aggregate and the two apoproteins of cytochrome b_{559} are also present. This was confirmed by blotting with specific antibodies (performed at Imperial College). No polypeptides corresponding to the 47 and 43 kDa subunits were observed.

3.2.2 Pigment composition of the PSII reaction centre complex

The ratio of the number of chlorophyll *a* to cytochrome b_{559} molecules of the reaction centre complex was estimated. The chlorophyll *a* concentration was calculated from the amplitude of the absorbance peak at 675nm and an extinction coefficient of

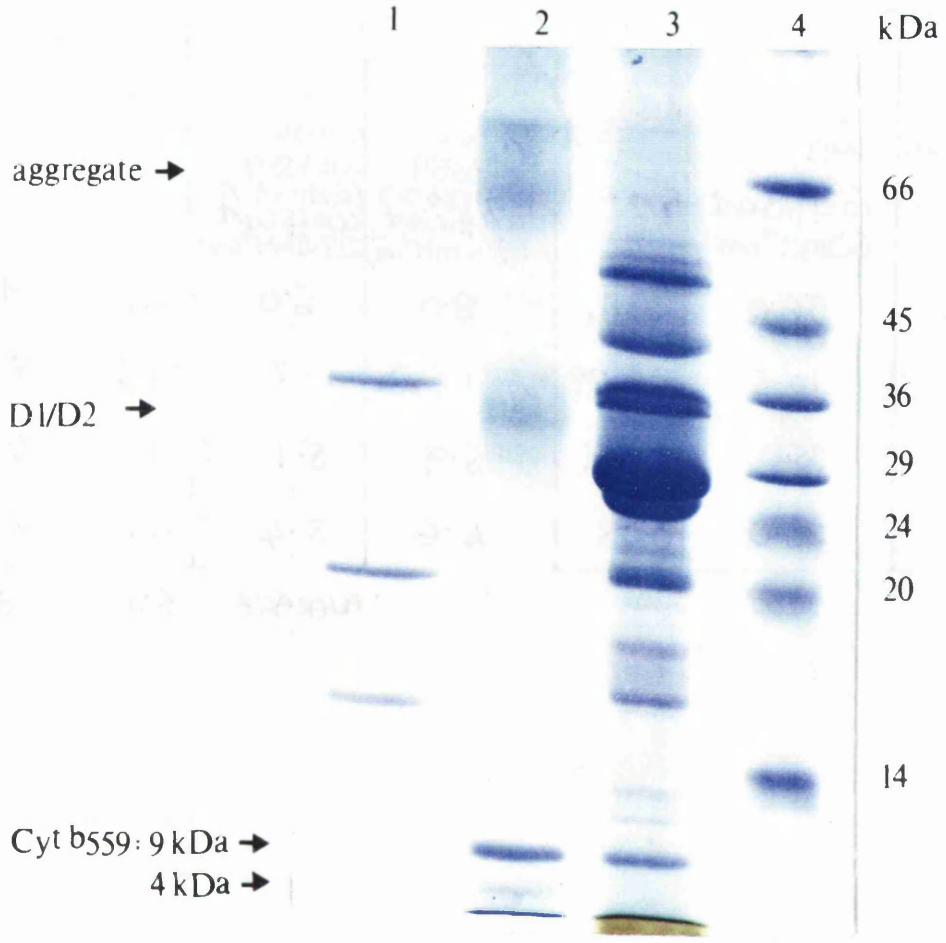

Figure 3.2. 12.5% polyacrylamide slab gel of the polypeptide constituents of PSII particles and PSII reaction centres

The polypeptide composition of pea PSII particles is shown in Lane 3 .The broad band at approximately 24-29 kDa represents the LHCII polypeptides. The 47 and 43 kDa intrinsics and the two apoproteins of cytochrome b_{559} are visible but D1 and D2 are obscured. The three polypeptides of the OEC removed as a result of the tris wash are shown in Lane 1. The profile of the reaction centre containing fraction (Lane 2) reveals a diffuse band of 30 kDa (attributed to D1/D2). An aggregate of 60 kDa and the two apoproteins of cytochrome b_{559} are also visible. The molecular weight markers are as shown in Lane 4. The gel was prepared and run as described in the Materials and Methods.

CHLOROPHYLL a		CYTOCHROME b559			RATIO CHL a : cyt b559	
Abs 675nm	μmoles Chl a (Extinction coefficient 60 $mM^{-1}cm^{-1}$)	Abs 559	i) μmoles cyt b559 (extinction coefficient 17.4 $mM^{-1}cm^{-1}$)	ii) μmoles cyt b559 (extinction coefficient 23.4 $mM^{-1}cm^{-1}$)	i)	ii)
3.35	56.0	0.14	8.0	6.0	7:1	9:1
0.63	10.5	0.028	1.6	1.2	6.5:1	8.8:1
2.10	35.0	0.12	6.9	5.1	5:1	6.9:1
1.40	23.0	0.08	4.6	3.4	5:1	6.8:1
				AVERAGE	6:1	8:1

$60mM^{-1}.cm^{-1}$(Barber et al, 1987).

The amount of cytochrome b_{559} was quantitated by recording the dithionite-reduced minus ferricyanide oxidised difference in absorbance at 559nm. Miyazaki et al (1989) have calculated a value for the extinction coefficient of cytochrome b_{559} of 23.4 $mM^{-1}.cm^{-1}$. However, Dekker et al (1989a) report a value of 17.4$mM^{-1}.cm^{-1}$. An estimate of the cytochrome b_{559} concentration was made using both these values. The pigment composition of the Triton X-100 reaction centre complexes was approximately 6-8 chlorophyll a : 1 cytochrome b_{559}, using the extinction coefficients 23.4 and 17.4$mM^{-1}.cm^{-1}$ respectively, (see table opposite).

The present model of the PSII reaction centre is based on analogies with the well characterised bacterial reaction centre which has 4 bacteriochlorophyll a per 2 bacteriopheophytin. However, the pigment composition of the PSII reaction centre may not follow that of the bacterial reaction centre. Dekker et al (1989a) have proposed that the reaction centre of PSII may contain more than 4 chlorophyll a molecules. They suggest that the Triton X-100 prepared reaction centres do not represent the in vivo situation and that exposure to Triton X-100 treatment is responsible for the removal of 2-4 pigments from the complex. The pigment stoichiometry of the reaction centre complex would be expected to vary

with different isolation procedures. The exact pigment composition of the intact PSII reaction centre requires further investigation.

3.2.3 Photochemical activity of the reaction centre complex

The photochemical activity in the column fractions was assessed by the detection of the spin polarised triplet (Figure 3.3) (Okamura et al, 1987: Rutherford et al, 1981). The AEEAAE polarisation pattern of the spectrum is interpreted as originating from the radical pair recombination between $P680^{+}$ and Phe^{-} (Rutherford et al, 1981). The line positions are described by the zero field splitting parameters, given as |D| and |E|.

The characteristic zero field splitting parameters were estimated to be |D| = 0.0297 cm^{-1} and |E| = 0.0041 cm^{-1}. The |D| and |E| values are consistent with a monomeric chlorophyll a. The spin polarised triplet did not originate from non-functional chlorophyll a since chlorophyll a molecules in solution have a polarisation pattern of EEE AAA (Thurnauer et al, 1975).

The reaction centre preparation was also characterised by the lack of major changes at g=2 upon illumination at 4K (Figure 3.3). Fractions containing

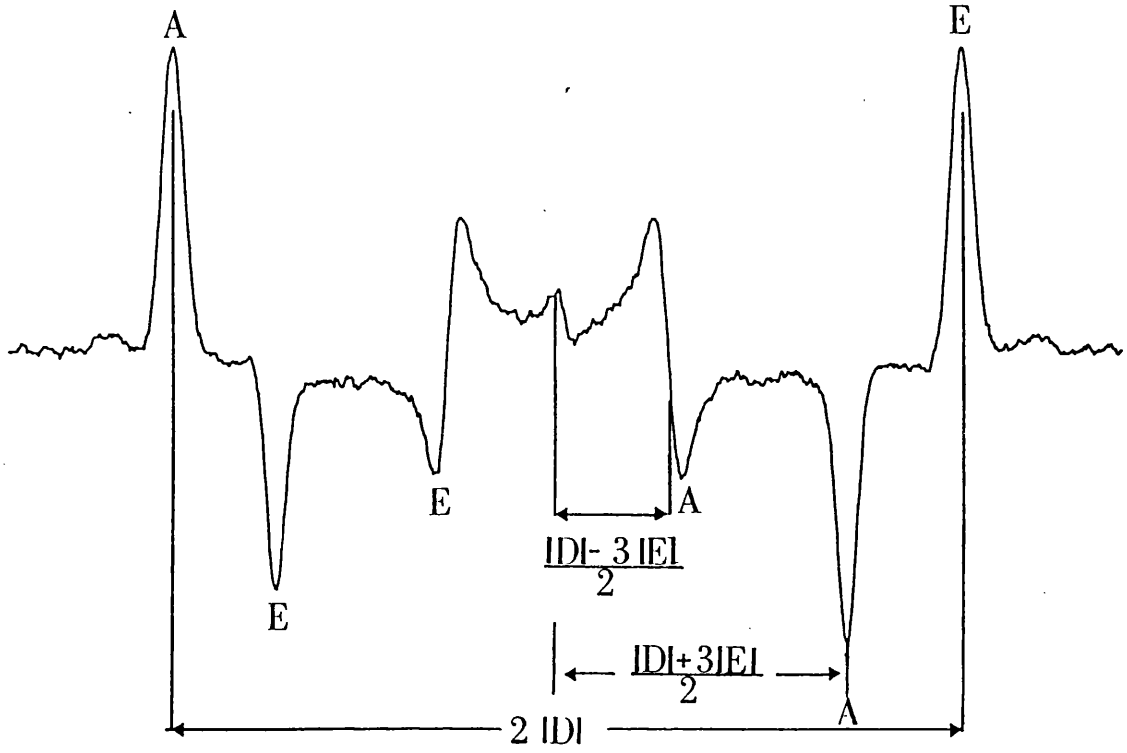

Figure 3.3 Esr spectrum of the spin polarised triplet observed in spinach reaction centre complexes (120 mM NaCl fraction).

The signal shown is a light minus dark difference spectrum. The triplet, with its absorption and emission peaks, is characteristic of a radical pair mechanism. The six peaks are observed symmetrically around g=2. The positions of the peaks are given by the zero field splitting parameters, |D| and |E|. |D| and |E| give information on the magnetic environment and the interactions of the two unpaired electrons that give the triplet its spin s=1. They also give an indication of whether an electron is delocalised over more than one molecule. Esr conditions; Microwave power 25uW, modulation width 1.25mT and temperature 4K.

the reaction centre polypeptides, but contaminated with the 43/47 kDa polypeptides (60 and 90mM NaCl fractions) did not form the spin polarised triplet, but gave changes at g=2 upon illumination. This indicates that these larger complexes have different electron transfer properties than the reaction centre complex itself.

3.3 Reactions centre complexes prepared from the alga Scenedesmus

Reaction centres were prepared from the LF1 mutant of Scenedesmus using the Triton X-100 method. The LF1 mutant is reported to have a D1 polypeptide 1.5 kDa larger than the D1 of the wild type. This was not evident using our SDS-PAGE system (Figure 3.4, lane 2). However, the mutant would not grow phototrophically, indicating that a lesion in photosynthetic ability was present. This effect may therefore be due to chosen SDS-PAGE system. The spin polarised triplet was observed in the LF1 reaction centre. The zero field splitting parameters of the triplet were the same as for the higher plant reaction centre preparation. The absorption spectrum also resembled that of the higher plant reaction centres.

3.4 Reaction centres prepared from P.laminosum

Figure 3.5, lane 2 shows the polypeptide composition of reaction centres prepared from P.

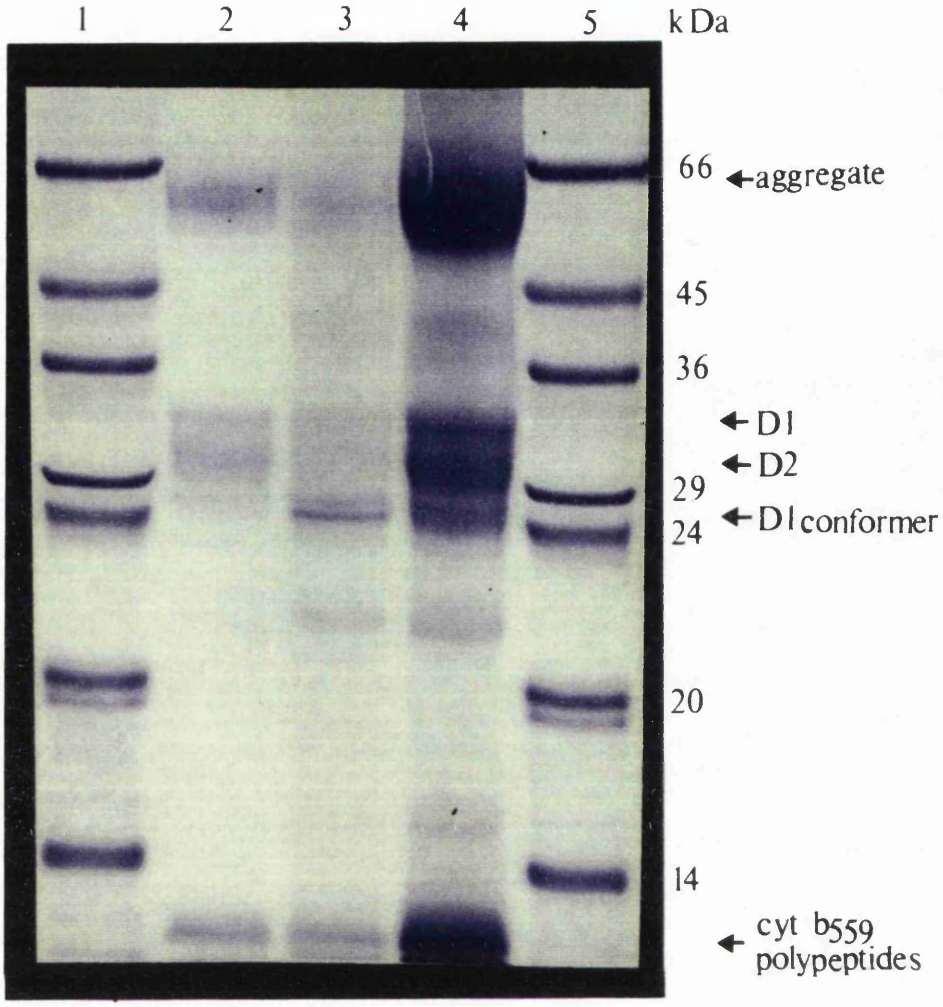

Figure 3.4. 12.5% polyacrylamide slab gel of the polypeptide composition of the D1/D2/cyt b_{559} complex of the LF1 mutant of Scenedesmus obliquus.

The reaction centre complex prepared from the LF1 mutant is shown in lane 2. For comparison, the profile of reaction centres of pea (lane 3) and spinach (lane 4) are also shown. In the absence of urea in the gel buffers, D1 runs with a higher molecular weight than D2 (the reverse is true in the presence of urea) (Barber et al, 1987). Hence, the three bands observed in the 30 kDa region represent the D1 polypeptide followed by D2. The third lower molecular weight band is the D1 conformer. A low level of contamination with other polypeptides is evident in Lanes 3 and 4. The molecular weight markers are in Lanes 1 and 5. The gel was prepared and run as described in the Materials and Methods.

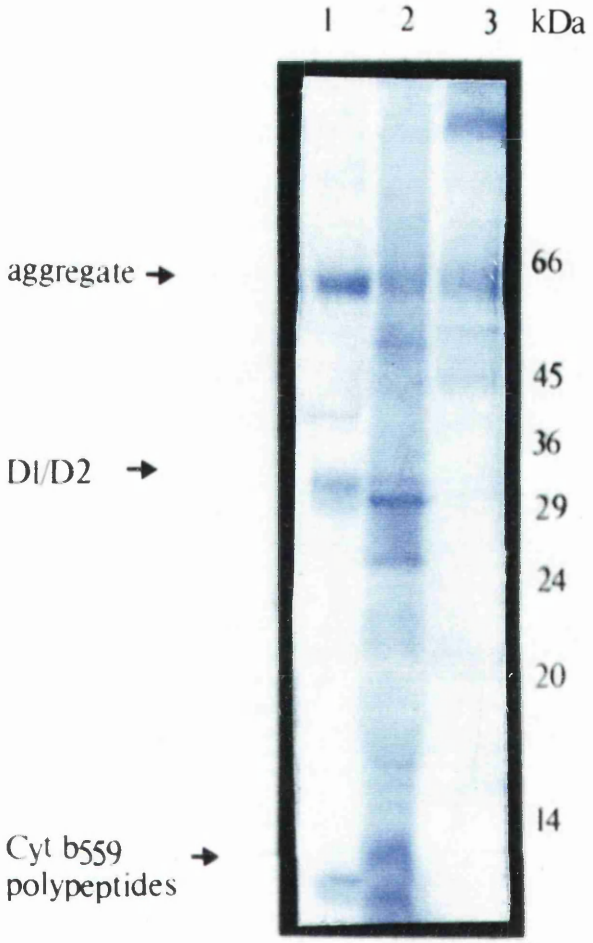

Figure 3.5. 10-22% gradient gel showing the polypeptide composition of the P.laminosum reaction centre complex and a PSII complex from deuterated Scenedesmus.

The polypeptides of the P.laminosum reaction centre preparation are shown in lane 2. The speculative reaction centre polypeptides are indicated. Lane 1 shows the profile of a higher plant reaction centre complex for comparison. Lane 3 shows the pigment-protein complex isolated from deuterated Scenedesmus PSII. The gel was prepared and run as described in the Materials and Methods.

laminosum using the Triton X-100 method. There are equivalent bands on SDS-PAGE which compare to those seen in the higher plant reaction centre. However, there are also a number of other bands present. Two protein bands in the 30 kDa region are visible which may represent the D1/D2 polypeptides. The 60 kDa band may represent the aggregate form of the D1/D2 polypeptides and two bands of approximately 12 and 4 kDa may be the two apoproteins of cytochrome b_{559}. The identity of these proteins would need to be confirmed by antibody binding studies.

The spin polarised triplet was observed in this preparation with identical zero field splitting parameters to that of the higher plant reaction centre complex. However, the complex contained a greater number of chlorophyll a molecules (8 chlorophyll a : 1 cytochrome b_{559})^ using an averaged extinction coefficient. Further work is required to refine the cyanobacterial reaction centre preparation.

Recently, Gounaris et al (1988) have reported the isolation of the reaction centre complex from the cyanobacterium, Synechocystis . The complex was shown to photochemically active. However, the molecular weights of the complex as resolved with SDS PAGE were found to be 50 kDa (aggregate), 38 kDa (D1) and 34 kDa (D2). It was also found that the cytochrome b_{559}

polypeptides were seldom resolved. This was not the case with P. laminosum. More work is required to determine the stoichiometry of the prosthetic groups and molecular weights of the polypeptides of the cyanobacterial reaction centre.

3.5 The preparation of a reaction centre complex from deuterated Sc. obliquus

The isolation of reaction centres from Sc. obliquus grown on deuterated media was attempted in order to investigate the effects this would have on lineshape of esr signals. PSII particles were prepared using the Triton X-100 method as for the LF1 mutant of Sc. obliquus. Reaction centres were prepared using the Nanba and Satoh method. A complex which gave four bands on SDS-PAGE was eluted at 120mM NaCl (>60 kDa, 60 kDa, approx. 45 kDa and 50 kDa) (Figure 3.5 Lane 3). The esr triplet signal was not observed in these preparations. However, the $P680^{+}$ and Phe^{-} esr signals were able to be investigated in this preparation (Chapter 4). The bands may represent the aggregate form of D1/D2 plus some 47/43 kDa polypeptide impurities.

3.6 Summary

A chorophyll a binding complex containing the D1/D2/cyt b_{559} polypeptides was isolated from higher plants and similar complexes were isolated from an alga

and a cyanobacterium. This suggests that this core complex is common to PSII containing organisms. The observation that the spin polarised triplet was present in the reaction centre complex suggests that the electron transfer components, P680 and pheophytin are bound to this complex.

The characteristics of the triplet i.e. the |D| and |E| values were the same in the higher plant, algal and cyanobacterial reaction centre complexes. These values indicate that P680 is a monomeric form of chlorophyll a. This will be discussed further in Chapter 4.

Chapter 4

ESR characterisation of the components in the isolated reaction centre complex.

4.1 Introduction

As discussed in Chapter 3, the D1/D2/cyt b_{559} complex is limited with respect to bound electron transfer components i.e. it contains the primary electron donor, P680, the accessory chlorophylls, and the primary acceptor, pheophytin but there is no associated quinone (Nanba and Satoh, 1987; Barber et al, 1987). As a result, photochemistry is limited and electron transfer cannot occur beyond pheophytin, the reduced pheophytin recombining with oxidised P680. This results in the formation of the spin polarised triplet (SPT) esr signal (Okamura et al, 1987; Takahashi et al, 1987).

The redox range for the formation of the SPT in reaction centre preparations has been determined by Telfer et al (1988). SPT formation occurs between +400mV and -530mV. At potentials more negative than this, the ability to form the SPT is lost, probably by the chemical reduction of Phe.

At more positive potentials, a radical at g=2 is formed upon illumination . It was suggested that the

non-haem iron atom may still be bound to the D1/D2/cyt b_{559} complex, this being the only component with a redox potential near +400mV. As a result, electron transfer could occur beyond the pheophytin, onto the oxidised non-haem iron, resulting in a loss in ability to form the SPT.

Electron flow beyond pheophytin has been demonstrated in the presence of the artificial electron donor diphenylcarbazide (DPC), when silicomolybdate (SiMo) is added to the D1/D2/cyt_{559} complex (Barber et al, 1987; Chapman et al, 1988). When SiMo was added alone, a reversible light induced absorbance change at 680nm, was observed following a 5 sec illumination period at 4°C, which was attributed to the formation of $P680^+$. The formation of this oxidised radical is attributed to electron transfer beyond the pheophyin to SiMo, stabilising the oxidised P680.

Experiments using isotope substitution and site directed mutagenesis have shown that the electron donors D and Z are probably tyrosine residues located symmetrically on D1 and D2 (Debus et al ,1988a; Debus et al, 1988b; Vermass et al, 1988; Takahashi et al, 1987). The oxidised species of D and Z both display a similar esr spectrum. We have performed experiments to try to detect these components in our reaction centre preparations.

Exposure of the photosynthetic apparatus to high light intensities results in a loss of photosynthetic activity. The primary event of this photodamage has been localised in PSII (Powles , 1984).

The exact site and mechanisms however are controversial. It has been suggested that the site of primary damage occurs at the Q_B site via reactions with oxygen radicals (Kyle et al, 1984). The radicals then selectively damage the D1 protein, generating a conformational change, which renders the protein susceptible to attack by an intrinsic membrane protease. A sequence of 14 amino acids in a loop between helices IV and V on D1 has been proposed as such a cleavage site yielding a 23.5 kDa degradation product (Greenberg et al, 1987). The D1 polypeptide has been found to turn over rapidly in the light (Kyle et al, 1984; Ohad et al 1985) and this turnover has been correlated with the photoinhibition of PSII.

Conversely, Cleland (1988) does not correlate photoinhibition with any loss of the D1 protein, but proposes that a cofactor involved in primary photochemistry may be the initial site of photoinhibition, which may then lead to D1 damage. The photodamage may be caused by the presence of oxygen radicals formed by the interaction of the triplet

states of the monomeric and/or P680 chlorophyll with oxygen.

Thompson and Brudvig (1988) have also proposed a mechanism for photoinhibition involving the phototoxidation of the accessory chlorophylls by $P680^{+}$. The absence of quinone electron acceptors in the reaction centre complex allows the role of the accessory chlorophyll in photosynthesis to be further investigated.

Subjecting the isolated reaction centre to high light intensities, in the absence of artificial electron acceptors, results in a shift to shorter wavelengths of the peak in the 674nm region of the absorption spectrum. The $P680^{+}$ signal obtained in the presence of SiMo by Telfer and Barber (1989) was recently reported to have an absorption shoulder towards the blue side of the spectrum at 672nm. This component was suggested to be due to the bleaching of the accessory monomeric chlorophyll.

This additional bleaching was thought to account for differences reported for the wavelength maxima of the $P680^{+}$ signal observed in PSII preparations by a number of authors. A number of values for the wavelength maxima for $P680^{+}$ have been reported, between the range of 674 to 672nm. (Doring et al, 1969; Nuijs

et al, 1986; van Gorkom et al, 1975; Allakhverdiev et al, 1986). These differences may be due to variable amounts of oxidised monomeric chlorophyll in these preparations.

The bleaching of the monomeric chlorophyll was proposed to indicate photodamage of the reaction centre. The oxidising potential of $P680^+$ is sufficient to oxidise the monomeric chlorophyll. Exposure of the reaction centre to illumination under anaerobic conditions has been found to provide some protection against photodestruction, suggesting a role for oxygen in the process (McTavish et al,1988; Telfer and Barber, 1989; Wasielewski et al, 1989).

In the experiments described in this Chapter, esr and laser flash spectroscopy were used to characterise the electron transfer reactions in the D1/D2/cyt b_{559} complex. It was found that $P680^+$ was stabilised in the presence of exogenous electron acceptors, resulting in the loss of ability to form the triplet state. The effect of deuteration on the linewidths of the $P680^+$ and the reduced pheophytin esr signals was determined using esr. Electron donation to the reaction centre chlorophyll, P680 by the monomeric chlorophyll and the tyrosine residue D/Z was investigated in the presence of exogenous electron acceptors.

RESULTS

4.2 Electron transfer in the D1/D2/cyt b_{559} complex in the presence of SiMo and FeCN ; the formation of a radical at g=2.

Figure 4.1 (a-c) shows that the addition of the electron acceptors ferricyanide (FeCN) and SiMo to the D1/D2/cytb_{559} complex allows electron transfer to occur at cryogenic temperatures. Figure 4.1a (left) shows the illuminated spectrum (with the dark spectrum subtracted) at 4K in a reaction centre sample with no additions . The spin polarised triplet can be observed but there is no radical at g=2 (Figure 4.1a right).

Reaction centre samples treated with 100uM SiMo prior to freezing in the dark, resulted in a 50% reduction in triplet yield and the formation of two radicals upon illumination at 4K, at g=1.94 (arrowed) and at g=2 (Figure 4.1b left). The g=2 region omitted in the spectra on the left is shown in more detail in Figure 4.1b right.

The SiMo used was in a mixed redox state. The addition to the reaction centre of SiMo which had been fully oxidised with FeCN (25uM), resulted in an almost total loss of triplet and a retention of the g=2 characteristics of the SiMo sample (not shown).

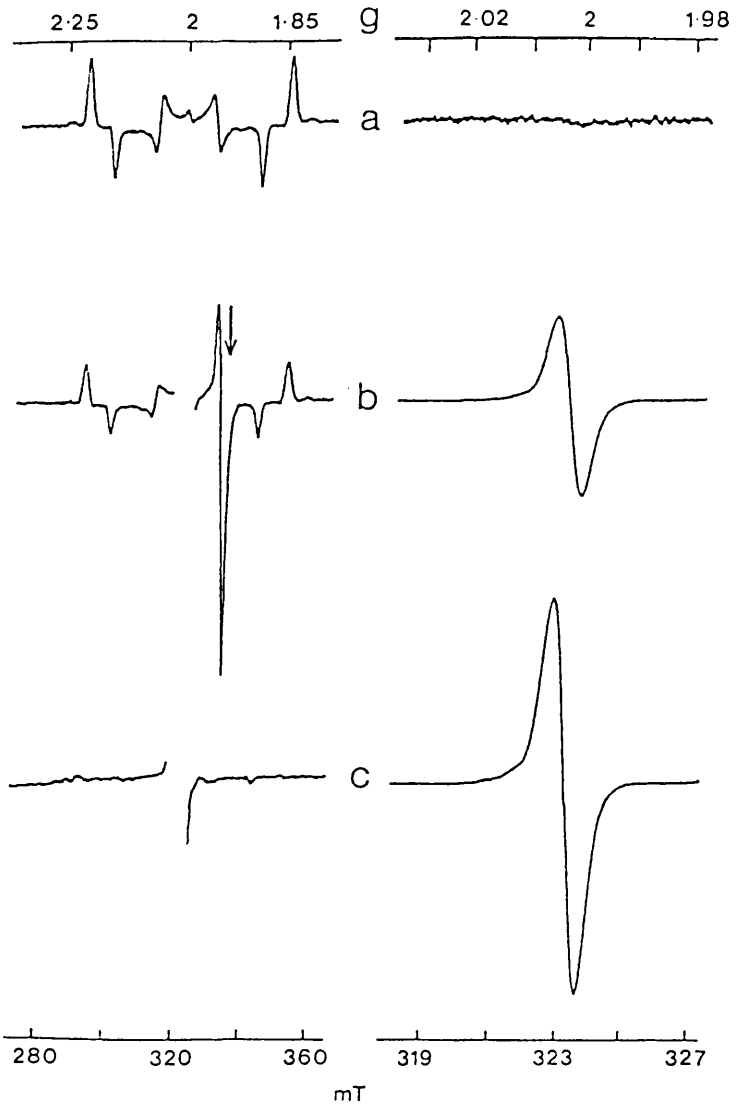

Figure 4.1. Esr spectra showing the effect of added electron acceptors.

4K illuminated minus 4K dark difference spectra of the D1/D2/cyt b_{559} preparation (30 ug Chl. ml^{-1}, 0.033% Triton X-100). (a) Untreated showing the spin-polarised reaction centre triplet. (b) with 100uM silicomolybdate added. The signal arising from the reduction of silicomolybdate is arrowed. (c) with 1mM potassium ferricyanide added. The large g=2 radical observed in b and c omitted from the left is shown on the right. Esr conditions;a-c Microwave power 25uW (left) and 10uW (right), modulation width 1.25mT (left) and 0.2mT (right) and temperature 4K.

The formation of the radical at g=2 and the reduction in triplet yield are indicative of electron transfer beyond the pheophytin. The possible electron acceptors in these samples are the non-haem iron, SiMo or cyt b_{559}.

The addition of the artificial electron acceptor, FeCN (1mM) resulted in the total loss of triplet formation (Figure 4.1c left) and induced a large radical near g=2 (Figure 4.1c right) as found previously (Telfer et al,1988). The g=1.94 signal was absent in this sample, confirming that the latter was due to the reduction of SiMo.

The characteristics of the g=1.94 signal suggest that it may be due to the reduction of SiMo VI to V (Palmer, 1985). Figure 4.2a shows the formation of a signal at g=1.942 in a sample containing SiMo alone, when reduced with ascorbate. This signal is similar to the major peak at g=1.94 as seen in reaction centre samples in the presence of SiMo. The dotted line in Figure 4.2a represents the SiMo oxidised by 25uM FeCN .

The characteristics of the putative Mo(V) signal in the D1/D2/cyt b_{559} complex were investigated further. Figure 4.2b shows the generation of the Mo (V) signal in a D1/D2/cyt b_{559} sample, upon illumination at 5K. No signal is observed in the dark in a reaction

centre sample where the SiMo is chemically oxidised by FeCN (Figure 4.2b, spectrum 1). Upon illumination at 4K, the 2.7mT wide Mo(V) signal is produced at g=1.942 (Figure 4.2b, spectrum 3). This was composed of a reversible and an irreversible component, since in the dark following illumination period , a large proportion of the signal was lost but an irreversible portion remained (Figure 4.2b, spectrum 2). The irreversible signal increased in size with length of time of illumination indicating a process leading to the stabilisation of charge separation. This result confirms that SiMo can act as an electron acceptor in the reaction centre complex at 4K.

In the FeCN sample, the electron acceptor must be either FeCN, cyt b_{559} or the non-haem iron. The esr signal of FeCN is too broad to monitor any light induced changes. The g=6 signal of the non-haem iron (Diner and Petrouleas, 1987) was not observed in the SiMo or FeCN oxidised samples, even in concentrated reaction centre samples (200ugchl/ml). No light induced changes were observed in the spectrum of cytochrome b_{559} at cryogenic temperatures. It is therefore assumed that FeCN also acts as an electron acceptor in the isolated complex at 4K.

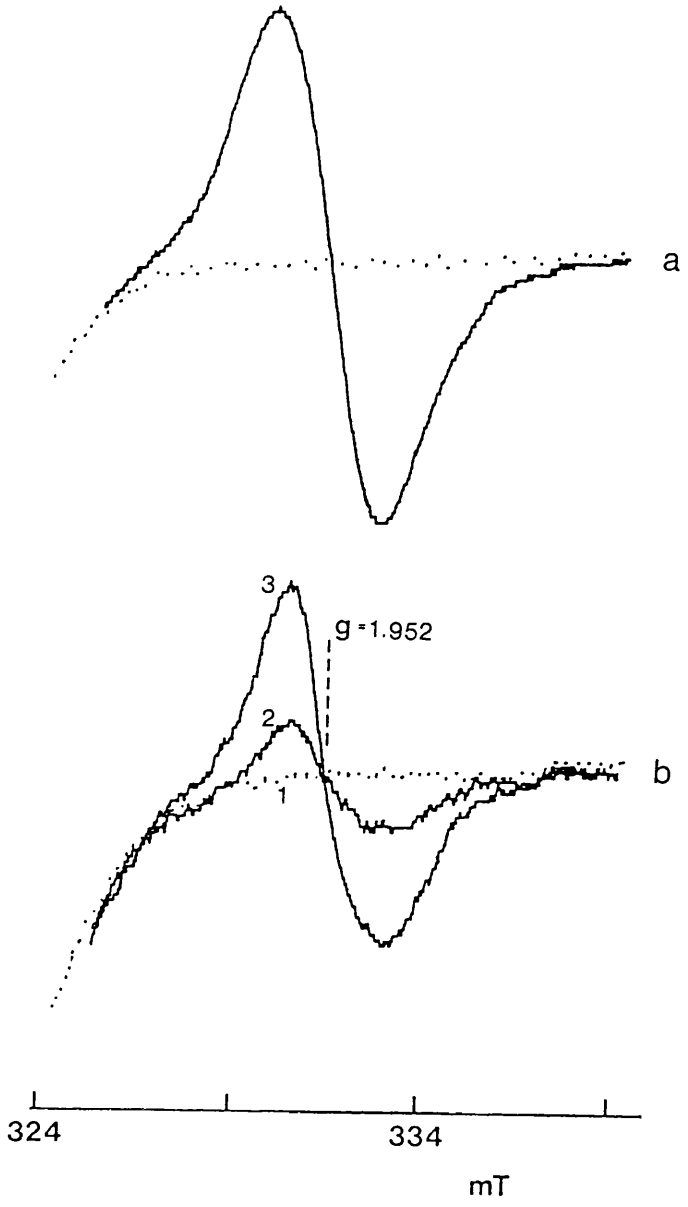

Figure 4.2. Esr of the g=1.942 spectrum of reduced SiMo (Mo V).

2a) Silicomolybdate sample oxidised by ferricyanide (dotted line) and reduced by sodium ascorbate (solid line), showing the characteristics of the Mo (V) signal. (b) D1/D2/cyt b_{559} complex with 100uM silicomolybdate oxidised by ferricyanide added. Spectrum (1) dark, (2), dark following illumination at 5K and (3), under illumination at 5K showing the generation of the Mo(V) signal in the complex. Esr conditions; Power 1mW, modulation width 0.25mT and temperature 5K.

4.2.1 Origin of the g=2 radical

The g=2 radical, formed on illumination in the presence of SiMo or FeCN, can be attributed to the presence of a hydrocarbon cation radical with the characteristic g value of 2.0026. This probably represents P680, the oxidised form of the monomeric accessory chlorophyll or carotenoid (Thompson and Brudvig, 1988; Grant et al, 1988).

Figure 4.3 A and B show that only a small g=2 radical is generated in untreated samples by illumination at 17K. Following the addition of FeCN, a g=2 radical was produced upon illumination at 17K (Figure 4.3C spectrum b), reaching a maximum size after 5 mins (Figure 4.3C, spectrum c). Spectra taken during this accumulation of the g=2 radical indicated a broadening of the radical from 0.8mT to 1.0mT with time. 20% of the signal in the FeCN sample was reversible when the light was turned off after 6 mins, leaving the 1.0mT irreversible portion of the signal. The 1.0mT radical has the linewidth characteristics of an oxidised monomeric chlorophyll (Thompson and Brudvig, 1988; Visser et al, 1977).

In SiMo samples, approximately 60% of the g=2 radical decayed rapidly on turning off the light. This correlated with the behaviour of the g=1.942 signal

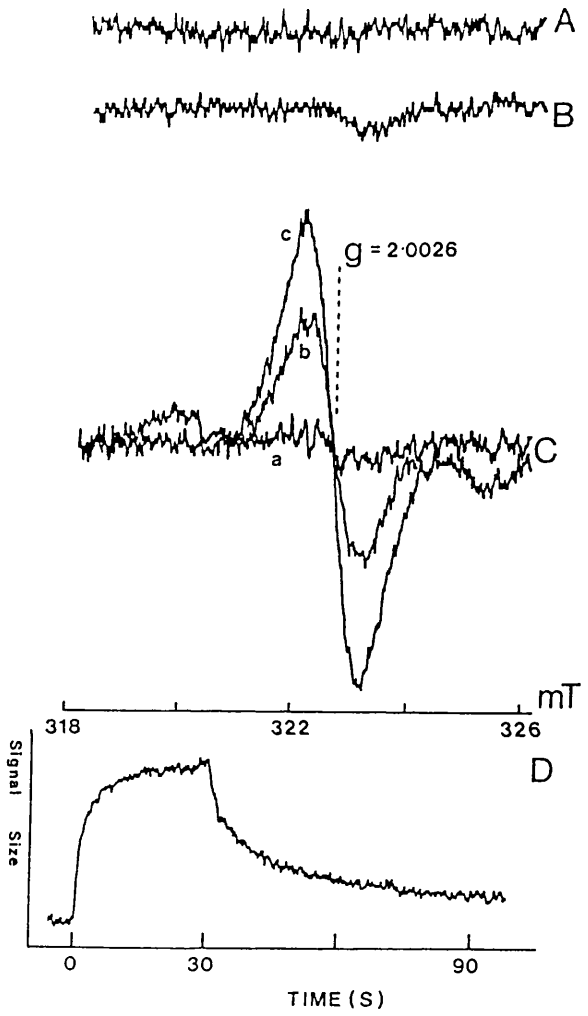

Figure 4.3. Esr characteristics of electron donation in the D1/D2/cyt b_{559} complex.

(A) untreated dark adapted sample (B) untreated sample illuminated at 17K for 5 min. Both (A) and (B) display a small g=2 radical (C) 1mM ferricyanide treated sample; a) in the dark and b) after 2 min illumination and c) 5 min illumination at 17K showing the photoaccumulation of a large g=2 radical. (D) The time course of changes at g=2.006 during illumination at 17K of a sample containing 100uM SiMo. The illumination period (0 to 30s) is indicated by the dotted line between the arrows. The time course reveals a biphasic decay of the g=2 radical. Chl concentration 20 ug Chl. ml^{-1}. Esr conditions; Microwave power 50uW, modulation width 0.2mT and temperature 17K.

from the SiMo (Figure 4.2b spectrum 2). The reversible signal had a linewidth of 0.8mT. The time course of the amplitude at g=2 in a reaction centre sample in the presence of SiMo is shown in Figure 4.3D. A rapid rise in signal size occurred upon illumination followed by a slow increase corresponding to the appearance of the 1.0mT signal. On turning off the light, two phases were observed, a rapidly reversible phase and a slow phase. Both g=2 signals were lost upon thawing to 275K and refreezing in darkness.

From these results it is concluded that in the presence of either SiMo or FeCN, $P680^{+}$ can be formed giving rise to the 0.8mT radical, since these compounds can act as electron acceptors. During the illumination period the monomeric chlorophyll donates to $P680^{+}$, giving rise to a 1.0mT radical and stabilising the charge separation at cryogenic temperatures.

The biphasic recombination, with the SiMo as an acceptor, may indicate recombination between reduced SiMo and $P680^{+}$ (rapid phase) and between reduced SiMo and Chl^{+} (slow phase). The formation of the chlorophyll radicals have been proposed to play a role in photoinhibition. An esr spectrum of oxidised carotenoid has an esr signal at g=2 with a linewidth of 1.3-1.4mT (Grant et al, 1988). This was not detected in the D1/D2/cyt b_{559} complex.

4.2.2 Power saturation of the g=2 radical

At non-saturating microwave powers, the amplitude of an esr signal varies linearly with the square root of the microwave power. This is indicated by the straight line in the log plot (Figure 4.4). The power saturation of each signal is determined from the intercept of the two lines of the power saturation curve. The power saturation of the g=2 radical as measured in a reaction centre sample in the presence of SiMo at 15K was calculated to be 25uW (Figure 4.4A). The signal was found to saturate at a higher power (63uW) at 77K (Figure 4.4B) . This is in agreement with the expected saturation level for organic radicals i.e. in the uW range at cryogenic temperatures and shows that the radical is not due to SiMo, which would saturate at higher power.

4.2.3 The effect of deuterium substitution on the g=2 radical.

Further evidence consistent with the g=2 radical being due to a chlorophyll cation was provided by investigating the reversible signal in reaction centre complexes prepared from Sc. obliquus grown on deuterated media. The deuterated complex was treated with 100uM SiMo in the same manner for normal reaction

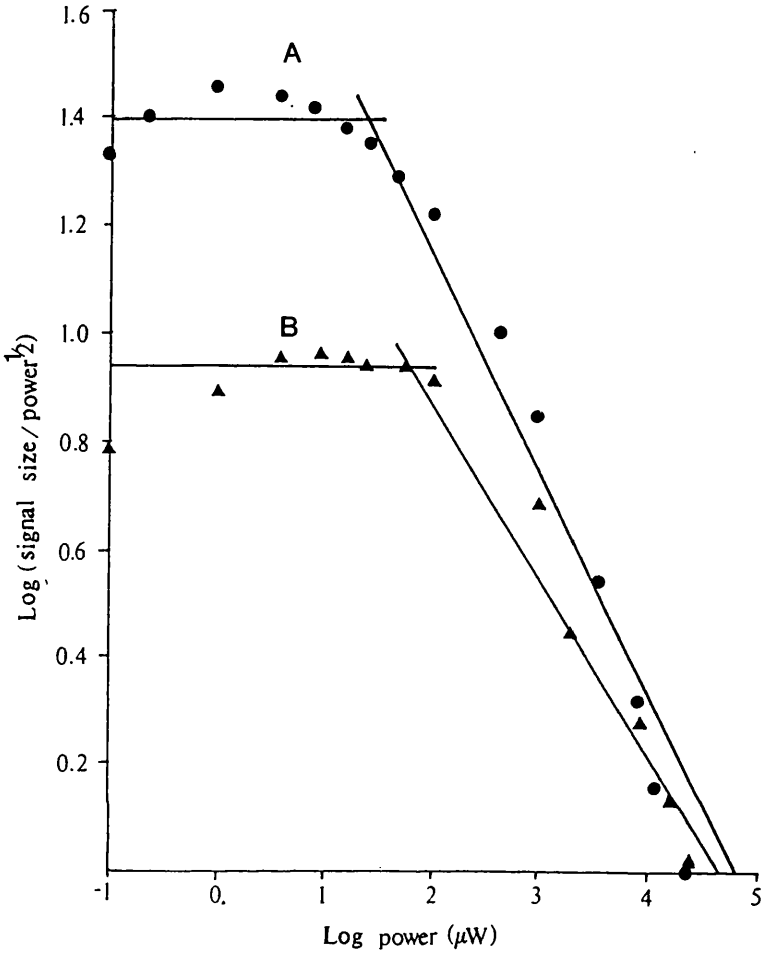

Figure 4.4. Microwave power saturation curve of the g=2 radical as measured in the D1/D2/cyt b_{559} complex in the presence of 100uM SiMo.

A) the power saturation curve of the g=2 radical following illumination (attributed to the formation of $P680^{+}$), recorded at 15K. B) as A, at 77K. The signal power saturates at higher power with increasing temperature. Esr conditions as for Figure 4.1.

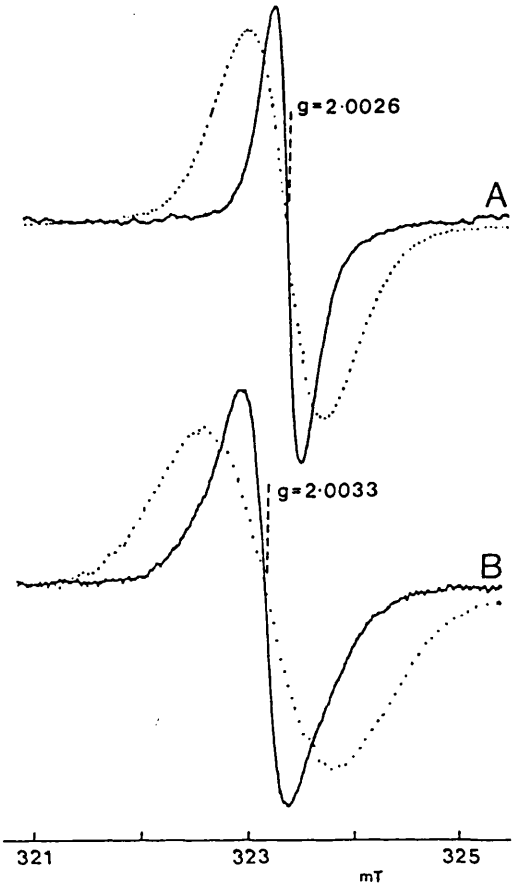

Figure 4.5. Comparison of the g=2 radicals generated in normal and deuterated D1/D2/cyt b_{559} complexes prepared from Sc. obliquus.

Dotted lines represent normal samples and solid lines the deuterated samples. (A) $P680^{+}$ esr signal, illuminated at 15K (with dark following illumination spectrum subtracted) of samples treated with 100uM SiMo. (B) Illuminated at 277K minus dark spectra of samples treated with dithionite at pH 10 showing Phe^{-} spectrum. The size of individual signals have been changed to give approximately equal amplitudes. The linewidths are (A) solid line 0.35mT, dotted line 0.8mT. (B) solid line 0.54mT, dotted line 1.35mT. Chl concentration 5 ug Chl. ml^{-1}. Esr conditions; Microwave power 10uW, temperature 15K and modulation width 1.25mT solid lines and 2.0mT dotted lines.

centres. For chlorophyll cations that contain one unpaired electron, the major interaction of the unpaired electron is with the protons of the chlorophyll macrocycle. Deuteration replaces the large magnetic moment of ^{1}H by ^{2}H , narrowing esr spectra where ^{1}H is important in the linewidth. This decrease in linewidth is due to the magnetic moment of ^{1}H being 6.514 times larger than the magnetic moment of ^{2}H.

Figure 4.5A shows a narrowing of the g=2 signal from 0.85mT to 0.35mT. This reduction by a factor of 2.4 is close to the reduction observed when bacteriochlorophyll is deuterated. This indicates that the extensive delocalisation of the unpaired electron mainly involves hydrogen-electron interactions consistent with a chlorophyll cation.

4.2.4 Investigation of the g=2 radical under anaerobic conditions.

Anaerobic conditions are known to stabilise the reaction centre since the reaction between radicals and oxygen to form oxygen radicals can cause damage to nearby components (Telfer and Barber, 1989; Thompson and Brudvig, 1988; Wasielewski et al, 1989).

The effect of prolonged illumination on the reaction centre at 4K under anaerobic and aerobic conditions was investigated. Under both these

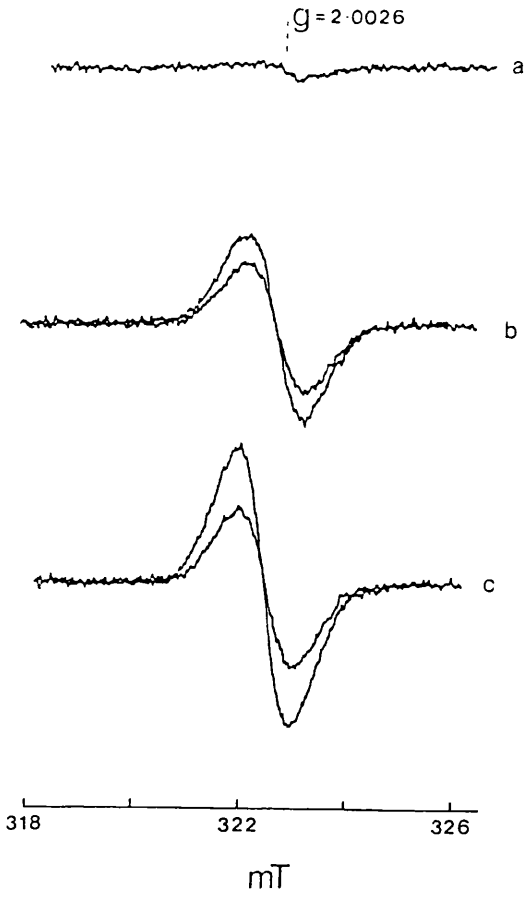

Figure 4.6. Esr spectra of the g=2 radical formed in the D1/D2/cyt b$_{559}$ complex under aerobic and aerobic conditions

(a) Spectrum following illumination for 1 min at 4°C minus the dark spectrum of an untreated sample observed at 4K. (b) As a, but sample containing 100uM silicomolybdate. The outer larger spectrum is an anaerobic sample, the inner spectrum an aerobic sample (c) As b, but sample containing 1mM ferricyanide. Chl concentration 25 ug Chl ml^{-1}. Esr conditions; Microwave power 25uW, temperature 14K and modulation width 0.2mT. Other conditions as Materials and Methods.

conditions, the radical formed should be the irreversible (or very slowly reversible) 1.0mT chlorophyll radical.

Figure 4.6 shows that the 1.0mT radical was the major radical formed during longer periods of illumination (30s to 5 mins) at 4K in samples of the D1/D2/cyt b_{559} complex either in the presence of SiMo or FeCN (Figure 4.6b and 4.6c respectively). These periods of illumination caused a blue shift in the peak in the 674nm region of the absorption spectrum and a loss in activity was also reported by Telfer and Barber, 1989). However the absorption shift and loss of activity were lessened in samples prepared under anaerobic conditions. In both the FeCN and SiMo anaerobic samples, a larger g=2 radical was produced (Figure 4.6b and 4.6c outer peaks) indicating a greater retention of photochemical activity. The most likely photoproduct(s) of oxygen is the singlet oxygen radical . Porphyrins are very efficient generators of these radicals (Marsh and Connolly, 1984; Valenzeno , 1987).

4.3 Laser flash spectroscopy experiments performed on the reaction centre complex in the presence of SiMo/FeCN

Figure 4.7 shows the rise and decay at 820nm of

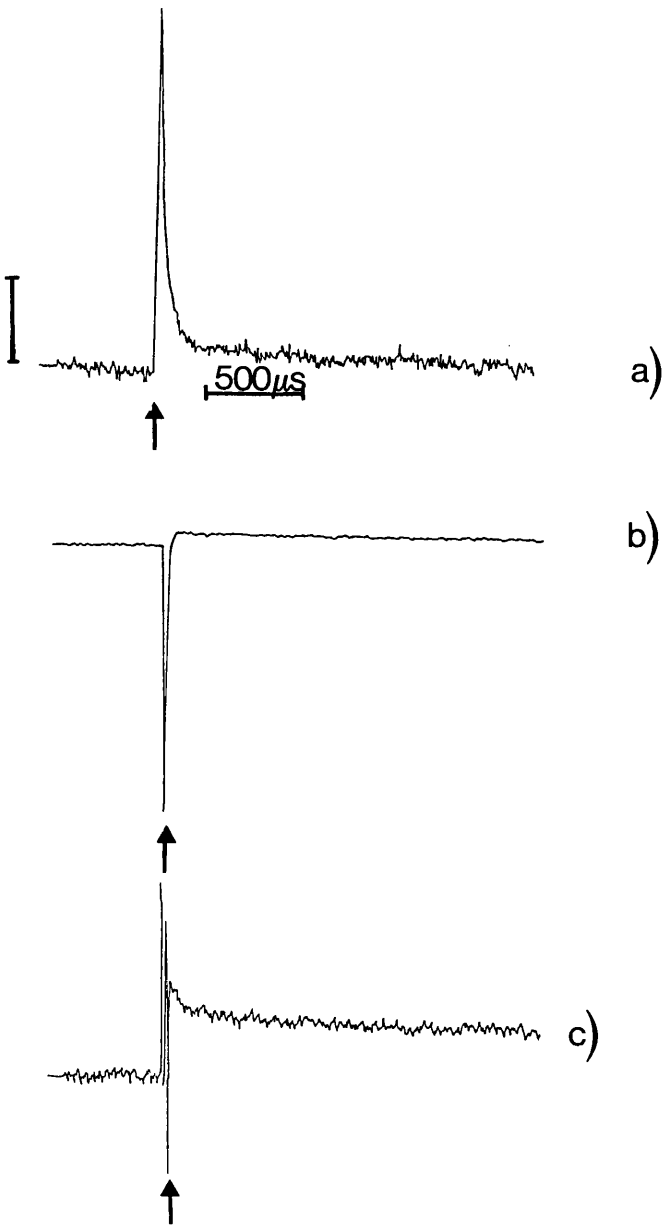

Figure 4.7 Absorbance changes of the D1/D2/cyt b_{559} complex at 820nm induced by a laser flash at 337nm

a) No additions, b) with 100uM silicomolybdate added, c) with 1mM potassium ferricyanide added. Each spectrum is the average of 32 flashes at 0.5 Hz measured at room temperature. The arrow indicates the position of the laser flash. The vertical bar represents an absorbance change of (a) 2×10^{-4}, (b) 4×10^{-5}, (c) 4×10^{-5} absorbance units. Chlorophyll concentration 10ug. ml^{-1}, 50mM Tris/HCl, 0.2% Triton X-100, 120mM NaCl, pH 7.2, pathlength 1cm. Other conditions as described in the Materials and Methods.

the absorption changes due to P680 in the D1/D2/cyt b_{559} complex following 32 flashes. In reaction centre samples with no additions, (Figure 4.7a) the decay was a monophasic fast phase of 20us which is indicative of the back reaction of the reduced Phe to the oxidised P680, forming the P680 triplet (Takahashi et al, 1987; Mathis et al, 1989). The $t_{1/2}$ of a reaction centre sample (no additions) in degassed cuvettes increased from 20 to 80 us. This property is indicative of the formation of a triplet species.

The addition of SiMo to the reaction centre complex resulted in the total loss of the fast phase attributed to triplet formation (Figure 4.7b). This was replaced by a slow component with a half-life of 3.5ms, indicating that SiMo was acting as an electron acceptor. The decay observed in reaction centre samples in the presence of FeCN however was biphasic with a fast phase of 40us (60%) and a slow phase of 3.0ms (40%) (Figure 4.7c).

The millisecond component observed in the presence of both SiMo and FeCN is probably due to electron donation of reduced SiMo or FeCN to $P680^+$. An alternative pathway may include the reduction via cyt b_{559} from SiMo or FeCN. However, this is unlikely due to the midpoint redox potentials of SiMo and FeCN being

too high to be reoxidised by cyt b_{559}. The kinetic data therefore suggests that both SiMo and FeCN act as electron acceptors at room temperature. This is consistent with the esr data presented earlier.

The fast phase observed in the biphasic decay in the presence of FeCN probably represents the formation of P680 triplet. It may be concluded from this that FeCN is not as efficient an electron acceptor as SiMo at room temperature.

4.4 The detection of reduced pheophytin in the reaction centre complex

Figure 4.8A shows the esr signal of reduced pheophytin. This is produced when reaction centre samples are frozen in the light in the presence of dithionite. The trapped pheophytin signal is approximately 1.35mT wide and situated at g=2. The SPT was not formed in this sample as expected. Figure 4.8B shows the generation of the SPT in an untreated sample. The reduced pheophytin spectrum was also observed in reaction centres prepared from P. laminosum and had the same characteristics as that of the higher plant preparation (Nanba and Satoh, 1987; Okamura et al, 1987; Telfer et al, 1988).

As seen with the P680 radical, a narrowing of the

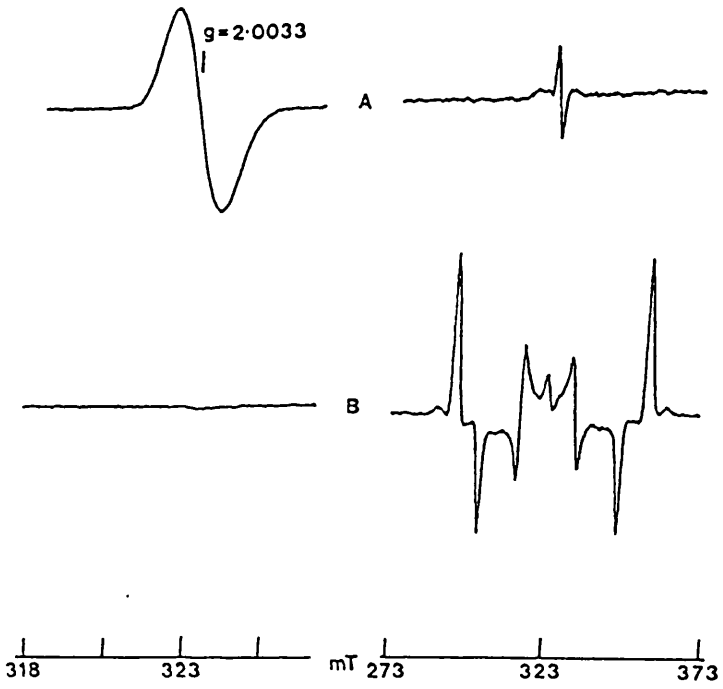

Figure 4.8. Esr spectra showing the loss of spin polarised triplet formation on reduction of pheophytin (Phe).

D1/D2/cyt b_{559} complex at 30 ug Chl. ml^{-1}. (A) Sample at pH 10 reduced by sodium dithionite and then frozen under illumination showing the trapped Phe^{-} radical (left) and the absence of triplet (right). (B) as A but frozen in the dark showing the spin polarised triplet.The spectra on the right are the illuminated minus dark after illumination, difference spectra. Esr conditions; Microwave power (left) 10uW, temperature 15K;(right) microwave power 25uW, temperature 4K.

pheophytin signal was observed from 1.35mT to 0.54mT in reaction centre preparations of deuterated Scenedesmus (Figure 4.5b). The pheophytin signal is wider than that of chlorophyll due to the fact that the pheophytin macrocycle has two additional protons.

4.5 Triplets

The characteristics of the spin polarised triplet have already been discussed in Chapter 3. The possibility that the location of the SPT lies on the monomeric chlorophyll, as opposed to P680, cannot be ruled out and will be discussed later stage in this Chapter.

4.5.1 Power saturation of the SPT

The triplet signal was found to saturate at low microwave powers (25uW) (Figure 4.9a) and the amplitude of the signal to increase as the temperature was lowered (Figure 4.9b). However, a small amount of the triplet is still detected even at 28K. No change in lineshape, as observed in the triplet spectrum of purple bacteria when the semiquinone Q_A^- (Hore et al, 1988) was detected at these higher temperatures. Hore et al (1988) reported a change in the polarisation pattern from AEEAAE to AEAEAE at 100K when the semiquinone was bound.

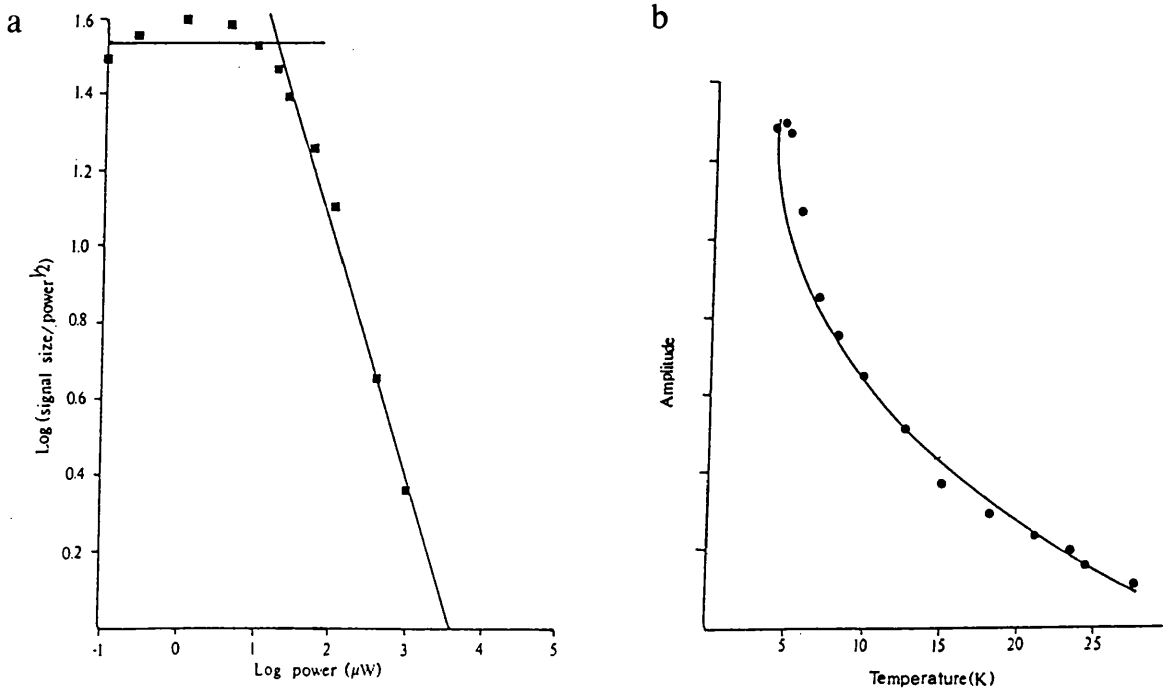

Figure 4.9. Power saturation curve (4.9a) and temperature dependency (4.9b) of the spin polarised triplet esr signal.

The optimal conditions for the observation of the triplet are low temperatures (below 8K) and low power (25uW). Esr conditions are as for Figure 4.1.

4.5.2 An additional light induced triplet species

An additional light induced signal was observed in the reaction centre preparations together with the main SPT. The signal was symmetrical about the g=2 region with peaks observed in the low and high field regions of the major triplet. Figure 4.10 shows the extreme low field peak of the main SPT and the additional triplet. A similar peak appears to the right of the high field peak of the SPT. The pattern suggests the possibility of an additional spin polarised triplet with a |D| $=0.0350cm^{-1}$. The full spectrum would be required to confirm the polarisation pattern but this is obscured by the major triplet.

The |D| value is larger than would be expected from a chlorophyll triplet (Thurnauer and Norris, 1977) or P700 triplet (Rutherford and Mullet, 1981; Frank et al, 1979) but similar to that obtained for monomeric pheophytin a in solution although with a different polarisation pattern (Thurnauer et al, 1975). This probably represents centres where the excitation energy has migrated out onto a nearby pheophytin molecule. The pheophytin triplet has since been observed in the D1/D2/cyt b_{559} complex by Frank et al, (1989).

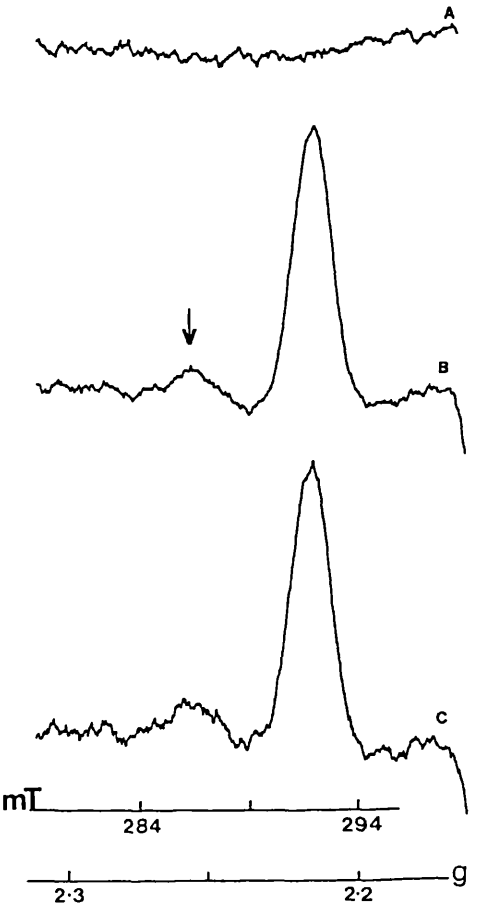

Figure 4.10. Esr spectra showing the extreme low-field peaks of both the light induced triplets in the D1/D2/cyt b_{559} complex

A) Spectrum obtained in the dark at 4K. B) spectrum obtained under continuous illumination at 4K. The additional triplet is arrowed. C) Illuminated spectrum with the dark spectrum subtracted. Chl concentration 30 ug Chl. ml^{-1}. Esr conditions ; 25uW, modulation width 1mT and temperature 4K.

4.5.3 Confirmation that the system is in a triplet state

Figure 4.11b shows the generation of a further light induced signal in the reaction centre complex. The signal consists of an irreversible peak at g=4 at 1605 gauss. This signal was attributed to the formation of the $\Delta m_s=2$ triplet which is observed at low field (called a 'half-field transition'). The signal corresponds to transitions for which $\Delta m_s = 2$ (m_s = spin quantum number). This triplet represents the two parallel spins making the transitions T_{-1} to T_{+1} and T_{+1} to T_{-1} , as opposed to the SPT where the transitions are T_0 to T_{+1} and T_0 to T_{-1}. Therefore the power saturation of the $\Delta m_s=2$ triplet is higher than that of the SPT (500uW), (Figure 4.12).

The $\Delta m_s=2$ triplet is an example of a weakly allowed transition and only occurs in a small number of centres. The observation of a half-field transition is a strong confirmation that the system is in a triplet state.

4.6 Evidence for the presence of the tyrosine electron donor D/Z in the reaction centre complex

Figure 4.13 shows the effect of pre-illuminating the reaction centre complex for 15secs at room

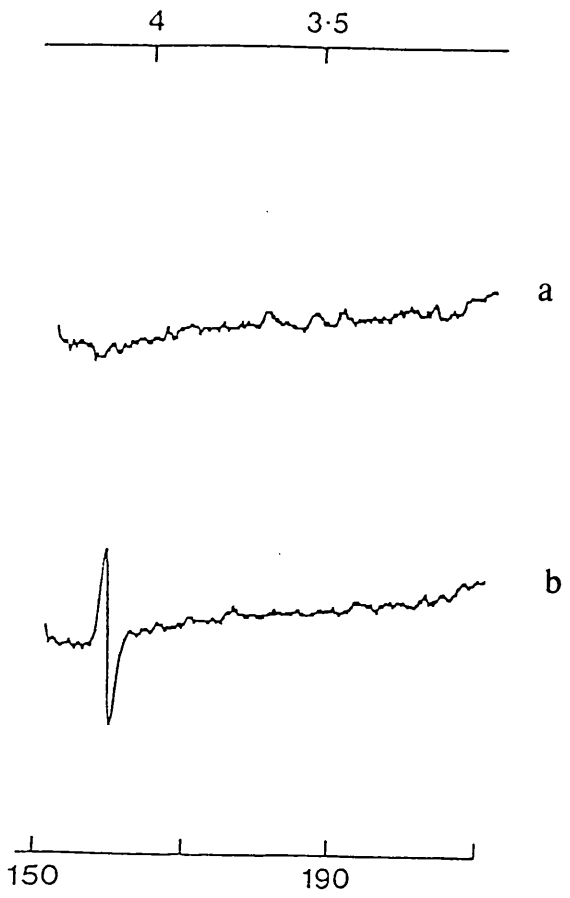

Figure 4.11. Esr spectrum of the $\Delta m_s=2$ transition at half field

a) spectrum in the dark following illumination b) the spectrum on illumination at 4K showing the generation of the $\Delta m_s=2$ transition triplet. Esr conditions;100uW, modulation width 1.25mT and temperature 4K. D1/D2/Cyt b_{559} complex at 177 ug Chl ml^{-1}.

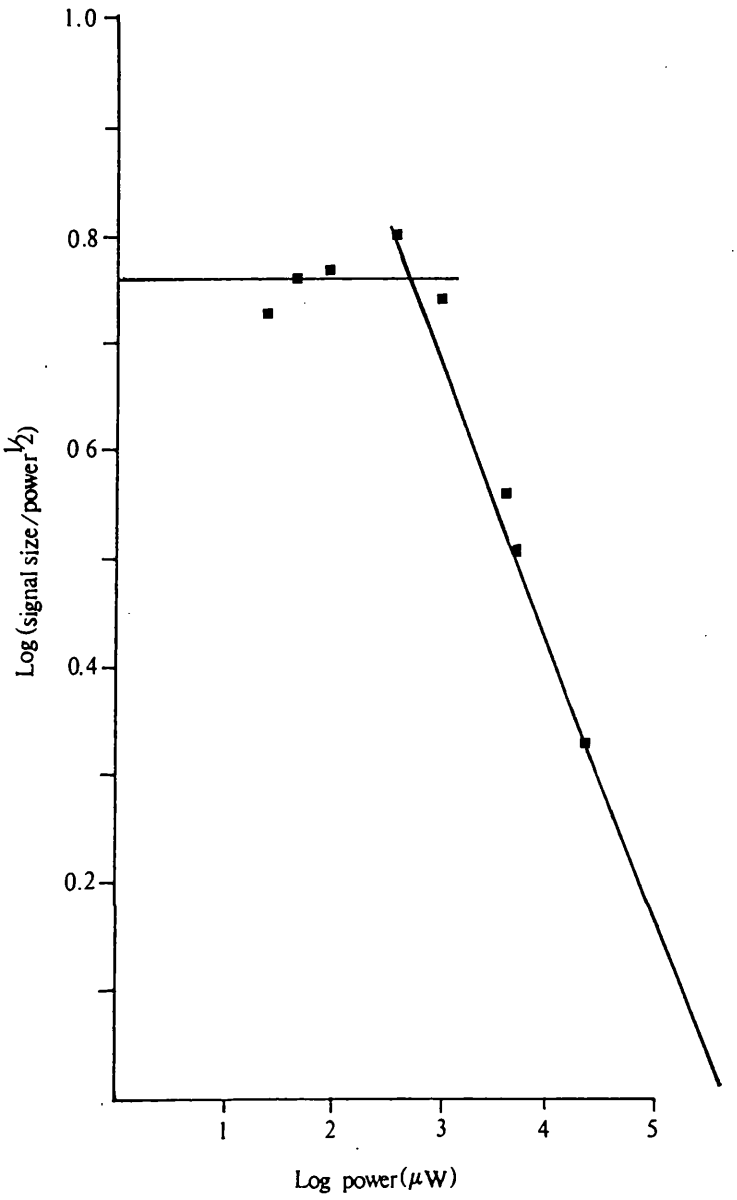

Figure 4.12. Microwave power saturation of the $\Delta m_s=2$ transition triplet.

The half-field transition triplet is a forbidden transition and therefore saturates at a higher power than the spin polarised triplet. Esr conditions as for Figure 4.11.

temperature and subsequently freezing the sample under illumination. Untreated samples show no esr signals in the g=2 region in the dark or upon illumination in the cryostat at 4K (Figure 4.13a). The addition of SiMo or FeCN prior to the illumination period resulted in the formation of broad signals near g=2 detected at 14K in the dark (Figure 4.13b). These signals were stable at 77K but decayed rapidly if the sample was thawed to 4°C.

The esr characteristics of the solid line spectrum suggest it may be composed of two components, a broad and a narrow radical. The narrow radical may represent the 1.0mT monomeric chlorophyll radical also detected by illumination at 4K. The broad component resembled the signal from the tyrosine radical (D^{+} or Z^{+}) (Barry and Babcock, 1987; Debus et al, 1988a ;Debus et al 1988b; Vermaas et al,1988; Takahashi and Styring, 1987), (Figure 4.13c).

Z^{+} and D^{+} have a similar esr spectrum. Comparison of the broad signal with that of D^{+} induced in oxygen evolving PSII particles (Figure 4.13c), revealed that the two spectra were similar. Moreover, the esr characteristics of the broad signal such as the power saturation and the g value (greater than g=2.004) were consistent with the assignment to D^{+} or Z^{+}. The

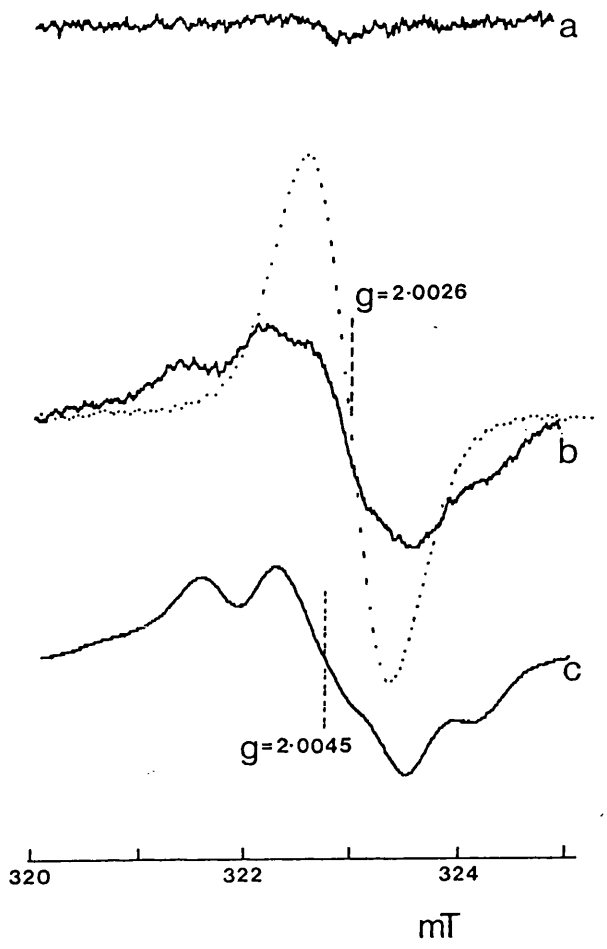

Figure 4.13. Esr spectra of the radicals produced by illumination at 4°C.

30 ug Chl. ml^{-1} D1/D2/Cyt b_{559} complex. (a) Illuminated at 4°C for 15s minus dark spectrum, of an untreated sample. (b) solid line, illuminated as a) minus the dark spectrum of sample containing 100uM silicomolybdate showing the formation of a broad signal at g=2. Dotted line , illuminated at 4K minus dark spectrum of same sample showing the formation of 1.0mT radical. (c) spectrum of D^{+} in dark adapted oxygen-evolving PSII .Esr conditions; Microwave power 25 uW, temperature 14K and modulation width 0.2mT.

addition of the electron donor diphenylcarbazide (DPC) reduced the size of the signal, confirming that it was due to the presence of an electron donor in the preparation.

The number of centres with a functional D/Z was estimated by calibrating against the D^+ signal from a PSII particle preparation. It was found that approximately 5% of the centres were involved in the formation of D^+/Z^+ signal assuming 1 cyt b_{559} per reaction centre. This low yield may be due to number of reasons, a) it may represent the trapping of only a small steady state population of D^+ or Z^+ due to rapid rereduction, b) measuring D^+/Z^+ in only a few centres, c) contamination with polypeptides other than the reaction centre ones. The latter can be be ruled out since the level of contamination was less than 5%. It is more likely that the isolation procedure resulted in the modification of the characteristics of the tyrosine electron donors.

4.7 The effect of SiMo on the cytochrome b_{559} esr spectrum

Figure 4.14 shows the g_y and g_z peaks of the esr spectrum of cytochrome b_{559}, which is usually in its oxidised form in the reaction centre preparation. In the presence of SiMo, it was found that the peaks of

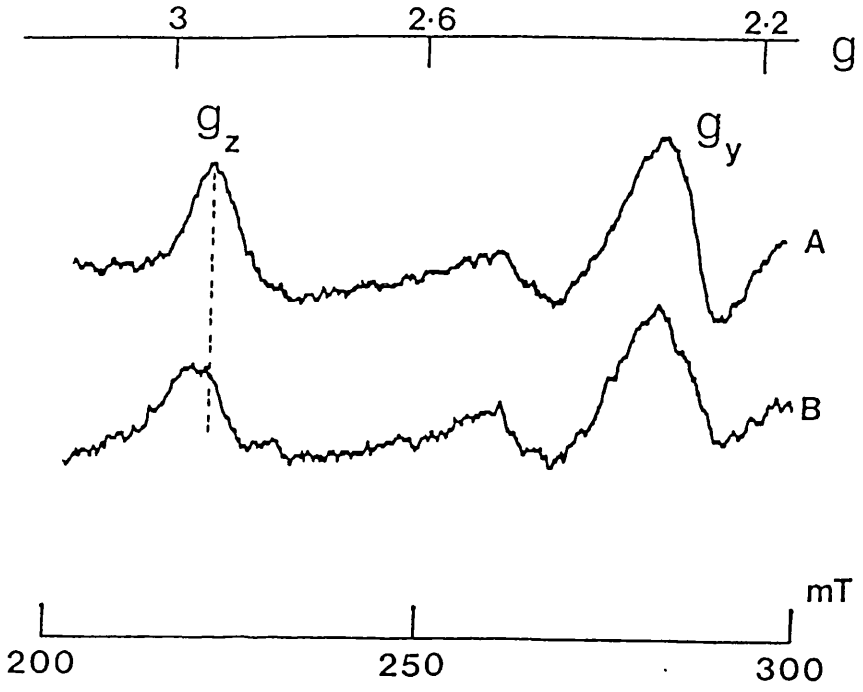

Figure 4.14. Esr spectra of cytochrome b_{559} in the D1/D2/cyt b_{559} complex.

(A) 50 ug Chl. ml^{-1}, 0.05% Triton X-100, showing the g_y and g_z peaks of the oxidised low potential cytochrome b_{559}. (B) With 100uM silicomolybdate added. The dotted line shows the shift in the peak position. Esr conditions: Microwave power 5mW, modulation width 1.25mT and temperature 13K.

the cytochrome b_{559} spectrum were broadened, suggesting the binding of the SiMo close to the cyt haem (Figure 4.14A and B). Photoreduction of the cytochrome was not observed under these conditions.

Discussion

4.8 The PSII reaction centre chlorophyll ; monomer or dimer?

The analogy between the L and M subunits of the bacterial reaction centre and the D1/D2 polypeptides of higher plants have led to the idea that the crystal structure of the bacterial reaction centre can be used as a viable model for the PSII reaction centre. The model has P680, pheophytin, Q_A and Q_B bound to the D1/D2 heterodimer.

The bacterial reaction centre chlorophyll is dimeric. However, the spectroscopic data available for the arrangement of PSII reaction centre chlorophyll is not consistent with this proposal.

In the case of Rhb. sphaeroides, the linewidth of the dimeric chlorophyll is narrowed by /2 as compared to the monomer ($P870^+$ dimer 0.9mT, BChl a^+ monomer 1.3mT). The reduced linewidth of the P680 radical (0.79mT compared to 1.0mT of monomeric form) could therefore be interpreted as being due to the dimeric

form (Norris et al, 1971).

Unfortunately, reduction in linewidth can also be caused by environmental factors (Davis et al, 1979a). The bacteriochlorophyll dimer of Rps. viridis, P960 only shows a small reduction in esr linewidth (Plato et al, 1988). This is thought to indicate that the charge distribution on the Rps. viridis dimer is asymmetric (Davis et al, 1979b; Plato et al, 1988). Therefore, the observed reduction in linewidth cannot be taken as an indication of a monomeric or dimeric form of the chlorophyll radical.

The zero field splitting parameters of the spin polarised triplet of P680 are consistent with a monomeric chlorophyll a structure. Rutherford , (1986) has also suggested that the P680 triplet is oriented parallel to the membrane. In contrast, the zero field splitting parameters of the triplet of Rhb. sphaeroides are characteristic of a dimeric bacteriochlorophyll a and the triplet is oriented perpendicular to the membrane.

However, the bacteriochlorophyll b dimer of Rps. viridis has been shown to have a triplet state with characteristics of a monomer (Norris et al, 1971). Therefore the possibility that P680 is a chlorophyll a dimer with its triplet located on one of the accessory

monomeric chlorophylls cannot be ruled out. This would also explain the parallel orientation of the P680 triplet in the membrane.

4.9 Components of the reaction centre complex

4.9.1 Electron acceptors

The esr characteristics of the D1/D2/cyt b_{559} complex show that it is depleted of some of the PSII electron transfer components, such as the quinones Q_A and Q_B and the non-haem iron. However both SiMo and FeCN are able to act as electron acceptors in the complex even at cryogenic temperatures as described above. Esr experiments performed by Takahashi et al (1989) confirm the proposal that SiMo can act as an electron acceptor in the reaction centre complex.

Both FeCN and SiMo allow the observation of the $P680^{+}$ radical, making it a good system for further study of this radical, as shown by the deuteration experiments.

It has been proposed that SiMo binds at or near the non-haem iron due to the observation that washing chloroplasts with SiMo displaces bicarbonate (Stemler, 1977; Vermaas and van Rensen, 1981). The positively charged bicarbonate site probably makes a good site for binding anions such as SiMo and FeCN. Graan has also

demonstrated that SiMo interacts non-competitively with the herbicide DCMU suggesting binding to or near the Q_B site. No evidence for a high level of nonspecific binding was found. This result explained why it was previously thought that as SiMo binding was DCMU insensitive and that SiMo was accepting electrons at a site prior to that of Q_B. This may also explain why identical results were seen irrespective of the order of addition of the SiMo and FeCN since the FeCN does not compete with SiMo binding.

4.9.2 Electron donors

Although only a small number of centres displayed the signal assigned to the tyrosine electron donor, this still provides additional evidence that the D1/D2 heterodimer is involved in binding Z and D respectively. This low level may be an indication that additional polypeptides are required to maintain activity within the complex.

The 47 kDa polypeptide has been proposed thought to play a conformational role in addition to its role as a chlorophyll binding polypeptide. A complex consisting of the 47 kDa/D1/D2/cyt b_{559} polypeptides has been reported, using dodecylmaltoside and a combination of cation and anionic exchange chromatography (Dekker et al, 1989b). No bound quinone

was detected in the complex. However, in the presence of FeCN, a signal assigned to the formation of Z^{+} was detected in 70% of the centres.

The 47 kDa polypeptide could therefore play an essential structural role in the PSII complex and could account for the low yield of the signal observed in our preparations. However, the possibility that the isolation procedure used by Dekker et al (1989b) is less damaging to the complex cannot be ruled out.

A monomeric chlorophyll has been shown to function as an electron donor in the D1/D2/cyt b_{559} complex under conditions of prolonged illumination. The oxidation/reduction potential of P680/$P680^{+}$ is estimated to be +1.17V, which is much greater than the reduction potential of the primary donors of PSI and of the photosynthetic bacteria (+0.25–+0.5V). P680 is therefore able to oxidise its antennae chlorophyll. The close proximity of the accessory chlorophylls to the reaction centre will increase their susceptibility to photooxidation. Therefore the 1.0 mT radical observed at g=2 could be attributed to the photooxidation of the accessory chlorophyll. The photooxidation of monomeric chlorophyll at cryogenic temperature has been reported by de Paula et al (1985). This was also inferred to be an accessory chlorophyll.

The interaction of the oxidised monomeric chlorophyll, or P680 , with oxygen to form oxygen radicals has been implicated to play a primary role in photoinhibition. These oxygen radicals react with nearby components e.g P680 or the monomeric chlorophylls. The β -keto-ester group in ring V of chlorophyll a is particularly sensitive to oxidative reagents (Wasielewski et al 1982). Other forms of degradation may involve the splitting of the porphyrin ring and the removal of Mg.

The observation that the oxidation of the monomeric chlorophyll decreases under aerobic conditions (Figure 4.6) supports the observations reported by other authors (McTavish et al, 1988; Wasielewski et al 1989, Telfer et al, 1989). It is therefore possible that a primary site of photoinhibition is located at the reaction centre P680 and/or the monomeric chlorophyll.

The lack of carotenoid radicals and the sensitivity of the complex to light suggests that the carotenoid within the complex is not functioning normally by protecting the P680 by reaction with chlorophyll triplets. Using Resonance Raman spectroscopy, Ghanotakis et al (1989) established that the beta carotene was in the all-trans form. This is in contrast to the bacterial reaction centre where the

carotenoids are all in the cis form. The isolation procedure may therefore uncouple the beta carotene from the reaction centre. The beta carotene can then undergo photoisomerisation from the cis to the all-trans form. The cis form may be the form required for protection, and therefore does not carry out its role in the isolated reaction centre.

The shift in the cytochrome b_{559} spectrum in the presence of SiMo implies that they are in close proximity to each other. Although a definite role of the cytochrome has yet been determined, it may play a role in photoinhibition (Cleland , 1988; Brudvig and Thompson, 1988). This is discussed in more detail in Chapter 5.

In the next Chapter, experiments attempting to reconstitute the reaction centre complex with exogenous quinones are described.

CHAPTER 5

Reconstitution of the D1/D2/cyt b_{559} complex with exogenous quinones.

5.1 Introduction

The D1 polypeptide has been shown to bind herbicides by using photoaffinity labelling of thylakoids with an azido-derivative of atrazine (Pfister et al, 1981). Many herbicides and inhibitors are known to interfere with photosynthetic electron flow at PSII. They block electron transfer between Q_A and Q_B, probably by displacing PQ at the Q_B binding site (Kyle, 1985).

Inhibitors of Q_A oxidation include members of the triazines (atrazine) ureas (DCMU=Diuron), cyanophenols (ioxynil), nitrophenols (dinoseb) and benzo- and napthoquinones. The binding of the phenolic herbicides may also involve the 47 and 43 kDa polypeptides of PSII (Johanningmeier et al, 1983 ; Trebst and Depka, 1985), while the atrazines and ureas bind to D1 only (Pfister et al, 1981). These herbicides bind in such a way , that Q_B can no longer bind in its proper orientation and location to accept electrons from Q_A.

The D1/D2/cyt b_{559} complex is deficient in plastoquinone-9 (PQ-9) (Nanba and Satoh, 1987). In contrast, reaction centres from the purple bacterium Rhb.

sphaeroides can be prepared with bound ubiquinone-10 (UB-10) present at the Q_A and Q_B sites. This has been attributed to the presence of the H subunit of bacterial reaction centres, which may preserve the binding pocket of the quinone due to its close association with the L and M subunits.

The UB-10 at the Q_A site in purple bacteria can be replaced by a wide variety of benzo-, naptho- and anthraquinones, many of which can function as electron acceptors in the reaction centre (Cogdell et al, 1974 ; Okamura et al, 1975).

Parallel efforts to functionally reconstitute the Q_B binding site were thought to be limited to quinones with the native UQ configuration. However, the Q_B site is now known to have a broad specificity for a variety of herbicides. Giangiacomo et al (1989) have recently reported the reconstitution of Q_B activity with a variety of benzo-and napthoquinones to the Q_B site of Rhb sphaeroides.

Reconstitution of the D1/D2/cyt b_{559} complex with decylplastoquinone (DPQ) has shown that DPQ may bind at the Q_A/Q_B site. The photoreduction of cytochrome b_{559} has been observed in the reaction centre complex in the presence of added DPQ and $MnCl_2$ (Chapman et al, 1988), indicating that electron flow through DPQ to cytochrome

b_{559} may occur . Gounaris et al (1988) have observed similar results when performing reconstitution experiments with the native PQ-9. The reconstitution was dependent upon high levels of quinone and an optimum Triton X-100 concentration of 0.2% at pH 8.0. These results were interpreted as binding of the artificial quinone at the Q_A/Q_B site. The quinone then accepts electrons from the pheophytin and passes them onto the cytochrome b_{559}.

In this Chapter the reconstitution of the D1/D2/cyt b_{559} complex was attempted using a variety of exogenous quinones.

Results

5.2 The effect of detergent exchange on the stability of the reaction centre complex

Figure 5.1A and 5.1C shows that a decrease in the Triton X-100 concentration from 0.2% to 0.03% respectively in the reaction centre preparation resulted in an increase in yield of the spin polarised triplet . A similar result was obtained when the Triton X-100 was exchanged with dodecylmaltoside (results not shown). This is in agreement with the detergent effects already discussed in Chapter 4.

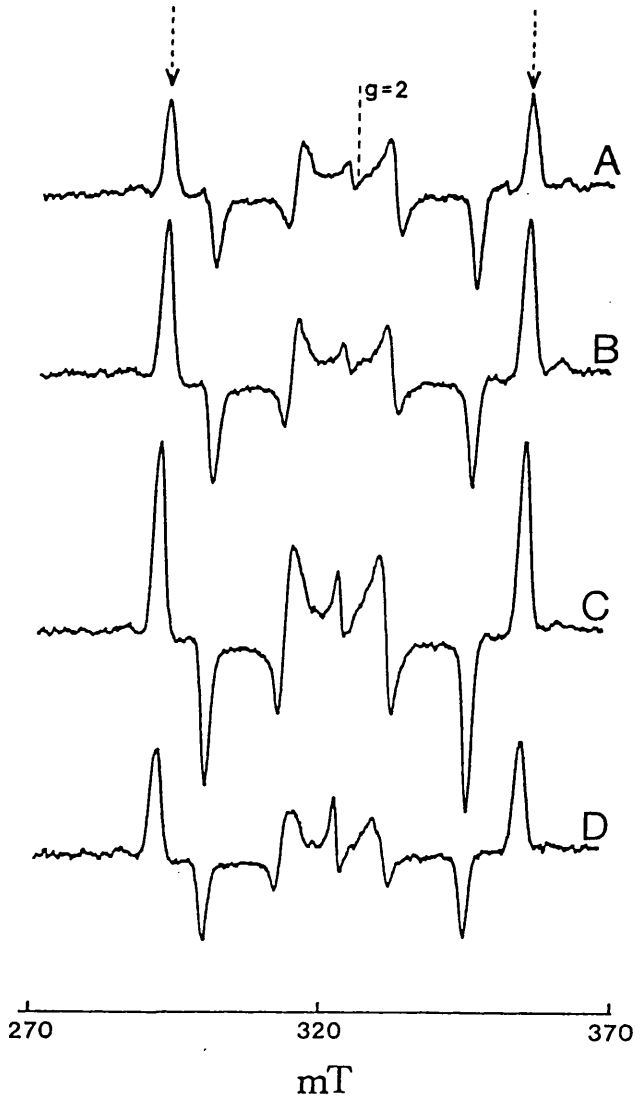

Figure 5.1. Esr spectra of triplets observed in the D1/D2/cyt b_{559} complex.

A-D 4K illuminated spectrum (with the dark following illumination spectrum subtracted) (A) 0.2% Triton X-100, the outer peaks of the spin polarised triplet are arrowed. (B) 0.2% Triton X-100 plus 100uM DPQ. (C) 0.033% Triton X-100 (D) 0.033% Triton X-100 plus 100uM DPQ. Esr conditions; Microwave power 25uW, modulation width 1.25mT, temperature 4K. Chl concentration of the Triton X-100 reaction centres was 30 ug Chl. ml^{-1}.

5.3 Reconstitution of the reaction centre complex with decylplastoquinone

The addition of the artificial quinone, (DPQ) to the D1/D2/cyt b_{559} complex, resulted in a change in both the lineshape and the yield of the spin polarised triplet observed at 4K. In the 0.2% Triton X-100 sample (Figure 5.1B) an increase in triplet yield was seen upon addition of the DPQ. There was also an increase in the size of the ratio of the outer pair of peaks (arrowed) to the inner peaks. This was shown not to be as a result of solvent effects, since the addition of ethanol or dimethylsulphoxide alone, equivalent to that added with DPQ, produced no changes.

In contrast, a decrease in the triplet yield was observed in the 0.033% Triton X-100 sample in the presence of DPQ (Figure 5.1D). The change in the outer peaks was again more marked resulting in a lineshape change. The drop in triplet yield may be attributed to electron transfer to the quinone although no other evidence of electron transfer at cryogenic temperatures was detected.

Changes in triplet yield are unreliable as a sole indication of electron transfer. However, a net photoreduction of the cytochrome b_{559} at 4°C was observed

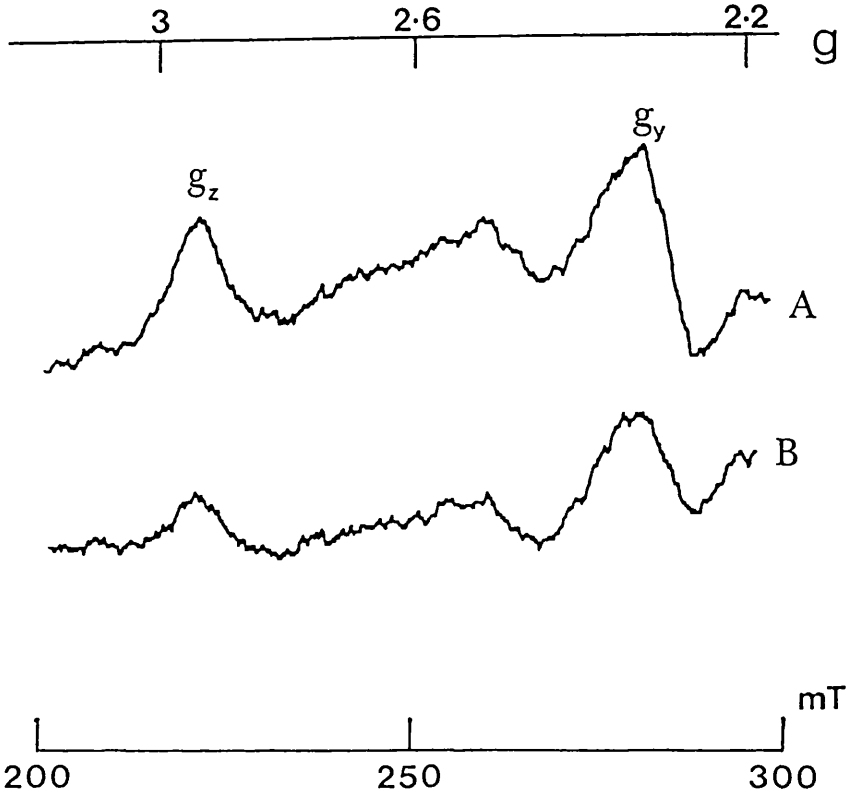

Figure 5.2. Esr spectra of the photoreduction of cyt b_{559} in the D1/D2/cyt b_{559} complex.

(A) shows the g_z and g_y peaks of the oxidised low potential cytochrome in a reaction centre sample (50 ug Chl. ml^{-1}; 0.2% Triton X-100) containing 100uM DPQ and 1mM DPC prior to illumination at 4°C. (B) sample in (A) following 30s illumination at 4°C, showing the photoreduction of the cytochrome. Esr conditions; Microwave power 5mW, modulation width 1.25mT and temperature 13K.

in the D1/D2/cyt b_{559} complex upon the addition of DPQ but only in the presence of the electron donor DPC (Figure 5.2). The addition of DPC prior to the samples being frozen had no effect on the triplet yield (not shown).

Figure 5.2A shows the g_y and g_z peaks of the esr spectrum of cytochrome b_{559}, which is usually in its oxidised form in the reaction centre preparation. Figure 5.2B shows the decrease in the cytochrome peaks in samples containing DPQ and DPC after illumination at 4°C. This decrease in size indicates that cytochrome b_{559} accepts electrons from the photoreduced DPQ, which presumably binds to the Q_A and Q_B site as suggested previously (Chapman et al, 1988; Gounaris et al, 1988). However, no evidence of a semiquinone radical at g=2, indicating specific binding of DPQ, was observed. Illumination at 4K caused no changes to the cytochrome b_{559} spectrum (not shown). The reduction of the cytochrome with dithionite did not lead to the ability to photoxidise the cytochrome at cryogenic temperatures. This suggests that the reduced cytochrome b_{559} cannot compete withn the back reaction from pheophytin.

5.4 Reconstitution of the reaction centre complex with dibromothymoquinone

Experimental evidence for the specific binding of

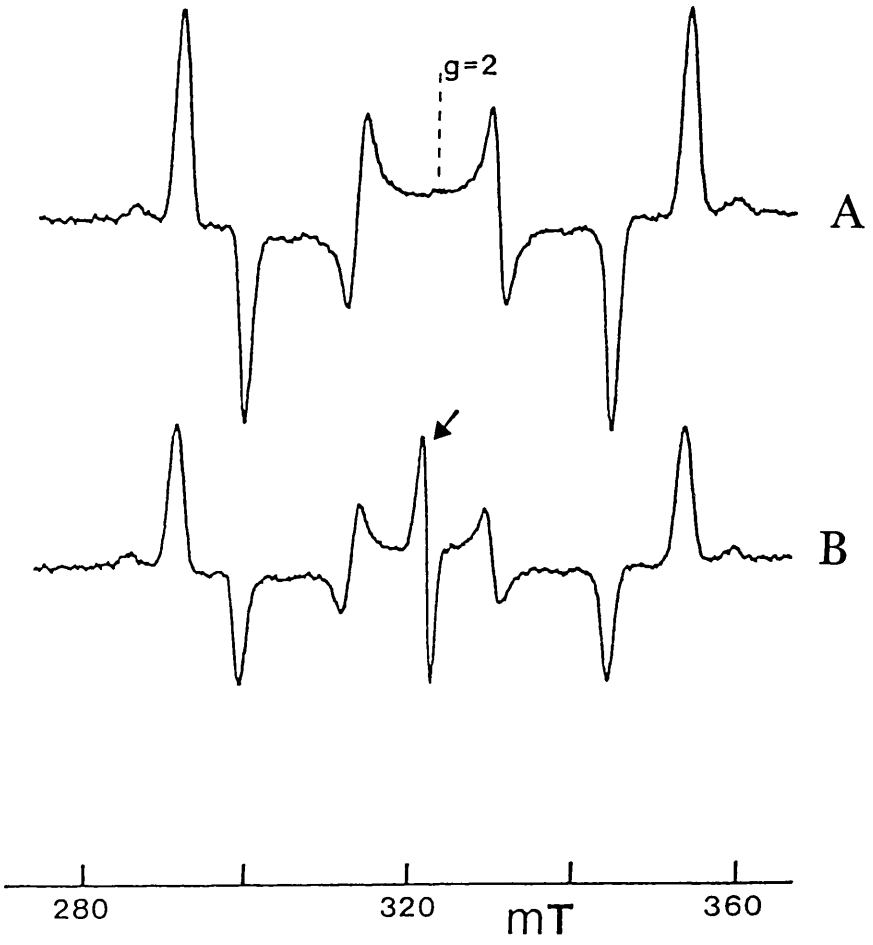

Figure 5.3. Esr spectra showing the effect of DBMIB addition to the D1/D2/cyt b_{559} complex on the amplitude of the triplet signal.

(A) and (B) are illuminated spectra (with the dark following illumination spectrum subtracted). (A) D1/D2/cyt b_{559} complex isolated in 4mM dodecylmaltoside, no additions. (B) as (A) with 100uM DBMIB added, showing a reduction in triplet amplitude. Esr conditions as for Figure 5.1.

exogenous quinone to the D1/D2/cyt b_{559} complex, was obtained when the DPQ was replaced with the artificial quinone, dibromothymoquinone (DBMIB) (Figure 5.3). These reconstitution experiments were carried out with reaction centres isolated at the final elution stage with the detergent, dodecylmaltoside. Following the addition of 100uM DBMIB, an approximate 50% decrease in triplet amplitude was observed, together with the generation of a radical at g=2 of approximately 1.2mT linewidth (Figure 5.3B arrowed). This could be interpreted as being as a result of quinone binding to the Q_A or Q_B site, allowing $P680^+$ to be observed with the DBMIB acting as an electron acceptor.

However, neither the g=1.82 or g=1.9 signal of the iron semiquinone were detected even when exogenous iron (4mM Fe^{2+}) was added to the sample. The inversion of the inner peaks of the triplet seen in Rps. viridis when the semiquinone Q_A was present as reported by Hore et al (1988) was also not observed. The addition of the inhibitor DCMU (250uM) prior to the addition of the DBMIB in the reaction centre sample had no effect on the reduction of triplet yield in the DBMIB samples.

The addition of the natural PQ-9 to the reaction centre complex isolated with Triton X-100 did not have an effect on the yield or lineshape of the triplet.

5.5 Laser flash spectroscopy experiments

Figure 5.4 shows the effect of DBMIB upon the decay kinetics of $P680^+$ in Triton X-100 prepared reaction centres. In a reaction centre sample with no additions, the decay is monophasic, with a fast phase of 20-60 us (Figure 5.4A). This fast phase is comparable to one observed in reaction centre complexes with no additions as discussed in Chapter 4 and is attributed to the formation of the triplet species (Takahashi et al, 1987; Mathis et al, 1989).

The addition of 100uM DBMIB to the reaction centre caused changes in the flash induced absorption spectrum. The decay was diphasic with a fast phase of 20-60us and a slow phase < 1 ms (Figure 5.4B). As in the case of the decay kinetics of reaction centre samples with SiMo/FeCN added (Chapter 4), the slow phase is indicative of electron transfer beyond Phe.

The fast phase could represent the formation of triplet in some centres. However, Mathis et al, (1989) have observed a similar decay component in the D1/D2/cyt b_{559} preparation, of 25 us which they do not attribute to triplet, as the decay kinetics are not altered by oxygen concentration. This kinetic phase is comparable to a 22 us phase which has been observed in tris washed PSII which as yet has no assigned function (Mathis et al,

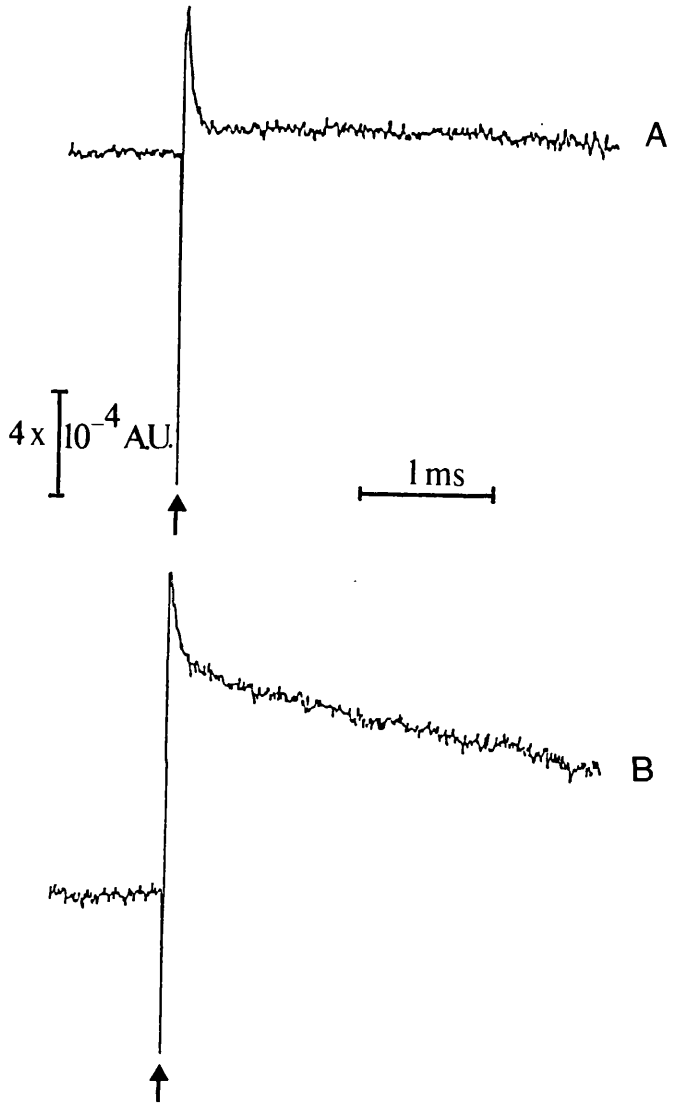

Figure 5.4. Absorbance changes of the D1/D2/cyt b_{559} complex at 820nm induced by a laser flash at 337nm.

A) No additions B) 100uM DBMIB added. Each spectrum is the average of 32 flashes at 0.5 Hz measured at room temperature. The arrow indicates the position of the laser flash. Chlorophyll concentration was 10 ug. ml^{-1}, 50mM Tris/HCl, 0.2% Triton X-100, 120mM NaCl, pH 7.2 , pathlength 1cm . Other conditions as described in Materials and Methods.

1989; Boska et al, 1983).

The >1ms component may represent the reduction of $P680^+$ by either reduced cytochrome b_{559} or DBMIB. This slow decay is comparable to one reported by Mathis et al (1989) observed in the D1/D2/cyt b_{559} complex in the presence of DBMIB. This decay is attributed to electron donation from reduced cytochrome b_{559} to $P680^+$, in a small number of centres. The photoreduction of cytochrome b_{559} by DBMIB at room temperature supports this observation. We therefore propose that the slow component represents the reduction of $P680^+$ by the cytochrome.

The reduction of $P680^+$ by Z occurs in the time range of a few microseconds (Gerken et al, 1988; Mathis et al, 1989). It was not possible to resolve such a fast component with our equipment, but it is possible that the fast phase observed in the presence of DBMIB (20-60 us) included contributions from the 5 us component. The kinetic data therefore support the role of DBMIB as an electron acceptor.

Discussion

5.6 The effect of detergent exchange on the stability of the reaction centre complex

Triton X- 100 was found to cause instability in the reaction centre complex as shown by the increased triplet

yield of the reaction centre sample at a lower Triton X-100 concentration. Reaction centres prepared using dodecylmaltoside were consistently more stable, possibly as a result of subtle structural changes, and subsequently the complexes retained activity for longer periods.

5.7 Reconstitution of the complex with exogenous quinones

Although electron transfer to the quinone was not observed in the presence of DPQ, the esr results could be interpreted as binding of the artificial quinone to the reaction centre complex causing a change in the triplet lineshape. The change in lineshape is unlikely to be due to triplet quenching as this does not explain the opposing effects observed at different Triton X-100 concentrations. No evidence to support the binding of the natural PSII quinone, PQ-9 to the reaction centre was obtained.

Electron transfer to the quinone was observed in dodecylmaltoside reaction centre samples containing DBMIB using both esr and laser flash spectroscopy. It is proposed that DBMIB is acting as an electron acceptor, with electron transfer occurring from the pheophytin. This results in the partial loss of triplet formation and the presence of a radical at g=2. These esr

characteristics are similar to those observed in reaction centre preparations in the presence of SiMo and FeCN.

An iron-semiquinone signal was not observed by esr in samples containing DBMIB. This may have been due to the loss of the non-haem iron during the isolation process. The FeQ signal was not restored in samples where exogenous iron was added to excess (4mM). The linewidth of the radical observed at g=2 (1.2mT) upon illumination at 4K was wider than that for the monomeric chlorophyll formed by SiMo or FeCN. This may therefore represent the presence of a combination of the semiquinone g=2 radical and the monomeric chlorophyll radical.

5.8 The photoreduction of cytochrome b_{559}

The photoreduction of cytochrome b_{559} was observed only in the presence of both DPQ and the electron donor DPC, suggesting that cytochrome b_{559} accepts electrons from DPQ. Thompson and Brudvig (1988) have proposed a mechanism for the prevention of photoinhibition whereby cyclic electron transport occurs around PSII under high light intensities. In this cycle, the monomeric chlorophyll is reduced by cytochrome b_{559} which is in turn reduced by the quinone acceptors (refer to the schematic diagram of this cycle overleaf).

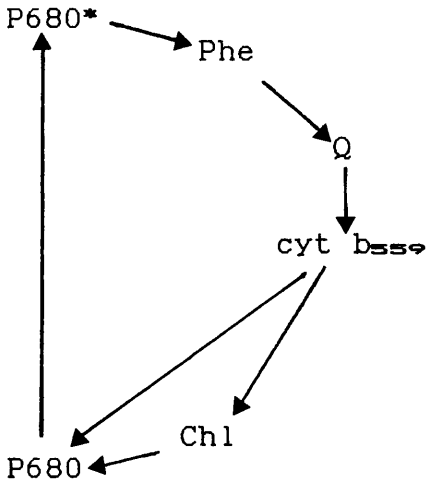

In support of this proposal is the formation of oxidised monomeric chlorophyll at cryogenic temperatures when cytochome b_{559} is oxidised as demonstrated in Chapter 4.

DBMIB acts as an electron acceptor at cryogenic temperatures. The change in the kinetic decay of P680 in the presence of DBMIB can also be interpreted as DBMIB acting as an electron acceptor at room temperature. Therefore this cycle may operate in the D1/D2/cyt b_{559} reaction centre complex in the presence of exogenous qunones such as DBMIB or DPQ.

Although the PSII reaction complex can be partially reconstituted with artificial quinone, a preparation containing bound quinone has not yet been reported. The H subunit of the bacterial reaction centre makes extensive contact with the L and M subunits via a region which

runs along the surface of the L/M complex near the quinone binding sites. This contact is thought to stabilise the reaction centre structure.

The removal of the H-subunit has been found to impair electron transport from Q_A^- to Q_B^- which may be attributed to a loosening of the structure of the L/M complex. This may increase the exposure of the quinone binding sites to exogenous agents or stabilising groups situated on the H-subunit may be lost and as a consequence, lower the binding constant of Q_B. Unsuccessful attempts at isolating the PSII reaction centre with bound quinone could be due to the lack of an analogous H-subunit.

It may be possible that the 47/43 kDa polypeptides may be necessary for high affinity binding of quinone in the PSII reaction centre. Indeed, recently Yagamuchi et al (1988) have reported the isolation of a D1/D2/47 kDa/cyt b_{559} complex using treatment with the chaotropic reagent potassium thiocyanate followed by separation by digitonin-polyacrylamide gel electrophoresis. The complex was estimated to contain 1.8 molecules of plastoquinone. It is therefore possible that Q_A is primarily bound to D2 but that the 47 kDa is required for high affinity binding of the quinone. The isolation of a complex with bound quinone may require the presence of the 47 kDa

polypeptide. However, it is also possible that the increased integrity of the complex prepared by Yagamuchi et al (1988) is due to the isolation procedure.

5.9 The number of copies of cytochrome b_{559} in PSII

Based on the analogy between the reaction centres of bacteria and PSII, it is suggested that there are two monomeric chlorophylls adjacent to P680. One of the accessory chlorophylls may act as a bridge for excitation between the antenna chlorophylls and P680. Its oxidation would therefore decrease light limited electron transfer, and also increase the susceptiblity of the second chlorophyll to oxidation by $P680^{+}$. This is consistent with the observations of Callahan et al (1986) which show that both D1 and D2 are synthesised during the recovery from photoinhibition and the cyclic system of Thompson and Brudvig (1988). If this is the correct situation of the reaction centre, two copies of the cytochrome b_{559} would be required to rereduce the two photooxidisable monomer chlorophylls in its photoprotective role.

The exact stoichiometry of the pigment composition of the PSII reaction centre is still undetermined partly due to inconsistencies with the extinction coefficient used for cytochrome b_{559}. Variations in the isolation procedure and the detergent used would also account for differences. In addition, the stoichiometry of the

pigments of the reaction centre complex is based on the assumption that for each reaction centre chlorophyll, there are two pheophytins, in analogy with the bacterial reaction centre. Further work is required to establish the stoichiometry of the prosthetic groups of the different preparations reported, by using a reliable method such as HPLC.

CHAPTER 6

Final Discussion

It is established that the D1/D2/cyt b_{559} complex binds the reaction centre components of PSII in higher plants, algae and cyanobacteria. Although the D1/D2/cyt b_{559} complex is depleted in electron transfer components (i.e. quinone, non-haem iron), it can still perform electron transfer reactions in the presence of exogenous electron acceptors/donors.

The complex can be partially reconstituted with the exogenous quinone, DBMIB (Chapter 5). Both SiMo and FeCN can act as electron acceptors in the reaction centre complex resulting in charge stabilisation, and the observation of a radical attributed to $P680^{+\cdot}$. Under these conditions, it has been shown that electron donation to P680 via the electron donors D/Z and the momomeric chlorophyll, can occur (Chapter 4). A role for cytochrome b_{559} has been proposed whereby the cytochrome partakes in electron transfer around PSII under high light intensities as discussed in Chapter 5. Figure 6.1 summaries these reactions and these results are published in Demetriou et al, 1988 and Nugent et al, 1989.

The analogy between the PSII reaction centre and that of purple bacteria originally suggested from amino acid sequence homology appears to be strong. The

Figure 6.1 Summary diagram of the electron transfer reactions of the D1/D2/cyt b_{559} complex in the presence of exogenous electron acceptors

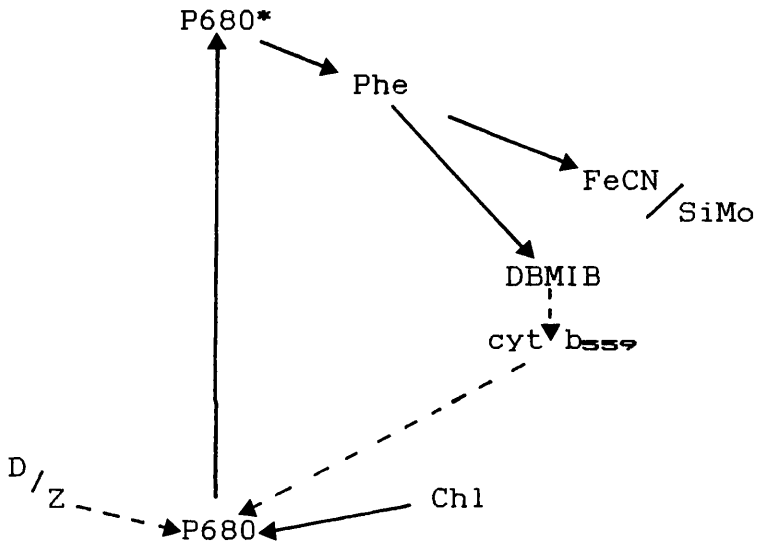

_____ Electron transfer reactions at cryogenic temperature

_ _ _ Electron transfer reactions at room temperature

reaction centre components are bound to the D1/D2 complex in a similar fashion and forward electron flow appears to involve similar components. However, there are major differences between the two systems:

1) The sensitivity of PSII to photoinhibition. This may be due to the high redox potential of P680/P680^{+} (1 V), which is much higher than the redox potential of the primary electron donors of PSI and photosynthetic bacteria (0.25-0.5 V). This is the probable reason for the oxidation of the accessory chlorophyll. A possible role of cytochrome b_{559} in protecting PSII against damage due to chlorophyll oxidation has already been discussed.

2) The loss of bound quinone in the PSII reaction centre complex which may be attributed to the lack of an H subunit analog and/or the loss of the non-haem iron.

Further work is required to improve the isolation procedure to give a more stable reaction centre preparation. The emphasis here would lie on the isolation of a reaction centre complex with bound quinone. Individual steps in the isolation procedure require investigation in order to find the stage at which the quinone is lost. Modifications in the isolation procedure at the appropriate step could then

be made. The possible role of the 47 kDa polypeptide in binding the reaction centre constituents also requires further investigation.

Increased stability of the preparations will result in a reaction centre complex more amenable to spectroscopic studies. A stable preparation is also required for attempts at the successful crystallisation of the reaction centre complex.

REFERENCES

Allen, J.P. and Feher, G. (1984) Proc. Natl. Acad. Sci. U.S.A. 81, 4795-4799.

Allen, J.P., Feher, G., Yeates, T.O., Rees, D.C., Deisenhofer, J., Michel, H. and Huber, R. (1986) Proc. Natl. Acad. Sci. U.S.A. 83, 8589-8593.

Akabori, K., Tsukamoto, H., Tsukihara, J., Nagatsuka, T., Motokawa, O. and Toyoshima, Y. (1988) Biochim. Biophys. Acta 932, 345-357.

Akerlund, H.E. and Jansson, C.(1981) FEBS Lett. 124, 224-232.

Akerlund, H.E., Jansson, C. and Andersson, B. (1982) Biochim. Biophys. Acta 681 , 1-10.

Allakhverdiev, S.I., Shafiev, M.A. and Klimov, V.V. (1986) Photobiochem. Photobiophys. 12, 61-65.

Anderson, J.M and Andersson, B. (1982) Trends Biochem. Sci. 6 , 288-292.

Andersson, B. and Akerlund, H.E. (1978) Biochim. Biophys. Acta 503 , 462-472.

Arnon, D.I. (1949) Plant Physiol. 24, 1-15.

Babcock, G.T and Sauer, K. (1973) Biochim. Biophys. Acta, 325, 483-519.

Babcock, G.T., Widger, W.R., Cramer, W.A., Oertling, W.A. and Metz, J.G (1985) Biochemistry 24 , 3638-3645.

Babcock, G.T. (1987) in Photosynthesis : New Comprehensive Biochemistry Vol. 15, pp 125-158 Elsevier (Amesz J ed).

Barber, J. (1982) Bioscience reports 2, 1-13.

Barber, J. (1987) Trends Biochem. Sci. 12, 123-124.

Barber, J., Chapman, D.J. and Telfer, A. (1987) FEBS Lett. 220, 67-73.

Barry, B.A. and Babcock, G.T. (1987) Proc. Natl. Acad. Sci. U.S.A. 84 , 7099-7103.

Beck, W.F., de Paula, J.C. and Brudvig, G.W. (1985) Biochemistry 24 ,3035-3043.

Berthold, D.A., Babcock, G.T. and Yocum, C.F. (1981) FEBS Lett. 134 , 231-234.

Bishop, N.I (1971) Methods Enzymol. 23, 372-408.

Boska, M., Sauer, K., Buttner, W. and Babcock, G.T (1983) Biochim. Biophys. Acta 722, 327-330.

Bouges-Bouquet, B. (1973) Biochim. Biophys. Acta 314, 250-256.

Brok, M. Ebskamp, F.C.R and Hoff, A.J. (1985) 809, 421-428.

Brudvig, G.W. and Crabtree, R.H. (1986) Proc. Natl. Acad. Sci. U.S.A. 83, 4586-4588.

Callahan, F.E., Becker, D.W. and Cheniae, G.M. (1986) Plant Physiol. 82, 261-269.

Castenholz, R.W. (1970) Schweiz. Z. Hydrol. 32 , 538-531.

Chang, C.H., Schiffer, M., Tiede, D. , Smith, U. and Norris, J. (1985) J. Mol. Biol. 186 , 201-203.

Chang, C.H., Tiede, D., Tang, J., Smith, U., Norris, J. and Schiffer, M. (1986) FEBS Lett. 205 ,82-86.

Chapman, D.J., Gounaris, K. and Barber, J. (1988) Biochim. Biophys. Acta 933, 423-431.

Chua, N.M. and Benoun, P. (1975) Proc. Natl. Acad. Sci. U.S.A. 72,2175-2179.

Cleland, R.E. (1988) Aust. J. Plant Physiol. 15, 135-150.

Cogdell, R.J., Brune, D.C. and Clayton, R.K. (1974) FEBS Lett. 45 , 344-347.

Commoner, B., Heise, J.J. and Townsend, J. (1956) Proc. Natl. Acad. Sci. U.S.A. 42, 710-718.

Davis, M.S., Forman, A. and Fajer, J. (1979a) Proc. Natl. Acad. Sci. U.S.A. 76, 4170-4174.

Davis, M.S., Forman, A., Hanson, L.K., Thornber, J.P and Fajer, J. (1979b) J. Phys. Chem. 83, 3325-3332.

Debus, R.J., Barry, B.A., Babcock, G.T. and McIntosh, L. (1988a) Proc. Natl. Acad. Sci. U.S.A. 85, 427-430.

Debus, R.J., Barry, B.A., Sithole, I., Babcock, G.T and McIntosh, L. (1988b) Biochemistry 27, 9071-9074.

Deisenhofer, J., Epp, O., Miki, K., Huber, R. and Michel, H. (1984) J.Mol. Biol. 180, 385-398.

Deisenhofer, J., Epp,O., Miki, K., Huber, R. and Michel, H. (1985a) Nature 318, 618-624.

Deisenhofer, J., Michel, H. and Huber, R. (1985b) Trends Biochem. Sci. 10, 243-247.

Deisenhofer, J. and Michel, H. (1989) EMBO Journal 8, 2149-2170.

Dekker, J.P., Bowlby, N.R. and Yocum, C.F. (1989a) FEBS Lett. 254, 150-154.

Dekker, J.P., Peterson,J., Bowlby, N.R., Babcock, G.T. and Yocum, C.F. (1989b) In: Current Research in Photosynthesis (Baltscheffsky, M. ed) 1, 263-267, Kluwer Academic Publishers.

Delepaire, P. and Chua, N.H. (1981) J. Biol. Chem. 256, 9300-9307.

Demetriou, C., Lockett, C.J. and Nugent, J.H.A. (1988) Biochem. J. 252, 921-924. Diner, B.A. and Petrouleas, V. (1987) Biochim. Biophys. Acta 893 , 138-148.

Diner, B.A. and Petrouleas, V. (1987) Biochim. Biophys. Acta 893,138-148.

Dismukes, G.C and Siderer, Y. (1980) FEBS Lett. 121, 78-80.

Dismukes, G.C. (1986) Photochem. Photobiol. 43 , 99-1.

Dismukes, G.C (1988) Chemica. Scripta. 28A, 99-104.

Doring, G., Renger, G., Vater, J. and Witt, H.T. (1969) Z. Naturforsch 24 , 1139-1143.

Duysens, L.N.M and Sweers, H.E. (1963) in Studies on Microalgae and photosynthetic bacteria, 353-372. University Tokyo Press.

Evans, M.C.W. (1977) In: Topics in Photosynthesis ;Primary Processes of Photosynthesis (Barber, J. ed) 2, 435, Elsevier Scientific Publishing

Company.

Feher, G. (1983) Biophys. J. 41, 2-7.

Feher, G., Allen, J.P., Okamura, M.Y. and Rees, D.C. (1989) Nature 339, 111-116.

Ford R.C. and Evans M.C.W. (1983) Febs Lett. 160, 159-163.

Ford, R.C. and Evans, M.C.W. (1985), Biochim. Biophys Acta 807 , 1-9.

Frank, H.A., Mclean, M.B. and Sauer, K (1979) Proc. Natl. Acad. Sci. U.S.A. 76, 5124-5128.

Frank, H.A., Hansson, O. and Mathis, P. (1989) Photosynthesis Research 20, 279-289.

Fuijita, F., Davis, M.S. and Fajer, J. (1978) J. Am. Chem. Soc. 100, 6280-6282.

Gast, P., Michalski, T.J., Hunt, J.E., Norris, J.R. (1985) FEBS Lett. 179, 325-328.

Gerken, S., Brettel, K., Schlodder, E. and Witt, H.T. (1988) FEBS Lett. 237, 69-75.

Ghanotakis, D.F., de Paula, J.C, Demetriou, D.M., Bowlby, N.R., Peterson, J., Babcock, G.T and Yocum, C.F. (1989) Biochim. Biophys. Acta 974 ,44-53.

Giangiacomo, M and Dutton, P.L. Proc. Natl. Acad. Sci. (1989) U.S.A 86, 2658-2662.

Glazer, A.N. (1984) Biochim. Biophys. Acta 768, 29-51.

Gounaris, K., Barber, J. and Harwood, J.L. (1986) Biochem. J. 237, 313-326.

Gounaris, K., Chapman, D.J. and Barber, J. (1988) FEBS Lett. 240,143-147.

Grant, J.L, Kramer, V.J., Ding, R. and Kispert, L.D. (1988) J. Am. Chem. Soc. 110, 2151-2157.

Greenberg, B.M., Gaba, V., Mattoo, A.K. and Edelman, M. (1987) The EMBO Journal 6, 2865-2869.

Haworth, P., Watson, J.L. and Arntzen, C.J. (1983) Biochim. Biophys. Acta 724, 151-158.

Hore, P.J., Hunter. D.A., van Wijk, F.G.H., Schaafsma,

T.J. and Hoff, A.J. (1988) Biochim. Biophys. Acta 936, 249-258.

Ikeuchi, M. and Inoue, Y. (1988) FEBS Lett. 241,99-104.

Johanningmeier, V., Neumann, E and Oettmeier, W. (1983) J. Bioenerg. Biomembr. 15, 43-66.

Joliot, P., Joliot, A., Bouges, B. and Barbieri, G. (1971) Photochem. Photobiol. 14 , 287-305.

Kahn, A. and Wettstein, D. (1961) J. Ultrastr. Res. 5, 557-574.

Kirmaier,C, Holten, D., Debus, R.J., Feher, G. and Okamura, M.Y. (1986) Proc. Natl. Acad Sci. U.S.A. 83, 6407-6411.

Klimov, V.V., Klevanik, A.V., Shuvalov, V.A. and Kranovsky, A.A. (1977) FEBS Lett. 82, 183-186.

Klimov, V.V., Dolan, B. and Ke, B. (1980) FEBS Lett. 112, 97-100.

Kohl, D.H. and Wood, P.M. (1969) Plant Physiol. 44, 1439-1445.

Kok, B., Forbush, B. and McGloin, M (1970) Photochem. Photobiol. 11, 457-475.

Kuhlbrandt, W. (1984) Nature 307, 478-480.

Kuwabara, T. and Murata. N. (1982) Plant Cell Physiol. 23, 533-539.

Kuwabara, T. and Murata, N. (1983) Plant Cell Physiol. 24, 741-747.

Kyle, D.J., Ohad, I. and Arntzen, C.J. (1984) Proc. Natl. Acad. Sci. U.S.A. 81 , 4070-4.

Kyle, D.J. (1985) Photochem. Photobiol. 41, 107-116.

Laemmli, U.K. (1970) Nature 227, 680-685.

Marder, J.B. and Barber, J. (1989) Plant cell and environment 12, 595-614.

Marsh, K.L. and Connolly, J.S. (1984) J. Photochem 25,183-195.

Mathis, P., Satoh, K and Hansson, O. (1989) FEBS Lett 251, 241-244.

McIntosh, L. (1988) Biochemistry 27, 9071-9074. 85, 427-430.

McTavish, H., Picorel, R. and Seibert, M. (1988) Plant Physiol. 89, 452-456.

Metz, J.G., Bishop, N.I. (1980) Biochim. Biophys. Acta 94, 560-566.

Metz, J.G and Siebert, M (1984) Plant Physiol. 76, 829-832.

Metz, J.G., Bricker, T.M. and Siebert, M. (1985) FEBS Lett. 185, 191-196.

Metz, J.G., Wong, J Bishop, N.J (1988) FEBS Lett. 114, 61-66.

Miyao, M. and Murata, N (1983) Biochim. Biophys. Acta 725 , 87-93.

Miyao, M., Murata, N., Lavorel, J., Maison-Peteri, B., Boussac, A., and Etienne, A.L. (1987) Biochim. Biophys. Acta 890, 151-159.

Miyazaki, A., Takahashi, S. Toyoshima, Y., Gounaris, K. and Barber, J. (1989) Biophys. Biochim. Acta 975, 142-147.

Murata, N. and Miyao, M. (1985) Trends Biochem. Sci. 10, 122-124.

Nakatani, H.Y., Ke, B., Dolan, E. and Arntzen, C.J (1984) Biochim. Biophys. Acta 765 , 347-352.

Nanba, O. and Satoh, K. (1987) Proc. Natl. Acad. Sci. U.S.A. 84, 109-112.

Norris, J.R., Uphaus, R.A., Crespi, H.L. and Katz, J.J (1971) Proc. Natl. Acad. Sci. U.S.A. 68, 625 -628.

Nuijs, A.M., van Gorkom, H.J., Plitjer,J.J. and Duysens, L.N.M.(1986) Biochim. Biophys. Acta 848 ,167-175.

Nugent, J.H.A., Diner, B.A. and Evans, M.C.W. (1981) FEBS Lett. 124, 241-244.

Nugent, J.H.A., Demetriou, C. and Lockett, C.J (1987) Biochim. Biophys. Acta 894, 534-542.

Nugent, J.H.A., Corrie, A.R., Demetriou, C., Evans, M.C.W. and Lockett, C.J. (1988) FEBS Lett. 235, 71-75.

Nugent, J.H.A., Telfer, A., Demetriou, C. and Barber, J. (1989) FEBS Lett. 255, 53-58.

Ohad, I., Kyle, D.J. and Hirschberg, J. (1985) EMBO J. 4, 1655-1659.

Okamura, M.Y. Isaacson, R.A and Feher, G. (1975) Proc. Natl. Acad. Sci. U.S.A. 72 , 3491-5.

Okamura, M.Y., Satoh, K., Isaacson, R.A. and Feher, G. (1987) In: Progress in Photosynthesis Research (Biggins, J. ed) 1, 379-381, Martinus Nijhoff, Dordrecht.

O'Malley, P.J and Babcock, G T, (1984) Biochim. Biophys. Acta 765 , 370-9.

Palmer, G. (1985) Biochem. Soc. Trans 13 , 548-560.

de Paula, J.C., Innes, J.B. and Brudvig, G.W. (1985) Biochemistry, 24, 8114-8120.

Pfister, K., Steinback, K.E., Gardner, G. and Arntzen, J. (1981) Proc. Natl. Acad. Sci. U.S.A. 78, 981-985.

Plato, M., Lubitz, W., Lendzian, F. and Mobius, K. (1988) Is. J. Chem. 28, 109-119.

Powles, S.B. (1984) Annu. Rev. Plant Physiol. 35, 15-44.

Rutherford, A.W. and Mullet, J.E (1981) Biochim. Biophys. Acta 635 , 225-235.

Rutherford, A.W., Paterson, D.R. and Mullet J.E. (1981) Biochim. Biophys. Acta 635, 205-214.

Rutherford, A.W. and Mathis, P. (1983) FEBS Lett. 154 , 324-328.

Rutherford, A.W. and Zimmerman, J.L. (1984) Biochim. Biophys. Acta 767, 168-175.

Rutherford, A.W. (1986) Biochim. Biophys. Acta 807, 189-201.

Rutherford, A.W, Siebert, M. and Metz, J.G. (1988) Biochim. Biophys.Acta 932, 171-176.

Rutherford, A.W. (1989) Trends Biochem. Sci. 14, 227-232.

Satoh, K. (1979) Biochim. Biophys. Acta 546, 84-92.

Sauer, K. (1986) In: Photosynthesis III- Photosynthetic membranes and light harvesting systems, Encyclopedia of Plant Physiology (Staehelin, L.A. and Arntzen, C.J. ed) 19, p89, Springer-Verlag.

Schatz, G.H. and Witt, H.T. (1984) Photobiochem. Photobiophys. 7 ,1-14.

Shopes, R.J. and Wraight, C.A. (1985) Biochim. Biophys. Acta 806, 348-356.

Seibert, M., Picorel, R., Rubin, A.B. and Connolly, S. (1988) Plant Physiol. 87, 303-306.

Stemler, A. (1977) Biochim. Biophys. Acta 460 , 511-522.

Stewart A.C. and Bendall D.S. (1979) FEBS Lett. 107, 308-312.

Stiehl, H.H. and Witt, H.T. (1969) Z. Naturforsch. 24, 1588-1598.

Sullivan, P.D. and Bolton, J.R (1968) J.Am. Chem. Soc. 90 , 5366-5370.

Swartz, H.M., Bolton, J.R. and Borg, D.C. (1972) In: Biological Applications of Electron spin resonance, Wiley Interscience.

Tabata, K., Itoh, S., Yamamoto, Y., Okayama, S. and Nishimura, M (1985) Plant Cell Physiol 26 , 855-863.

Takahashi, Y., Hansson,., Mathis, P. and Satoh, K. (1987) Biochim. Biophys. Acta 849, 49-59.

Takahashi, Y and Styring, S (1987) FEBS Lett 223, 371-375.

Takahashi, Y., Satoh, K. and Itoh, S. (1989) FEBS Lett. 255 133-38

Telfer, A., Barber,J and Evans M.C.W.(1988) FEBS Lett. 232c,209-213.

Telfer, A. and Barber,J. (1989) FEBS Lett. 246, 223-228.

Thompson, L.K. and Brudvig, G.W. (1988) Biochemistry 27, 6653-6658.

Thurnauer, M.C., Katz,J.J and Norris, J.R (1975) Proc. Natl. acad. Sci. U.S.A. 72, 3270-3274.

Thurnauer, M.C and Norris, J.R (1977) Chem. Phys. Lett 47, 100-105.

Trebst, A. and Depka, B. (1985) Z.Naturforsch 40, 391-399.

Trebst, A., Depka, B., Ridley, S.M. and Hawkins, A.F. (1985) Z. Naturforsch. 40, 391-399.

Trebst, A. (1986) Z. Naturforsch 41, 240-245.

van Gorkom,H.J., Tamminga,J.J., Haveman,J and van der Linden, I.K.(1974) Biochim. Biophys. Acta 347, 417-438.

van Gorkom, H.J., Pulles, M.P.J. and Wessels, J.S.C. (1975) Biochim. Biophys Acta 408 , 331-339.

Valenzeno, D.P. (1987) Photochem. Photobiol. 46, 147-160.

Velthys, B.R and Visser J.W.M. (1975) FEBS Lett. 55 , 109-112.

Vermaas, W.F.J. and van Rensen, J.J.S. (1981) Biochim. Biophys. Acta 636, 168-174.

Vermass, W.F.J., Renger, G. and Dohnt, G. (1984) Biochim. Biophys. Acta 764 , 194-202.

Vermass, W.F.J. and Rutherford, A.W. (1984) FEBS Lett. 175 , 243-248.

Vermass, W.F.J., Rutherford., A.W and Hansson, O. (1988) Proc. Natl. Acad. Sci. U.S.A. 85 , 8477-8481.

Visser, J.W.M., Rijgersberg, C.P and Gast,P. (1977) Biochim. Biophys. Acta 460, 36-46.

de Vitry, C., Carles,C. and Diner, B.A. (1986) FEBS. Lett 196 , 203-206.

Wasielewski, M.R. (1982) Synthetic approaches to photoreaction centre structure and function. In 'Light reaction Path of Photosynthesis' (Ed. F.K. Fong) Molecular Biology, Biochemistry and Biophysics. Vol.35, pp.234-276. (Springer-Verlag:Berlin).

Wasielewski, M.R., Johnson, D.G., Seibert, M. and Govidjee (1989) Proc. Natl. Acad. Sci. U.S.A. 86, 524-528.

Webber, A.N. and Gray, J.C. (1989) FEBS Lett. 249, 79-82.

Weyer, K.A., Lottspeich, F., Gruenberg,H., Lang, F., Oesterhelt, D and Michel, H. (1987) EMBO J. 6 , 2197-2202.

Yagamuchi, N., Takahashi, Y. and Satoh, K. (1988) Plant Cell Physiol. 29, 123-129.

Yamamoto, Y., Doi, M. Tamura, N. and Nishimura, M. (1981) FEBS Lett. 133 , 265-268.

Zuber, H. (1986) Trends Biochem. Sci. 11, 414-419.